# STUDY OF TRPML CHANNELS REVEALS INSIGHT INTO ENDOCYTIC MALFUNCTION, ORGANELLE CROSSTALK, AND THE ACTIVATION OF PRO-APOPTOTIC PATHWAYS

by

**Grace Ann Colletti**

B.S., Rider University, 2006

Submitted to the Graduate Faculty of

the Kenneth P. Dietrich School of Arts & Sciences in partial fulfillment

of the requirements for the degree of

Doctor of Philosophy

University of Pittsburgh

2011

UNIVERSITY OF PITTSBURGH

THE KENNETH P. DIETRICH SCHOOL OF ARTS & SCIENCES

This dissertation was presented

by

Grace Ann Colletti

It was defended on

November 29th, 2011

and approved by

Jeffrey Hildebrand, Associate Professor, Department of Biological Sciences

William Saunders, Associate Professor, Department of Biological Sciences

Michael Grabe, Assistant Professor, Department of Biological Sciences

Ora A. Weisz, Professor, Department of Medicine and Department of Cell Biology and Physiology

Dissertation Advisor: Kirill Kiselyov, Associate Professor, Departmental of Biological Sciences

**STUDY OF TRPML CHANNELS REVEALS INSIGHT INTO ENDOCYTIC MALFUNCTION, ORGANELLE CROSSTALK, AND THE ACTIVATION OF PRO-APOPTOTIC PATHWAYS**

Grace Ann Colletti, PhD

University of Pittsburgh, 2011

Mucolipidosis type IV (MLIV) is a lysosomal storage disease resulting from mutations in the gene *MCOLN1*, which codes for a transient receptor potential family ion channel TRPML1 (Mucolipin-1). MLIV has an early onset and is characterized by developmental delays, motor and cognitive deficiencies, gastric abnormalities, retinal degeneration and corneal cloudiness. The degenerative aspects of MLIV have been attributed to cell death, whose mechanisms remain to be delineated in MLIV and most other lysosomal storage diseases. The function of TRPML1 is still not completely understood in the cell. In order to address the function of this channel as well as the consequences of its loss, we have studied TRPML1 and a closely related channel TRPML3 using proteomic, transcriptional, and ion channel activity assays. Structure/function analyses of TRPML (Mucolipin) channels revealed that the closely related TRPML3 channel conducts $K^+$, $Na^{2+}$, $Ca^{2+}$, and $Fe^{2+}$, but does not conduct transition metals such as $Cu^{2+}$ and $Co^{2+}$. The permeability of the channel can be disrupted by mutations to the pore domain and a constitutively active channel mutation abolishes transition metal block of both TRPML1 and TRPML3. The similarities in TRPML sequence and the activity of the constitutively active mutants suggests that these channels may share similar activity profiles, which supports previous reports that TRPML1 may function to regulate lysosomal $Ca^{2+}$ and $Fe^{2+}$ in order to promote proper lysosomal fission/fusion events and function. Our proteomic and transcriptional analyses reveal that acute downregulation of TRPML1 results in apoptosis in a cathepsin B and Bax

dependent manner. This is the first evidence that acute TRPML1 loss is linked to apoptosis and my work provides a preliminary mechanism for this process. Furthermore, TRPML1 loss results in increased NFκB levels as well as altered transcription of genes outside the previously identified lysosomal gene expression network. This suggests that loss of TRPML1 results in cellular changes that affect downstream transcriptional targets and induces cellular responses, such as apoptosis. Taken together, these data shed light on the importance of TRPML1 function and may help us understand the cellular role of this channel and how its loss results in cell death.

## TABLE OF CONTENTS

## LIST OF TABLES

## LIST OF FIGURES

## PREFACE

I would like to thank many people who have helped me with this work throughout my graduate career. First, I would like to thank my advisor, Kirill Kiselyov for his unrelenting guidance and trust. He has helped me through the hardest parts of this dissertation work and always reminded me of my capabilities, pushing me to accomplish what he knew I was capable of. Kirill provided the perfect balance of guidance as well as independence, allowing me to pursue questions and hypotheses which helped me grow as a scientist. He is a wonderful advisor as well as friend and I am very thankful to have him as my graduate mentor.

I would also like to thank the members of my lab. Although labs change over the years, I was lucky enough to be accompanied throughout my graduate career by wonderful, supportive lab mates. I was able to mentor many of them enriching my experience as a teacher as well as graduate student. In particular, I'd like to thank Emina Hodzic, Ira Kukic, Youssef Rbaibi, and Jeffrey Lee for their friendship and optimism throughout my years here. I would also like to thank all of the past members who have contributed to this work, whether through experimental help, discussion, or just support and guidance!

I would like to thank my thesis committee: Dr. Jeffrey Hildebrand, Dr. William Saunders, Dr. Michael Grabe, and Dr. Ora A. Weisz for all of their help! They really kept me on track and helped me work through difficult times in my work. Thank you for your criticism, support, and guidance which made me a better scientist! I would also like to extend my thanks

to members of the Weisz lab including Jennifer Bruns and Mark T. Miedel for their collaboration on this project.

I would not be as happy and as successful if it was not for my friends and family. First, I need to thank my undergraduate research mentor, Dr. Jonathan Karp. Jonathan has not only been a wonderful advisor but also a great friend who inspired me to pursue my interest in science and has always reminded me why I love what I do! Next I want to thank my family, especially my mom and dad. They have also always supported my work and I thank them for all of their love and guidance! I definitely could not have gotten to this point without them and I am so lucky that they are always there for support! And finally, I'd like to thank my fiancé, Matthew Farber. Matt was always there to encourage me, push me forward, and make me laugh (especially when I desperately needed one!). He has helped me stay focused and reminded me of what is important. We wrote our dissertations during the same time, and although most might think this could hurt a couple, it has definitely made us stronger. He is my favorite person to be around so writing with him just made the process that much easier. So Matt, thank you for all your help and I love you!

# 1.0 INTRODUCTION

## 1.1 OVERVIEW

TRPML1 is a member of the Transient Receptor Potential (TRP) family of ion channels. Unlike most TRP channels, TRPML1 and its relative TRPML2 and TRPML3 primarily reside in the membranes of the endocytic pathway (1-6). TRPML1 localizes to the lower portions of the endocytic pathway (late endosomes and lysosomes), due to the presence of a lysosomal localization tag on its N-terminal (5). TRPML1 was shown to be an inwardly rectifying cation channel (ions flow out of the lysosomal compartment), whose activity is potentiated by $PI(3,5)P_2$ and by low, typically lysosomal, levels of pH (7, 8). TRPML1 activation by $PI(3,5)P_2$, a lipid predominantly found in late endosomes and lysosomes, provides physiological context for its localization suggesting that it is either activated by delivery to the lysosomes or it serves as a proximity sensor in lysosomes and late endosomes (9). TRPML1 was suggested to regulate fusion/fission of vesicles in the endocytic pathway, and/or some aspect of lysosomal ion homeostasis such as pH or $Fe^{2+}$ content (7, 10).

TRPML1 loss is due to mutations in the gene *MCOLN1* resulting in the rare lysosomal storage disease Mucolipidosis type IV (MLIV) (2, 11). The disease is associated with the buildup of storage bodies and has a profound neurodegenerative profile, which, in mouse models, has been linked to retinal degeneration and demyelination of corpus callosum, deep layer neocortex,

and cerebellar white matter tracts (12, 13). As with most lysosomal storage diseases, the mechanisms of cell death in MLIV are unclear. It was previously suggested that lysosomal deficiencies in MLIV and, perhaps, other storage diseases, lead to autophagic deficits and buildup of effete mitochondria, which may expose cells to pro-apoptotic effects of stimulation (14, 15). Nonetheless, the selectivity of cellular loss in storage diseases remains puzzling. We believe that the key to identifying the cell death pathway in MLIV lies in deconstructing the early events accompanying the loss of TRPML1 as well as understanding the function and activity of TRPML1 itself. Previous studies in patients' cells have provided conflicting and often convoluted data likely due to the contribution of secondary effects due to chronic accumulation of storage material. This accumulation of lysosomal substrates may have little to do with the core cause of the disease; therefore, a system lacking secondary defects is needed to understand the underlying effects of TRPML1 loss. Furthermore, human skin fibroblasts from MLIV patients, predominantly used in experiments, perform fairly well in culture suggesting that the mechanisms responsible for cell death in MLIV are suppressed and/or do not fully manifest in these cells.

To delineate the early events associated with the loss of TRPML1 we used siRNA mediated knockdown (KD) to acutely downregulate TRPML1 in HeLa cells. A KD of palmitoyl-protein thioesterase 1 (PPT1), an enzyme mutated in another lysosomal storage disease, Infantile Neuronal Lipofuscinosis, was used as a comparative control (16, 17). We show that TRPML1 loss specifically causes, within 48 hours after KD, a cytoplasmic buildup of the lysosomal protease CatB and Bax/CatB dependent apoptosis (Section 2). These results illustrate, for the first time, the early events leading to cell death in TRPML1 deficient cells.

Interestingly, acute TRPML1 KD, but not PPT1 KD, induced NFκB upregulation and altered expression of NFκB regulated genes (Section 3). The genes altered by TRPML1 KD were not part of a previously identified lysosomal gene network, suggesting that these changes are not due to the same lysosomal dysfunction which activates the lysosomal network (18) but rather to changes caused by TRPML1 KD, possibly at the protein level. Further work will be needed to delineate the pathways that result in NFκB upregulation and transcriptional changes.

The final portion of this work focuses on characterizing the activity of mucolipin channels and how they are affected by transition metals. Proper transport of transition metals from endocytic compartments to the cytosol has been shown to be critical for proper cell function and is necessary to prevent destructive ROS production. Therefore the permeability of several transition metals was evaluated in mucolipin channels. To do this, we performed structure/function studies using whole cell patch clamp analysis. TRPML1 does not show activity when using whole cell patch clamp analysis, as it is not targeted to the plasma membrane (5, 19). However, its close relative TRPML3 does localize to the plasma membrane when overexpressed (8, 20-26). Therefore we used TRPML3 as a model to study mucolipin activity and transition metal block. We tested the conductance of several ions including $Na^+$, $K^+$, $Ca^{2+}$, and several transition metals such as $Co^{2+}$, $Cu^{2+}$, $Ni^{2+}$, $Fe^{2+}$, and $Zn^{2+}$ both in wildtype and mutated forms of the channel. Mutations were made in conserved residues within the pore domain and surrounding residues of the channel. We report that TRPML3 conducts $Na^+$, $K^+$, $Ca^{2+}$, and $Fe^{2+}$ but is blocked by micromolar concentrations of $Co^{2+}$, $Cu^{2+}$, $Ni^{2+}$ and $Zn^{2+}$. A cysteine residue near the channel pore contributes to TRPML3's sensitivity to transition metals. The *varitint-waddler* (*Va*) TRPML3 spontaneously active mutant is insensitive to transition metal block. Interestingly the *Va* mutation in TRPML1 results in TRPML1 plasma membrane

expression which can be detected by whole cell patch clamp analysis. The *Va* TRPML1 channel conducts ions similarly to the TRPML3 *Va* mutant. Both mutants are resistant to transition metal block showing that these channels may share common conductance profiles.

This dissertation is divided into 4 sections: 1) background information, 2-3) the effects of TRPML1 downregulation including transcriptional changes and apoptosis, 4) the characterization of mucolipin channel activity and the effect of transition metal toxicity on cells and the possible role of mucolipins. The following introduction provides a review of lysosomes, cathepsin-mediated apoptosis, TRPML1, MLIV, and the role of the endocytic pathway in transition metal toxicity.

## 1.2 LYSOSOMES

The discovery of lysosomes appears to have arisen from a laboratory mishap. Christian De Duve's lab performed tissue fractionation through differential centrifugation and tested each fraction for acid phosphatase activity. Interestingy, another sample set was left in the refrigerator for 5 days and then assayed for acid phosphatase activity. The refrigerated samples showed increased amounts of acid phosphatase activity. This lead De Duve's group to speculate that the enzyme was bound in a membrane compartment (originally thought to be mitochondrial) and that over time, the enzyme was liberated from the compartment (27). Over the next several years De Duve and his colleagues characterized these membrane compartments calling them lysosomes due to their abundance of hydrolytic enzymes (28, 29). Through lysosomal characterization, it has become clear that lysosomes are necessary for proper cell function,

playing critical roles in substrate degradation, absorption of endocytosed material, and autophagy, a central housekeeping and survival function (30-35).

Lysosomal hydrolases work in the specific pH environment of the lysosome, maintained through several channels and transporters; therefore, the regulation and maintanence of this lysosomal environment is critical for cell survival. Several diseases are caused by the improper delivery or loss of function of both lysosomal transporters and hydrolytic enzymes. These "lysosomal storage disorders" result in severe neurodegenerative and motor defects, highlighting the importance of proper lysosomal activity. Therefore it is necessary that lysosomal components are both functional and properly delivered to this organelle. The following sections will discuss lysosomal formation and function, the biosynthesis of lysosomal proteins, and lysosomal-related diseases.

### 1.2.1 Lysosomal function and formation

Lysosomes function at deep levels of the endocytic pathway degrading substrates from late endosomes, autophagosomes, and chaperone-mediated autophagy as well as expelling nutrients into the extracellular environment through exocytosis. In this section, I will briefly discuss the role of lysosomes in autophagy, delivery of late endosomal substrates to the lysosome, and the regulation of the lysosomal environment.

In autophagy, autophagosomes form double membranes around cytosolic domains, either containing proteins or effete organelles, such as dysfunctional, fragmented mitochondria. Autophagosomes are transported to lysosomes by dynein, either fusing to create a hybrid organelle called the "autolysosome" or briefly interacting with lysosomes to transfer autophagic substrates (36). Upon fusion, the inner autophagosomal membrane enters the lysosomal lumen

where it is degraded, while the outer membrane temporarily fuses with the lysosomal membrane. Autophagosome degradation, but not docking, is dependent on proper lysosomal acidification (37). The autophagic machinery, formation, and processes are well developed; therefore my work will focus on the interaction of autophagosomes with lysosomes.

Similar to the outer membrane of the autophagosome, the late endosomal membrane is not degraded upon interaction with the lysosomes. Rather, contents of late endosomes appear to be transferred to lysosomes through "kissing" events, formation of intervesicular tubules, and reversible fusion (38, 39). "Kissing" refers to the brief interaction between the two compartments where the compartments do not completely fuse together. Fusion results in a hybrid organelle containing both late endosome and lysosomal components. Tubule formation between late endosomes and lysosomes appears to mediate content mixing before the fusion of hybrid compartments (38). The late-endosome-lysosome hybrid organelle shares components of both organelles, is larger than either lysosomes or late endosomes alone, and is less dense than lysosomes (40). Formation of these hybrid organelles is reversible, restoring the components of the two compartments.

The fusion of lysosomes with autophagosomes and late endosomes is dependent on several factors, which coordinate the delivery, tethering, and fusion of these vesicles. Several steps leading to lysosomal fusion with late endosomes and autophagosomes are conveyed by the GTPase Rab7, which has been shown to coordinate lysosomal fusion, autophagic maturation, and drive late endosome/lysosome perinuclear localization (41-44). The Vps39 protein of the HOPS complex (composed of vacuolar protein sorting (VPS) proteins) is required for conversion of Rab5 (early endosomal GTPase) to Rab7, a necessary step in early endosomal maturation and has been shown to act as a Rab7 GEF (Guanine Nucleotide Exchange Factor) (45, 46). Two

downstream effectors of Rab7, RILP and ORLP1, coordinate dynein/dynactin mediated minus-end transport of late endosomes and lysosomes along microtubules (41, 47, 48). Therefore, Rab7 seems to play multiple roles in the maturation and delivery of endosomal vesicles.

The above mentioned HOPS complex is conserved between yeast and mammalian cells, and is thought to not only mediate Rab5 to Rab7 conversion, but to also act as a tether between late endosomes and lysosomes. The HOPS complex is composed of VSP proteins 11, 16, 18, 33, 39, and 41. While Vsp39 displays Rab7 GEF activity, Vsp41 is thought to anchor the HOPS complex directly to Rab7 (49). Rab7, in turn, mediates the interaction between the HOPS complex and SNARE complexes, discussed below (50).

Fusion of the lysosome and late endosome vesicles is accomplished by the formation of a *trans*-SNARE complex (SNARE complexes are on opposing membranes) composed of Syntaxin7, Vti1b, Syntaxin8 and VAMP7 (51). The specificity of this complex is conveyed through VAMP7, which is unique to lysosomal compartments (52). Autophagic/lysosomal fusion is instead mediated by a SNARE complex consisting of Vti1b and VAMP8, independent of syntaxin 7/8 and VAMP7 involvement (53). Lysosomal/late endosomal vesicle fusion is a $Ca^{2+}$ driven event, mediated by intraorganelle $Ca^{2+}$ stores, suggesting that late endocytic ion channels may play a role in regulating the fusion of these vesicles (54-56).

Upon the delivery to the lysosome, substrates are broken down by specific hydrolytic enzymes. These include proteases, peptidases, amylases, and lipases which function optimally in the acidic pH (~4.5-5.5) of the lysosome. Some lysosomal hydrolases, such as Cathepsin B, are active in a wider pH range, allowing them to cleave proapoptotic cytosolic substrates, which will be discussed later (57-59). However, most lysosomal enzymatic activity is dependent on the specific ionic environment of the lysosome, maintained through the activity of several membrane

channels and transporters. In addition, the acidity of the lysosome is necessary for proper sorting, fusion, and delivery to the lysosome (60-62). This acidity is mainly regulated by the V-type ATPase $H^+$ pump, which moves protons against the gradient into the lysosome, although other lysosomal transporters such as ClC-7 help regulate the activity of this pump (63, 64). In addition to acidification, regulation of other lysosomal ion concentrations is critical for proper function. Channels and transporters found in the lysosomal membrane include TRPML1, discussed in depth in section 1.3, TPCN1/2, Slc11a2 (also called DMT1, NRAMP2), and ClC-7 (65-67). The TPC channels were recently discovered to be $Ca^{2+}$ release channels, activated by the messenger NAADP (68). Slc11a2 is a metal transporter which is responsible for moving substrate bound metals to the cytoplasm (65). ClC-7 was identified in the past several years as a lysosomal $Cl^-/H^+$ antiporter, which is necessary for proper lysosomal acidification (69, 70). It is clear that maintaining the ionic environment of the lysosome is a tightly regulated process which is dependent on several components and is required for proper organelle function.

It is important that cells maintain proper lysosomal levels in order to respond to the need for cellular digestion. Formation or increase in lysosomes occurs through the synthesis and delivery of lysosomal components. *De novo* lysosomal formation has not been shown; therefore it appears that the increase in lysosomal number results in addition of newly synthesized lysosomal components into the endocytic system, driving up lysosomal numbers. It is well known that lysosome numbers change in response to specific lysosomal disruption (71, 72), suggesting that cells monitor the requirement for degradation and respond by altering lysosomal number and content. Such a response requires a coordinated change in gene expression, which was shown recently through the discovery of a "degradation" gene network (18, 73). Genes in this network contain the "CLEAR", Coordinated Lysosomal Expression And Regulation,

promoter element which is bound by the transcription factor EB (TFEB). Lysosomal disruption results in the coordinated upregulation of genes, mainly encoding lysosomal proteins, in this network through TFEB activation (18). Since the original study, the CLEAR network has been shown to drive expression of proteins in additional degradation pathways (73). This is the first evidence of a gene network that can alter lysosomal levels suggesting that cells can monitor and respond to changes in the endocytic pathway at a transcriptional level.

### 1.2.2 Synthesis and trafficking of lysosomal proteins

Lysosomal composition includes both hydrolytic enzymes as well as a system of transporters that play several important roles as discussed above. These include: (i) establishing and controlling acidic pH in the lysosomes, (ii) cleavage of specific substrates, (iii) absorption of digestive substrates, (iv) the release of $Ca^{2+}$ from the lysosomal lumen that drives the fusion of lysosomes with late endosomes, and (v) transport of metals bound to endocytosed proteins across the lysosomal membrane into the cytoplasm (30-32). Hydrolytic enzymes are targeted to the lysosomal lumen, while transporters are delivered to the membrane through vesicle fusion. Targeting to the lysosome can occur in mannose 6-phosphate dependent and independent manners through the biosynthetic and endocytic pathways. The following section will describe the trafficking and sorting of lysosomal proteins through these pathways.

All lysosomal proteins are co-translationally transported into the endoplasmic reticulum (ER) (74, 75). Hydrolytic enzymes are transported into the ER lumen while lysosomal membrane proteins (LMPs) are inserted into the ER membrane. I will first discuss the sorting of hydrolytic enzymes, which are delivered directly to lysosomes from the *trans*-Golgi network (TGN), modeled in Figure 1.1. In the ER the hydrolases are modified, specifically through

glycosylation on asparagine residues within the consensus motif Asn-X-Ser/Thr with high mannose oligosaccharides (76). These glycans are then processed by glucosidases and mannosidases before being transported to the Golgi complex (Fig 1.1.A) (77). Further processing may occur depending on the nature of the lysosomal protein, for example, specific cysteine residues are converted into $C_{\alpha}$-formylglycine residues in lysosomal sulfatases, a modification essential for proper sulfatase activity (78). The hydrolases are then transported to the Golgi complex via vesicular transport.

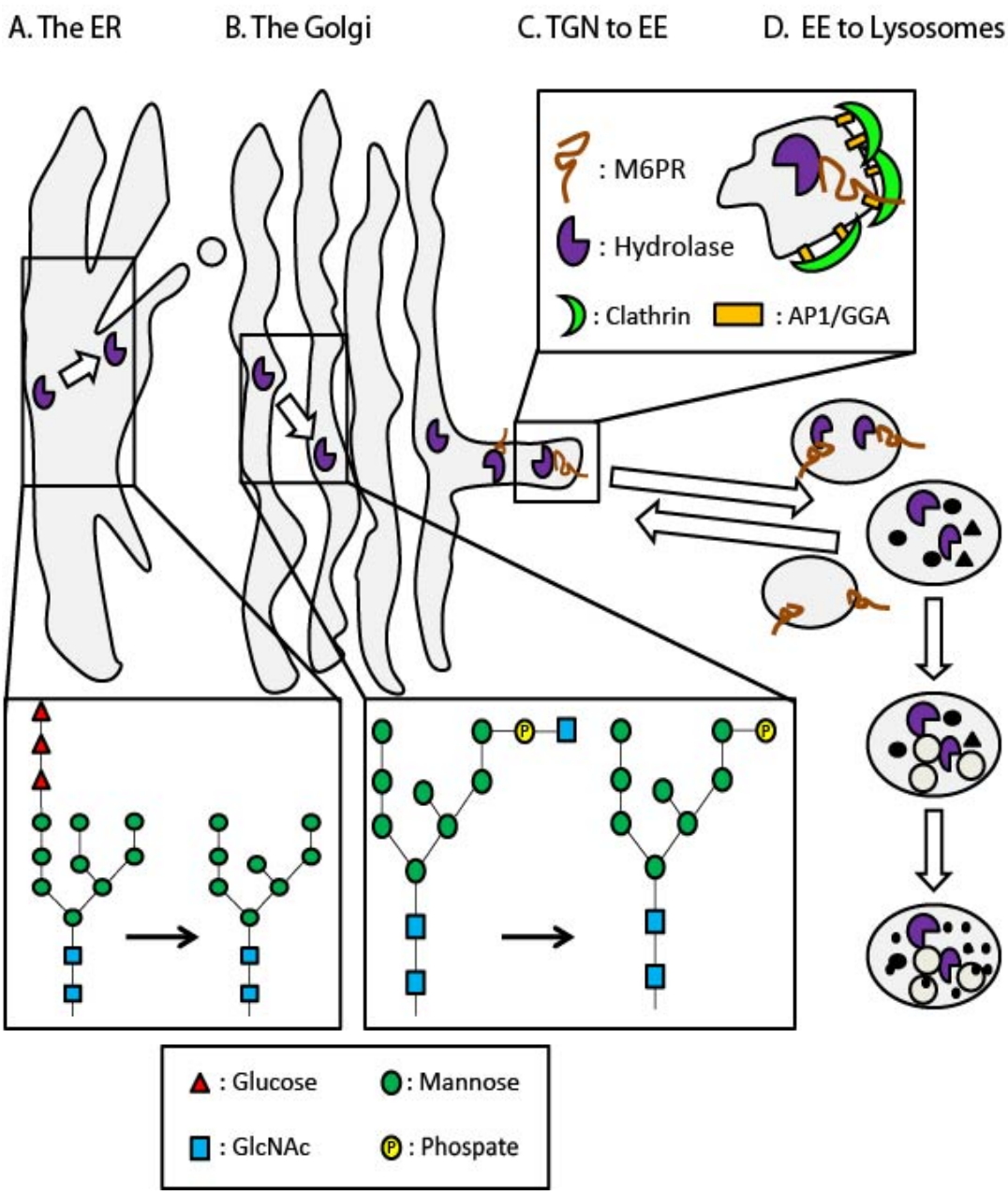


**Figure 1.1 Model of biosynthetic trafficking of lysosomal hydrolytic enzymes**
Schematic model of hydrolytic enzyme trafficking from the ER to the TGN to lysosomes. A. Hydrolytic enzymes are translated into the lumen of the ER, where they are glycosylated. This moiety is processed removing glucose residues and a mannose residue, before exiting the ER. B. In the early Golgi, a phosphodiester intermediate is formed mainly on the first mannose of the α-1,6 branch of the mannose chain. This is then hydrolyzed by the "uncovering enzyme" revealing the phosphate group. This structure is recognizing in the TGN by mannose-6-phosphate receptors (M6PRs) C. M6PRs associate with adaptor proteins such as AP-1, which mediates interaction with clathrin to form clathrin-coated vesicles. D. Clathrin coated vesicles from the TGN are transported to early endosomes. Here the M6PR dissociates with its cargo upon exposure to the acidic lumen of these vesicles. The M6PR is recycled back to the TGN or is transported to the plasma membrane. The early endosome matures/fuses with the late endosomes, which fuses or transfers cargo to the lysosome. In the lysosome the inactive hydrolases are activated. Model adapted from figures in Pohl et al., 2009 and Braulke and Bonafacino, 2009.

Upon reaching the Golgi, the high mannose chain is either mono- or diphosphorylated by GlcNAc-1-phosphotransferase, resulting in a phosphodiester intermediate (79, 80). The primary phosphorylation event occurs on the first mannose of the α-1,6 branch of the mannose chain, resulting in the name mannose-6-phosphate. The second phosphorylation site can occur on the first mannose of the α-1,3 branch (81, 82). Following these phosphorylation events, an enzyme called the "uncovering enzyme", or UCE, cleaves the GlcNAc revealing the mannose-6 phosphate (Fig 1.1 B) (83). The mannose-6 phosphate residues are recognized and bound by mannose-6-phosphate receptors, CD-MPR and CI-MPR, in the *trans*-Golgi compartment, segregating them from secretory proteins (84). The receptor-cargo complex is transported in clathrin coated vesicles, mediated by the association with AP-1 and GGA (Golgi-localized, γ-ear-containing, Arf-binding family of proteins) adaptors (Fig 1.1.C) (85), from the Golgi to pre-lysosomal compartments such as early and late endosomes. Upon fusion with the pre-lysosomal compartments the mannose 6-phosphate receptors dissociate from their cargo due to the acidic endosomal pH and are recycled to the Golgi complex or plasma membrane (86, 87). Delivery of acid hydrolases is completed when the late endosome fuses or transfers material to the lysosome, as seen in Figure 1.1.D. Lysosomal hydrolases arrive in an inactive "zymogen" form, but are then activated by homo- or heterocleavage by mature enzymes in the lysosome (88). Interestingly, it has been shown that increasing endocytic vesicle pH, through the treatment of modulators such as Bafilomycin A1, ammonium chloride, and chloroquine, results in acid hydrolases entering the secretory pathway (60, 61, 89), demonstrating that the acidic identity of these organelles is crucial for proper delivery of lysosomal components.

Although the mannose 6-phosphate receptor pathway is the most prevalent lysosomal sorting method, several mannose-6 phosphate receptor independent pathways have been

identified. For example, the receptor sortilin has been implicated in the sorting of prosaposin and acid sphingomyelinase (90, 91) and the lysosomal membrane protein LIMP-2 is suggested to mediate sorting of β-glucocerebrosidase (92). In addition, some secreted lysosomal proteins have been shown to be re-internalized through endocytosis, resulting in their delivery to the lysosomes. The final evidence for mannose-6-phosphate receptor independent delivery of lysosomal proteins stems from the observation that in cell systems lacking mannose-6-phosphate receptors, several tissues retain normal levels of properly delivered hydrolases (84).

Unlike hydrolytic enzymes, LMPs do not follow a mannose-6-phosphate receptor sorting pathway. These proteins contain targeting signals in their cytoplasmic tail domains and are sorted either directly from the TGN or through the plasma membrane (87). These signals are often linear tyrosine or di-leucine based motifs, however in the past several years other signals such as ubiquitin have also been shown to direct the delivery of LMPs (93). The sorting of LMPs through the plasma membrane is fairly well understood, while direct sorting through the TGN is not as well established. In indirect delivery, LMPs follow the secretory pathway to the plasma membrane where they are then endocytosed and are delivered through the endocytic pathway to the lysosome. The direct pathway suggests that LMPs follow a similar route as hydrolytic enzymes, without the need of mannose chains/mannose-6-phosphate receptor. However, the dynamics of this pathway are not well defined due to that fact that although LMPs have been shown to interact with the AP-1 and clathrin, which direct the formation and sorting of clathrin coated vesicles to early and late endosomes (94, 95), they are also properly sorted in systems lacking AP-1 and clathrin (96, 97). This suggests that additional sorting components may be able to compensate for the loss of these proteins, resulting in the proper delivery. Interestingly, it was recently shown that LMPs interact with ubiquitinated GGA3, an adaptor

protein which is thought to also interact with mannose-6-phosphate receptors, resulting in lysosomal delivery (98). This suggests that ubiquitin is a common sorting signal for LMPs.

### 1.2.3 Lysosomal storage disorders

Lysosomal storage disorders (LSDs) are a class of about 50 diseases caused by the malfunction, loss, or improper delivery of lysosomal or endocytic components, critical for proper lysosomal function. The majority of these disorders are autosomal recessive genetic diseases that arise from single gene mutations (2, 99-101). These disorders are often classified by the resulting substrate accumulation, although the basis and severity of this accumulation may differ (i.e. Mucopolysaccharidoses, Sphingolipidoses, and Glycoproteinoses). The first link between a disease and the loss of a lysosomal component was in 1963, identifying the loss of α-glucosidase as the cause of Pompe disease (102). Since then the majority of identified LSDs have been linked to defects in hydrolytic enzymes, resulting in the buildup of specific substrates. However several LSDs arise from the loss of LMPs; these disorders are not as easily treatable and do not result in the accumulation of specific substrates.

LSDs are characteristically neurodegenerative disorders (although there are exceptions such as type I Gaucher's disease and Pompe disease) resulting in motor defects, abbreviated life span, impaired vision, and peripheral defects. At a cellular level, LSDs often result in the accumulation of dense cellular inclusions filled with undigested substrates, although the composition of these inclusions differs between diseases (103-105). The buildup of undigested substrates appears to cause similar secondary defects shared between several disorders. These include oxidative stress, improper $Ca^{2+}$ handling, perturbed metabolic function, and impaired autophagy (14, 15, 106-109). The appearance of these secondary defects has become a problem

in studying the molecular mechanisms driving LSDs as they convolute the model system. For example, most LSD studies are performed in patient cells, which have already built up cellular inclusions and developed these secondary defects (110-114). Understanding these downstream effects is important for treatment, however these chronic models make it difficult to study the primary effects of dysfunction, especially in diseases that are not enzymatically based.

Deficiencies in lysosomal components often arise from genetic mutations resulting in improper delivery to the endocytic pathway, improper folding, or inactivation of lysosomal proteins. These defects can be directly related to the lysosomal components or affect components required for proper delivery or function of the enzyme. For example, mucolipidosis II & III result from mutations in the gene *GNPTA*, which results in the loss of UDP-*N*-acetylglucosamine-1-phosphotransferase (or GlcNAc-1-phosphotransferase) (115). As discussed in section 1.2.2., this enzyme is required for the production of the mannose-6-phosphate tag in the Golgi. Therefore, mannose-6-phosphate dependent trafficking is ablated, resulting in higher levels of secreted hydrolases and reduced lysosomal levels (116). Additional, non-lysosomal mutations such as the loss of $C_{\alpha}$-formylglycine generating enzyme (FGE), which is required to convert cysteine residues in sulfatases (as mentioned in section 1.2.2.) and the loss of sphingolipid activator proteins (called saponins), result in the disorders Multiple Sulfatase Deficiency and GM2 gangliosidosis respectively (99, 117, 118).

In addition to LSDs caused by the improper processing or trafficking of lysosomal enzymes, there are several disorders characterized by the loss of LMPs. Such is the case in Mucolipidosis Type IV (MLIV), which will be discussed more broadly in section 1.3. Other disorders classified by loss of LMPs include variants of neuronal ceroid lipofuscinosis (NCLs) caused by the loss of several uncharacterized transmembrane proteins: CLN3, CLN6, CLN7, and

CLN8 (119-122). The discovery of such disorders reveals that there are disorders that affect proteins which are responsible for regulating and maintaining the lysosomal ionic environment and that there are several classes of LMPs which are uncharacterized, displaying the complexity and thus unknown dynamics of the lysosome. Such discoveries display new opportunities in understanding the workings of the lysosome as well as the treatment of such disorders.

1 in 7000-8000 births is affected by LSDs, even though individual LSDs are far rarer (123-126). The prevalence of LSDs and the fact that they arise from lysosomal malfunction suggests this wide class of disorders may share similar molecular consequences and therefore may need both specific and non-specific treatments to address disease pathology. LSD treatments have progressed dramatically in the past several years including specific treatments such as enzyme replacement therapy, substrate reduction, pharmacological chaperones, and gene therapy. The most effective and broadly used specific treatment in both human and mouse models is enzyme replacement therapy. This approach is limited by the ability of the enzyme to cross the blood brain barrier (127, 128). In the past several years this problem has been addressed by such techniques as fusing the target enzyme to a protein that can cross the barrier, such as apolipoprotein B, and is then endocytosed into the cells (129, 130). Although this treatment does not completely correct disease pathology, it seems the development of such treatments can at least promise alleviation of some disease symptoms. Currently, enzyme replacement therapy is available for Gaucher, Fabry, mucopolysaccharidosis I & IV (MPS-I, MPS-VI), and Pompe disease (126).

Some “non-specific” treatments are being employed to address common pathologies in LSDs, such as inflammation. Such methods include the use of anti-inflammatory drugs and bone marrow transplant which have been shown effective in the treatment of specific disorders. Bone

marrow transplant is only beneficial when the disease is caused by enzyme deficiencies, with the donor macrophages and glia cells partially correcting enzyme levels in nearby neurons. Despite the neurological benefits of this approach, it is less effective in treating the motor and peripheral abnormalities of disease and must be administered before the onset of symptoms in order to be effective (131-133). Both bone marrow transplant and anti-inflammatory drug treatments have been shown effective in helping limit the inflammatory effects of LSDs, in mouse and human disease models (134, 135).

The most promising field in LSD treatment seems to be combining specific treatments (such as gene therapy and substrate reduction) with some non-specific treatments that address secondary/peripheral effects (such as bone marrow transplant or anti-inflammatory drugs) (126). Combined treatments help address multiple aspects of the disease; however, these treatments are targeted to diseases caused by enzyme deficiencies. A major question is how to treat LSDs that are not enzymatically based since enzyme replacement is not an option in these cases. In order to treat such disorders we must first understand the underlying causes of cell death in these diseases. Although we may treat the symptoms of these disorders, it is clear that addressing the cause of neurodegeneration and peripheral deterioration holds the key to treatment. To better understand how the loss or alteration of lysosomal components, such as LMPs, effects cell function we must study the direct effects of losing such components. These effects may hold the key to understanding the function of such proteins in the lysosome and how their loss contributes to disease pathology and cellular death. In the next section, I will discuss how the altered localization of a lysosomal component can indeed directly contribute to cell death.

### 1.2.4 Cathepsin-induced Apoptosis

Cathepsin proteins are major proteolytic enzymes localized to the lysosome. As previously discussed, specific Cathepsin proteins maintain activity in higher pH environments outside the lysosome. Interestingly, several Cathepsins have recently been linked to apoptosis suggesting that leakage of these lysosomal hydrolases may cleave pro-apoptotic factors driving cell death (58, 136-140). The role of Cathepsin B in apoptosis is investigated in this study therefore a brief background describing the role of Cathepsins in cell death is discussed below. This background section will focus mainly on Cathepsin B, although there are some similarities shared between this protease and other lysosomal proteases.

The Cathepsin family of papain-like proteins can be broken up into exopeptidases and endopeptidases and is further classified by the amino acids which coordinate their catalytically active sites. Cathepsin B is a cysteine protease which exhibits both endopeptidase and exopeptidase activity. It is unique among lysosomal cathepsins in this regard where cysteine Cathepsins D, H, L, and S and the aspartic Cathepsin D are strictly endopeptidases (141, 142).

Cathepsins are synthesized and trafficked as described in section 1.2.2. Upon entering the endocytic pathway, these proteases are in an inactive proenzyme form, called a zymogen, which contains a proregion blocking the catalytic domain. This domain must be cleaved in order to activate the enzyme. Cathepsin B contains an ~62 amino acid propeptide (143) which is cleaved by mature forms of Cathepsin B (144). Upon cleavage, the mature monomer (~20-30kD) is composed of two domains responsible for forming the catalytic pocket of the enzyme.

Similar to other Cathepsin proteases, mature Cathepsin B is defined by a left domain consisting of 3 α-helixes, and a right β-barrel domain. However, Cathepin B is unique in that it contains an insertion, called the occluding loop, which is thought to confer exopeptidase activity

to the enzyme, coordinated by an ion pair formed from a histidine and aspartate interaction (145, 146). The endopeptidase catalytic cleft of Cathepsin B is located between the left and right domains, coordinated by a cysteine residue in the left domain and a histidine and asparagine in the right domain (147, 148). This triad is conserved between cathepsins demonstrating its importance to proteolytic activity (149). The thiol group of the cysteine and the imidazolium ring of the histidine form an ion pair at acidic pH ranges. In the presence of a substrate, a neutrophile attack of the carbonyl carbon by the ionized thiol results in the formation of a covalent intermediate between the protease and its substrate, followed by proteolytic cleavage of the substrate. Cathepsin B's endopeptidase activity favors cleavage of amino acids upstream of bulky hydrophobic sidechains as well as arginine residues while the exopeptidase activity cleaves two C-terminal amino acids demonstrating preference for large aromatic side chains (150-152).

Cathepsin localization and the suitable pH conditions of the lysosome suggested that these proteases only operated in this organelle. However, in the past several years, it has been shown that release of specific cathepsins from the lysosome into the cytosol can promote apoptosis. It has been demonstrated that Cathepsin D plays a role in apoptosis under several conditions; however both Cathepsin B and Cathepsin L were also recently shown to play a role in apoptosis (57-59, 136, 137, 153-155). Cathepsin-mediated apoptosis in some cases appears to be caspase-independent (156, 157), however the majority of Cathepsin-mediated apoptosis is mediated by several pro-apoptotic cellular components including Bid, Bax, and caspases, such as caspase-8 and 3. The release of Cathepsins into the cytosol promotes cleavage of these substrates (i.e. Bid and caspases) resulting in mitochondrial fragmentation and subsequent apoptosis (58, 59, 138, 158, 159). However Bax and caspase-8 have both been shown to mediate

the release of Cathepsins from lysosomes. Therefore where Cathepsins lie in the apoptotic pathway is still unclear and may vary depending on the cell type and the apoptotic stimulus (59, 136). The diversity of these pathways shows that this process is complex, thus teasing apart these cellular systems could provide insight into how cells respond to their environment.

## 1.3 TRPML1

TRPML1 (or mucolipin-1) is the first member of the TRP family of ion channels that was found to function in deeper portions of the endocytic pathway. Mutations in the gene coding for TRPML1 (*MCOLN1*) cause the lysosomal storage disease mucolipidosis type IV (MLIV). TRPML1 localization in the lysosomes and the similarity of the MLIV phenotype to LSDs whose origin has been directly linked to lysosomal dysfunction, suggest that TRPML1 activity drives some vitally important processes within the endocytic machinery. The specific aspect(s) of TRPML1 activity that make it indispensable for proper endocytic function are currently unclear. Possible functions of TRPML1 are membrane fusion within the lower portion of the endocytic pathway possibly mediated by $Ca^{2+}$ release through TRPML1 itself or regulation of lysosomal ion homeostasis (pH or Fe content) (160-162). In addition to delineating the mechanisms of MLIV pathogenesis, identifying the role of TRPML1 in the endocytic pathway will lead to important developments in our understanding of this system and, due to the neurodegenerative nature of MLIV, how loss of this channel affects specific cell types. The

following section will focus on developments in identifying the TRPML1 function as well as established TRPML1 characterization.

### 1.3.1 TRPML1 characterization

TRPML1 was cloned by three labs in 2000 as a result of the search for the genetic determinants of MLIV (2, 11, 163). The gene *MCOLN1* (NG_015806, NM_020533) coding for TRPML1 is located on human chromosome 19 (19p13.2–13.3) spanning base pair positions 7,587,511–7,598,863. *MCOLN1* is fairly conserved within *Vertebrata*; no splice variants have been reported in the human gene, although variants have been reported in mice (164). In Drosophila, the entire TRPML family is represented by a single trpml gene (Dmel_CG8743, NM_140888, chromosome 3L, location: 76C2–76C2, base pairs 19,706,960–19,711,450). In *C. elegans*, TRPML is represented by the cup-5 gene (R13A5.1, NM_001027550, NM_001027548, NM_066263, NM_001027551, chromosome III, location: 378–564, base pairs: 7584129–7591495).

TRPML1 is a member of the TRPML (mucolipin) subfamily of the TRP family of ion channels. All TRPML channels function in the endocytic pathway, which sets them apart from other TRP channels. Like all TRP channels, TRPML1 is presumed to have 6 transmembrane domains; its putative pore lies between the 5th and 6th domains. The structure-functional determinants of TRPML1 function have not been explored in detail; it does not seem to possess the full TRP box signature domain or ankyrin repeats present in some other TRP channels, which may mediate the function and anchoring of TRP channels respectively. Both C- and N-termini of TRPML1 contain putative lysosomal localization signatures, although only the N-terminal di-

leucine motif has been verified (6). The significance of a large loop connecting the 1st and 2nd domains (1) and PKA-dependent phosphorylation sites (165) have not been explored in detail although some data suggest proteolytic cleavage of the loop and phosphorylation of the PKA-dependent domains as modulatory inputs.

### 1.3.2 Proposed Models of TRPML1 Function

There are two models of proposed TRPML1 function: a trafficking model and a metabolic model. The trafficking model suggests TRPML1 regulates delivery and fusion/fission of vesicles along the endocytic pathway while the metabolic model suggests that TRPML1 regulates the ionic environment of the lysosome driving proper enzymatic function. The trafficking model is supported by the initial set of conclusions regarding TRPML1 function, inferred from the conductance characteristics of the currents that were associated with TRPML1 expression and measurement of membrane traffic and lysosomal enzymatic activity in fibroblasts obtained from MLIV patients (primarily the WG0909 clone). A combination of the initial reports on $Ca^{2+}$ permeability through recombinant TRPML1 expressed in HEK293 cells (3, 160) or reconstituted into lipid bilayers (10, 166) and the delays in the lipid traffic reported in MLIV fibroblasts (167, 168) and in the *C elegans* MLIV model (169, 170) gave rise to the idea that TRPML1 is a lysosomal $Ca^{2+}$ release channel. According to this trafficking model, $Ca^{2+}$ release through TRPML1 drives the $Ca^{2+}$ dependent step of SNARE-mediated lysosomal-endosomal fusion. Without the TRPML1-mediated $Ca^{2+}$ release, substrate delivery is impaired, limiting the exposure of endocytosed material to active digestive enzymes, resulting in the buildup of undigested material within the endocytic pathway. A direct consequence of this model would be a general deficit in the membrane traffic within the endocytic pathway. Although such deficits

have been shown in MLIV fibroblasts and in the *C elegans* model (167-170), it is unclear whether they are a direct consequence of TRPML1 loss or a secondary effect of undigested material buildup.

The second model is built on the fact that membrane traffic delays similar to those reported in MLIV were also demonstrated in cells affected by LSDs of clearly "metabolic" origin (e.g. sphingolipid storage diseases) (171). This model suggests that TRPML1 regulates some aspects of lysosomal ion homeostasis and that dysregulation of this homeostasis in the absence of TRPML1 leads to chronic or acute loss of the lysosomal digestive function. This scenario is similar to the loss of lysosomal digestive function upon downregulation of the lysosomal $Cl^-$ channel ClC-7 (70). Both models present several unresolved questions concerning the causal relationships between TRPML1 loss and the resulting phenotypes that were used to formulate the models. Specifically, the core features of the trafficking model do not distinguish if the delays in lipid traffic are a direct result of TRPML1 loss or whether they are caused by the buildup of undigested material "clogging" the membrane traffic machinery. The metabolic model does not answer whether the ionic dysregulation observed in TRPML1 deficient cells is a direct effect of TRPML1 loss or whether it reflects a cellular response to TRPML1 loss, perhaps at a transcriptional level. In order to further delve into these models and study TRPML1 function, a new set of techniques has been recently established. The following section will discuss these approaches and their implications in understanding TRPML1 function and its link to disease. Table 1.1 summarizes the results used to formulate both models of TRPML1 function.

**Table 1.1 Models of TRPML1 loss and the resulting phenotypes**

| | |
|---|---|
| MLIV patients | Progressive neurodegeneration with early onset, mental retardation, corneal opacity, retinal degeneration, vacuolization of parietal cells, constitutive achlorhydria, elevated gastrin levels (172-182) |
| Mouse TRPML1 knockout | Neurological defects including gait deficits and hind-limb paralysis; elevated plasma gastrin, vacuolization in parietal cells, and retinal degeneration (13) |
| *Drosophila trpml* mutants | Neurodegeneration with accumulation of apoptotic cells in the brain, impaired synaptic transmission, impaired autophagy and mitochondrial function; lysosomal overacidification (15) |
| *C. Elegans* CUP-5 mutants | Impaired endocytosis and lysosomal biogenesis (4, 169, 183) |
| Human MLIV fibroblasts | Impaired membrane traffic (167, 168) and exocytosis (184) |
| Human MLIV fibroblasts & *Drosophila trpml mutants* | Impaired autophagy (14, 15, 165, 185) and mitochondrial function (14, 15) |
| MLIV fibroblasts, HeLa acute KD, *Drosophila trpml mutants* | Lysosomal overacidification (15, 162, 186) |
| HeLa acute KD, *Drosophila trpml mutants* | Normal membrane fusion in the endocytic pathway (15, 162) |
| Recombinant TRPML1 expression | Permeable to $Ca^{2+}$ (3, 8, 10, 160, 166, 187), $H^+$ (186), and $Fe^{2+}$ (188). Potentiated by $H^+$ (8) and inhibited by $H^+$ (166, 189) |

### 1.3.3 New techniques of studying TRPML1 function

The following techniques are being used to study TRPML1 function in a system which lacks secondary defects caused by substrate accumulation, so that we may better understand the role of this channel in the endocytic pathway. The first approach aims to identify the immediate consequences of TRPML1 loss on membrane traffic in the endocytic pathway. Two groups

downregulated TRPML1 expression using RNAi; the first studied the effects of acute TRPML1 knockdown using siRNA (162) while the second used a constitutively active shRNA expression system resulting in longer knockdown periods (190). Both studies documented delayed translocation of fluorescent lipids from lysosomes to the Golgi indicating that TRPML1 either modulates lipid modifications preceding lipid translocation from lysosomes to Golgi or it regulates membrane traffic events in this step. Analysis of pre-lysosomal trafficking defects in these studies produced varied results. Using stable line shRNA knockdown of TRPML1, a delay in lysosomal delivery of lipids from the lysosome to the Golgi was shown in TRPML1-deficient murine macrophages (190), while no delay was observed in acute 48 hour TRPML1 knockdown in HeLa cells (162). Further studies will elucidate whether the loss of TRPML1 results in trafficking defects along later portions of the endocytic pathway. It is interesting to note that delayed lipid delivery was seen in the stable TRPML1 knockdown line similar to delays seen in MLIV fibroblast cells (167, 168) suggesting that chronic loss of this channel could lead to secondary effects that result in trafficking delays. A detailed investigation of lipid hydrolysis and modification caused by acute TRPML1 loss will be necessary to clarify its role in lipid handling within the endocytic pathway. The acute model of TRPML1 knockdown provides an exciting new tool for studying the direct cellular responses to TRPML1 loss.

The next novel approach to studying TRPML1 function has been through structure-function analysis based on structural comparison with its relative TRPML3 and other voltage-gated ion channels. These studies have revealed a region resembling the linker sequence in the voltage-gated channels that translates the movement of the voltage-sensing domain to the opening and closing of the pore. Mutating this region in TRPML1 resulted in spontaneously active currents that, similar to previously published data, carried $Ca^{2+}$ (3, 8, 10, 160, 166, 187),

but contrary to some of the previously published data, was activated by low pH (8, 166, 189). Single channel recordings of TRPML1 activity confirmed its regulation by pH (191). These data provide support for the role of TRPML1 in $Ca^{2+}$ dependent maturation and fusion of endocytic compartments. However, one major caveat of the previously described studies was the inability to measure TRPML1 activity in the lysosomal environment. An exciting new technique was recently developed to enlarge lysosomes, making them accessible to patch clamp analysis. These studies demonstrated $Fe^{2+}$ permeability through TRPML1 (188). It is an interesting possibility indeed that TRPML1 is a $Fe^{2+}$ shunt that allows efflux from lysosomes that mitigates the effects of $Fe^{2+}$ buildup, which otherwise leads to, among other things, accumulation of lipofuscin (buildup of undigested lipid material) in the lysosomes. A detailed chemical and structural analysis of storage bodies in TRPML1 deficient cells and comparison of their content with classic $Fe^{2+}$ overload and lipofuscin buildup models will help test this interesting model.

The final line of research aimed at clarifying the role of TRPML1 in the endocytic pathway is focused on identifying the molecular context of TRPML1 activity, analyzing its activity and protein interactions in the lysosomal environment. As the first step towards this goal, the protein ALG-2 (EF-hand-containing protein apoptosis-linked gene 2 protein) suggested to be a sensor for mediating $Ca^{2+}$ dependent vesicle fusion (192), was found to bind to TRPML1 in a $Ca^{2+}$ dependent manner (55). That ALG-2 is a putative $Ca^{2+}$ binding protein suggests that $Ca^{2+}$ regulates TRPML1, or that the effects of $Ca^{2+}$ currents through TRPML1 are actuated by ALG-2. Further analysis of the functional consequences of TRPML1 interaction with ALG-2 and with other proteins will delineate how the environment of the lysosome modulates TRPML1 activity.

### 1.3.4 MLIV

MLIV is caused by mutations in the gene *MCOLN1,* coding for TRPML1. Onset of MLIV begins within a year of birth and has a severe neurodegenerative profile, presumably due to the loss of brain tissue. Other pathological manifestations of MLIV include corneal opacity, retinal degeneration and constitutive achlorhydria, and a decrease in gastric acid secretion (172-182). MLIV cellular pathology is characterized by the buildup of storage bodies and vacuoles throughout patient tissues (215). This disease is most prevalent in the Ashkenazi Jewish population with a reported carrier frequency of 1:100 (216), with the majority of mutations obliterating TRPML1; some mutations result in improper localization or channel function (1, 166, 217, 218). The mechanism of cell death in MLIV is poorly understood, despite the obvious benefits promised by delineating such pathways. Some recent data suggest autophagic dysfunction and buildup of dysfunctional mitochondria as a possible pathway of cell death in LSDs, specifically in MLIV (5, 14). Similar conclusions were obtained using the *Drosophila* model of MLIV obtained by knockout of the single TRPML coding gene in *Drosophila* (15). Understanding the underlying cause of TRPML1 loss as well as the downstream effects that may result in cell deterioration are critical for treatment of this disorder.

Like all LSDs, MLIV is marked by the buildup of undigested substrates in cellular inclusions. These inclusions have been shown to contain sphingolipids, mucopolysaccharides, and phospholipids, suggesting that loss of TRPML1 inevitably results in the dysfunction of several lysosomal hydrolases (167, 174). Differences between inclusion materials has been shown between cell types, possibly caused by cell-specific reactions to TRPML1 loss (219), controlled at the proteomic or transcriptional levels (220). One physiological example of such a reaction may be in the pronounced buildup of vacuoles in parietal cells, the stomach epithelial

cells that produce gastric acid, which underlie constitutive achlorhydria, low production of gastric acid, documented in MLIV patients (181). Parietal involvement and achlorhydria may directly point to TRPML1 function, or may result from a response of specific subsets of cells to the problems in the endocytic pathway caused by the TRPML1 loss. Delineating cell-specific responses to TRPML1 loss may reveal both the function of this channel as well as how cells differentially respond to endocytic insults.

Multiple roles of TRPML1 have been proposed, as discussed in section 1.3. Disparities between studies in patient fibroblast cells suggests that the key to delineating TRPML1 function and the cause of MLIV pathogenesis may lie in identifying cellular responses to acute TRPML1 loss. Furthermore, understanding the regulation of TRPML1 channel activity and its role in ion transport may reveal the endocytic role of this protein. The following work uses multiple approaches to answer the following questions: i) What is the cellular response to acute TRPML1 loss at the proteomic/lysosomal level, ii) Does TRPML1 loss induce specific transcriptional changes, and iii) Can we clarify the role of TRPML1 in ion transport using spontaneously active mutants and TRPML3 as a comparative model? By answering these questions, I hope to provide a better understanding of TRPML1 cellular function, separate primary effects of TRPML1 loss from secondary defects, and link cellular responses to TRPML1 loss to cell death.

### 1.3.5 Transition metal toxicity and TRPML1

Transition metals are well-known environmental hazards that cause systemic degenerative processes (193, 194). Excessive exposure to metals can occur from occupational

hazards, accidents, high dietary uptake, and genetic disorders which inhibit metal metabolism (193). $Fe^{2+}$ has been shown to overload the heart and liver, causing heart failure and even death (194). $Cu^{2+}$ toxicity also leads to liver and brain damage resulting in coma, hepatic necrosis, vascular collapse, and death (193). The accumulation of $Cu^{2+}$ in the genetic disorder Wilson's disease results in neuronal and cardiac defects such as cerebellar dysfunction, congestive heart failure, and cardiac arrhythmia (195). The wide spectrum of clinical representation of transition metal toxicity suggests that cell handling of these metals is crucial for maintaining proper function.

In tissues that absorb transition metals such as the brush border epithelial cells of the intestine or lung, liver and kidney, these metals enter the cytoplasm directly via plasma membrane transporters such as Slc31a1 (also called Ctr1) (196, 197) and Slc11a2 (also called DMT1, NRAMP2) (65, 66). Metals are removed from cells by metal-chaperones or through excretion pumps such as ATP7a or Slc40a1 (Fpn, MTP1) (197) (66). The effects of transition metals in the cytoplasm is the most widely studied model of metal toxicity and such studies provided the rationale for the use of metal chelators to combat acute transition metal toxicity.

In non-absorbing tissues, cells do not require a high metal intake, therefore they lack high levels of plasma membrane transporters and metals enter through the endocytosis of free metals and metal-bound proteins (65, 66, 197). In addition to $Fe^{2+}$ and $Cu^{2+}$ other transition metals such as $Fe^{3+}$, $Zn^{2+}$ and $Co^{2+}$ can enter the cell through this pathway. These metals travel through the endocytic pathway until they are excreted into the cytoplasm by transporters, such as Slc11a2 (DMT1), expressed at low levels in lysosomes (198). Under normal conditions, the majority of transition metals are bound to plasma proteins such as albumin, transferrin and ceruloplasmin (65, 66, 197). Degradation of these proteins in the endocytic pathway releases the metals into the

lysosomal lumen. The active chemical environment of the lysosomal lumen promotes Fenton-like chemical reactions (a reaction between a catalyst such as iron and hydrogen peroxide producing a hydroxide radical) resulting in generation of free radicals, which are damaging to the lysosomal membrane and result in the production of the inert chemical compound called lipofuscin (199, 200).

The acute exposure to high concentrations of transition metals has been linked to lysosomal storage phenotypes (194, 201, 202) and to lysosomal permeabilization (203, 204). Long-term exposure to transition metals, e.g. in postmitotic cells, has been linked to buildup of lipofuscin, which inhibits lysosomal function and autophagy (205, 206). Autophagy deficits have been shown in several models of LSDs (13-15, 112, 165, 207-210) and in transition metal overload (211, 212). According to the lysosomal-mitochondria axis models of aging and cell death in LSDs, the suppression of autophagy results in buildup of dysfunctional organelles, specifically mitochondria (205, 206). Our lab has previously suggested that the loss of mitochondrial $Ca^{2+}$ buffering capacity and of the $Ca^{2+}$-driven ATP production positive feedback loop makes cells vulnerable to the pro-apoptotic effects of stimulation with $Ca^{2+}$ mobilizing agonists (neurotransmitters, hormones, growth factors) as seen in Figure 1.2 (14, 209).

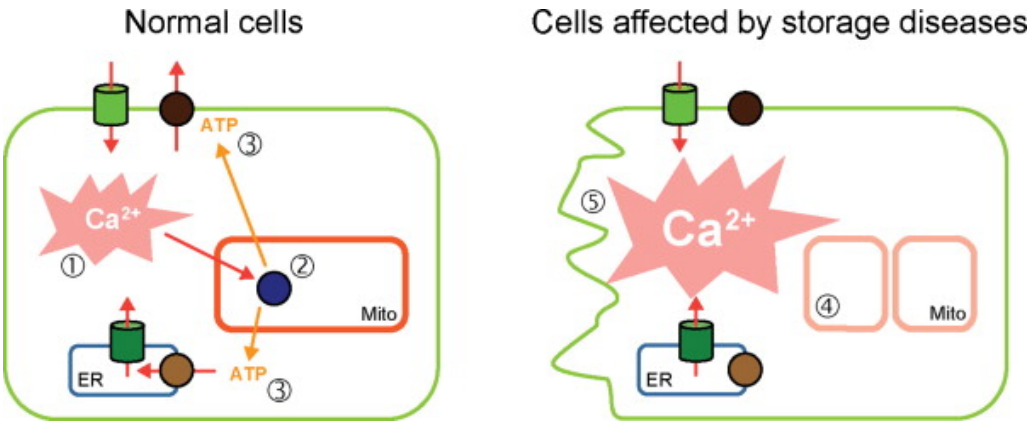


**Figure 1.2. Mitochondrial fragmentation in storage diseases due to defects in autophagy may promote proapoptotic pathways.**
In normal cells (left), mitochondria act as a buffering system for $Ca^{2+}$. The buildup of effete mitochondria (right) in storage diseases, due to impaired autophagy, may result in an increase in cytoplasmic $Ca^{2+}$. These increases may drive proapoptotic pathways, resulting in increased cellular death in LSDs. Model from Kiselyov et al., 2011 (213).

The detrimental effects of transition metals in the lysosomes, combined with the cellular requirements for transition metals necessitate extraction of the metals from the lysosomal lumen into the cytoplasm, where their effects can be mitigated by chelating proteins or by extrusion out of the cell (66, 197). Existence of such mechanisms has been shown before. Specifically, Slc11a1 (NRAMP1) and Slc11a2 (NRAMP2, DMT1) are ion transporters responsible for divalent cation uptake by cells (65, 66). The intracellular localization of Slc11a2 and its apparent role in export of divalent cations from the lumen of lysosomes led to the suggestion that this channel is, or is part of, the endocytic divalent cation absorption pathway. Recently published data suggests that Slc11a2 is not the only mechanism for transition metal absorption in the endocytic pathway and may implicate TRPML1 as a possible transition metal channel (188, 214).

TRPML1 has recently been proposed to function as a release channel for $Fe^{2+}$ and $Zn^{2+}$, exporting these transition metals from the lysosomal lumen into the cytoplasm to prevent Fenton reactions and the buildup of lipofuscin catalyzed by $Fe^{2+}$. Evidence in support of this function

was shown in MLIV patient fibroblasts which contain higher lysosomal levels of $Fe^{2+}$ than matched controls, further suggesting that TRPML1 may function as an $Fe^{2+}$ release channel (188). Furthermore, $Zn^{2+}$ accumulation was also demonstrated in MLIV fibroblasts and using a combination of electrophysiology and chemical analysis, $Zn^{2+}$ permeability through TRPML1 was observed (214). The limitations of recording physiological recordings from TRPML1 have hindered the complete understanding and dynamics of TRPML1 as a transition metal release channel, however future studies may elucidate its role. These studies provide an interesting possibility for existence of a novel metal export pathway from the lysosomes and suggest that transition metals may play a critical role in disease phenotype in MLIV and perhaps other LSDs.

## 1.4 GOALS OF THIS DISSERTATION

In the following chapters I will study TRPML function using models of acute endocytic disruption. In the first two chapters I will use acute siRNA-mediated knockdown of TRPML1 and measure the cellular effects of TRPML1 loss. I hope to identify direct cellular responses triggered by the loss of this protein, specifically in the context of cell death and differential gene expression. In the last chapter, I will study the closely related ion channel TRPML3 and its interaction with transition metals. Furthermore, I will test whether transition metals inhibit the endocytic pathway and if their interaction with TRPML3 mediates this dysfunction.

# 2.0 CATHEPSIN B MEDIATED APOPTOSIS IN TRPML1 DEFICIENT CELLS

## 2.1 ABSTRACT

Mucolipidosis type IV (MLIV) is a lysosomal storage disease caused by mutations in the gene *MCOLN1*, which codes for the transient receptor potential family ion channel TRPML1. MLIV has an early onset and is characterized by developmental delays, motor and cognitive deficiencies, gastric abnormalities, retinal degeneration and corneal cloudiness. The degenerative aspects of MLIV have been attributed to cell death, whose mechanisms remain to be delineated in MLIV and in most other storage diseases. Here we report that acute siRNA mediated loss of TRPML1 results in an upregulation and cytosolic leak of the lysosomal protease Cathepsin B (CatB). TRPML1 KD induces apoptosis, marked by increased Caspase-3 activity and cytochrome C release. Inhibition of either CatB or the proapoptotic protein Bax prevents TRPML1 KD mediated apoptosis. Bax inhibition did not affect CatB release, suggesting that Bax lies downstream of CatB release. This is the first evidence providing a mechanistic link between acute TRPML1 loss and cell death.

## 2.2 INTRODUCTION

TRPML1 is a member of the TRP family of ion channels. Unlike most TRP channels, TRPML1 and its relatives TRPML2 and TRPML3 primarily reside in the membranes of the endocytic pathway (1-6). TRPML1 localizes to the deeper compartments along the endocytic pathway (late endosomes and lysosomes), due to the presence of lysosomal targeting sequences on its N- and C-termini (5, 6). TRPML1 is an inwardly rectifying cation channel that is activated by low, typically lysosomal, levels of pH (7, 8). TRPML1 activation by $PI(3,5)P_2$ (9), a lipid predominantly found in late endosomes and lysosomes, provides a physiological context for its localization suggesting that it is either activated by delivery to the lysosomes or that it serves as a sensor for $PI(3,5)P_2$ rich compartments matching lysosomes and late endosomes for fusion. TRPML1 has been suggested to regulate fusion/fission of vesicles in the endocytic pathway (4, 160, 168, 184), and/or some aspect of lysosomal ion homeostasis such as pH, $Fe^{2+}$, or $Zn^{2+}$ content (9, 162, 186, 214).

TRPML1 downregulation due to mutations in the gene *MCOLN1* results in the rare lysosomal storage disease MLIV (2, 11). The disease is associated with the buildup of storage bodies of largely unknown origin. MLIV has a profound neurodegenerative profile, which, in mouse models, has been linked to retinal degeneration and demyelination of corpus callosum, deep layer neocortex, and cerebellar white matter tracts (12, 13). Gastric abnormalities including degeneration of parietal cells and hypochlorhydria have also been reported in MLIV patients and model mice (180-182, 221). As with most lysosomal storage diseases, the mechanisms of cell death in MLIV are unclear. We have previously suggested that lysosomal deficiencies in MLIV and, perhaps, other storage diseases, lead to autophagic deficits and buildup of effete mitochondria, which may expose cells to pro-apoptotic effects of cell stimulation with $Ca^{2+}$

modilizing agonists (14). Autophagy deficits have been confirmed in MLIV and several other lysosomal storage models (210, 222-227). Nonetheless, the selectivity of cellular loss in storage diseases remains puzzling. We believe that the key to identifying the cell death pathways in lysosomal storage diseases lies in deconstructing the early events accompanying the loss of TRPML1 or other components of the endocytic pathway. This task is difficult to accomplish in cells cultured from patients due to the possible and, indeed, likely, contribution of secondary effects due to chronic accumulation of storage material.

To delineate the early events associated with the loss of TRPML1, we used siRNA mediated KD to acutely downregulate TRPML1 in HeLa cells. A KD of PPT1, an enzyme mutated in another lysosomal storage disease, Infantile Neuronal Lipofuscinosis, was used as a comparative control (16, 17). We show that TRPML1 loss specifically causes, within 48 hours of KD, an upregulation and cytoplasmic release of the lysosomal protease CatB, followed by activation of pro-apoptotic caspase-3. Apoptosis in TRPML1 KD cells involved CatB as well as proapoptotic protein Bax. These results illustrate, for the first time, the early events leading to cell death in TRPML1 deficient cells.

## 2.3 EXPERIMENTAL PROCEDURES

*Cell Culture:* HeLa cells were maintained in DMEM (Sigma-Aldrich, St Louis, MO) supplemented with 7% FBS, 100 µg/mL penicillin/streptomycin, and 5 µg/mL Plasmocin prophylactic (Invivogen, San Diego, CA). For siRNA KD, antibiotic free media was used. Antibiotic free media supplemented with 100mM sucrose was used for sucrose treatments.

*siRNA-mediated KD*: siRNA were designed as described previously (162) and custom synthesized as ON-TARGET plus constructs by Dharmacon (Lafayette, CO). The TRPML1 siRNA probe targeting the sequence 5'-CCCACATCCAGGAGTGTAA-3' in *MCOLN1* was used for all TRPML1 KD. The PPT1 siRNA probe targeting the sequence 5'-GGTACTCACATAAATGCTT-3' in *PPT1* was used for all PPT1 KDs. Control siRNA #1 (Sigma) was used as a negative control. 6-well plates were transfected using Lipofectamine 2000 (Invitrogen Carlsbag, CA). 7-day long KDs were maintained by splitting cells every 3 days and retransfecting them in suspension. Transfections were performed as described by manufacturer's protocol using 300 nM siRNA per well. All KDs were confirmed using SYBR-green based quantitative real-time RT-PCR and Western blot analysis.

*Reverse Transcriptase and Quantitative qPCR*: RNA was isolated from cell using Trizol (Invitrogen) according to the manufacturer's protocol. cDNA was synthesized using the GeneAmp RNA PCR system (Applied Biosystems, Carlsbad, CA) with 2 μL oligo dT priming. qPCR was performed using 2 μL cDNA, 2X SYBR green (Fermentas, Glen Burnie, MD), and 5 μL of 4 μM primer per 50 μL reaction. The amount of cDNA loaded was normalized to starting RNA concentrations, with a final concentration of 6 ng of RNA loaded per experimental well. Six-point standard curves were generated for each primer using 1:2 dilutions of cDNA and loading 2 μL per well. Dilutions started at 20 ng of starting RNA. The following Quantitect primer assays were used: *ACTB* (β-actin, QT00095431), and *CTSB* (CatB, QT00088641). cDNA for the following genes were amplified using the indicated primers (IDT, Coralville, IA);

*MCOLN1*: Forward: 5'-TCTTCCAGCACGGAGACAAC-3'

Reverse: 5'-AACTCGTTCTGCAGCAGGAAGC-3'

*PPT1:* Forward: 5'-CCTGTAGATTCGGAGTGG TTTGGATT -3'

Reverse: 5’-CAGGCGGTCCTGTGTGTACA-3’

All primers were designed to span exons and negative RT controls were tested to ensure amplification of cDNA only. qPCR was performed using the Standard Curve method on the 7300 Real Time System (Applied Biosystems). Reactions were run on the following parameters: 2 min at 50°C, 10 min at 95°C, and 40 cycles at 95°C for 15 seconds followed by 60°C for 1 minute. All experimental samples were run in triplicate and normalized to a β-actin endogenous control. Microsoft Excel was used to generate standard curves and analyze qPCR results.

*Western blot analysis*: Cells were solubilized for 10 min at room temperature in a detergent solution (0.5 M EDTA pH 8.0, 1 M Tris pH 8.0, 0.4% deoxycholate, 1% NP-40 substitute) containing protease inhibitor cocktail mix III (Calbiochem, Gibbstown, NJ) and centrifuged at 16,000 g for 5 min. The supernatant was collected and protein concentrations were determined using a Bradford assay. Protein was incubated at 100°C for 5 min in sample buffer containing 14% β-Mercaptoethanol. Equal amounts of protein were loaded on a 12.5% SDS-PAGE precast Tris-HCl polyacrylamide gel (BioRad, Hercules, CA) for each experimental sample. Proteins were transferred to PVDF membrane (Millipore, Billerica MA) and blocked in 10% NFDM for 1 hr. The following primary antibodies were used: monoclonal Cathepsin B (CA10 clone, Calbiochem, IM27L) at 1:250 dilution, polyclonal PPT1 (Sigma, SAB1400222) at 1:250, polyoclonal Lysosomal Acid Lipase (Abcam, Cambridge MA, ab73445) at 1:500 dilution, monoclonal LAMP1 (H4A3 clone, Santa Cruz, Santa Cruz CA) at 1:1,000 dilution, monoclonal Cathepsin D (CTD-19 clone, Sigma), monoclonal HA (HA.C5, Abcam) at 1:500, monoclonal GAPDH (Millipore, Billerica, MA), monoclonal Cytochrome C (7H8.2C12 Clone, Invitrogen) at 1:1000, and monoclonal β-actin (AC-15 clone, Abcam) at 1:5,000 dilution. HRP conjugated goat anti-mouse or anti-rabbit secondary antibodies (Amersham, Piscataway, NJ) were used at

1:20,000 and 1:5,000 dilutions respectively. Immunodetection was performed with the Luminata Forte HRP substrate (Millipore). Band densities were measured using ImageJ (Bethesda, MD). For measurement of TRPML1 KD, cells were transfected with siRNA as described above. After 24 hr, 2 μg of HA-TRPML1 DNA was transfected into cells using Lipofectamine 2000 (Invitrogen) as described by manufacturer's protocol. Cells were then immunoblotted for the HA tag 24 hr later.

*Radioactive synthesis and degradation:* 2 days after siRNA knockdown, cells were starved for 30 min in media lacking cysteine and methionine. Cells were then labeled for 2 h at 37°C with 100μCi/mL of Tran$^{35}$S-label (MP Biomedicals, Solon, OH). Cells were chased with serum free DMEM media containing unlabelled cysteine and methionine. At indicated time points, cells were lysed using 1X detergent solution and labeled proteins were immunoprecipitated overnight at 4°C with the CatB monoclonal antibody (CA10 clone, Calbiochem, IM27L). Antigen-antibody complexes were collected using Pansorbin cells coated with Rabbit anti-mouse antibodies 24 h later. Pansorbin cells were washed 3 times in RIPA buffer, and then resuspended in 20 μL of 4X sample buffer, boiled for 3 min, and pelleted at 16,000 x g for 2 min. Supernatant was run on a 12.5% gel. Dried gels were analyzed using a phosphorimager and analyzed using Quantity One software (BioRad).

*CatB Secretion:* One day after KD, cell media was replaced with 0.5% FBS antibiotic free media. Media was collected 24 h later and concentrated on Millipore 10K Ambion filters. Concentrated protein was subjected to western blot analysis as described above.

*Membrane/Cytosolic Separation:* Cells were prepared as described in the Abcam Subcellular Fractionation protocol. Cells were solubilized using sonication (9 watt, 15 pulses). Nuclear and mitochondrial fractions were removed by 800 and 10,000 x g spins, respectively.

The cytosolic and membrane fractions were separate using a 100,000 x g spin for 1 hour at 4°C. The supernatant (cytosolic fraction) was concentrated using Millipore 10K Ambion filters (Millipore). The membrane pellet was washed 3 times with subcellular fractionation buffer and solubilized in detergent solution. β-actin was used as a loading control for both fractions. GAPDH was used as a loading control for the cytosolic fraction and to measure cytosolic contamination of membrane fractions. LAMP-1 was used to measure membrane contamination of the cytosolic fraction.

*Cathepsin B Activity:* Cathepsin B activity was analyzed using the EMD Innozyme Cathepsin B detection kit (Calbiochem, CBA001) following the manufacturer's protocol. The kit measures Cathepsin B activity using the substrate Z-Arg-Arg AMC (Benzyloxycarbonyl-L-arginyl- L-arginine-4-methylcoumaryl-7-amide), which fluoresces when cleaved. Fluorescence was measured using a fluorometer, at an excitation wavelength of 360 nm and an emission wavelength of 440 nm. Pre-cleaved substrates were used to create AMC standard curves and fluorescence in experimental samples was plotted against these curves to determine concentrations (in μM) of cleaved AMC. All values were normalized to the total protein load.

*Confocal and Electron Microscopy*: Confocal and electron microscopy was performed as previously described (162). Cellular inclusions were classified as vacuoles that showed a multimembranous or a dense profile. Size of inclusions was not a determining factor and the profiles of inclusions included in these counts are displayed in Figure 4.6. The following primary antibodies were used: monoclonal anti-TFEB (Abcam, ab56330), polyclonal anti-Lamin B1 (Sigma, SAB2101352), monoclonal LAMP-1 (H4A3 clone, Santa Cruz), and polyclonal Bax

(N-20, Santa Cruz). For indirect detection, a goat anti-mouse and goat anti-rabbit secondary antibodies from Invitrogen were used.

*Apoptosis assay*: Cells were prepared and measured using the EnzChek Caspase-3 Assay Kit #1 (Invitrogen) following the manufacturer's instructions. AMC substrate fluorescence was measured using a fluorometer at an excitation wavelength of 342 nm and an emission wavelength of 441 nm.

Statistical significance was calculated using a one-tailed, unpaired t-test with $p \leq 0.05$ considered significant. Data are presented as mean±S.E.M.

## 2.4 RESULTS

### 2.4.1 TRPML1 and PPT1 KD

Figs 2.1A,B show that our siRNA-mediated KD protocol resulted in a significant decrease in TRPML1 or PPT1 mRNA levels (a decrease of 78.0%±8.6 and 98.3%±3.7 respectively, $p<0.001$, $n=8$) 48 h after transfection of HeLa cells. Knockdown was verified using Western blot analysis of heterologously expressed recombinant HA-tagged TRPML1 or endogenous PPT1 (Figs 2.1A,B). Commercially available antibodies to TRPML1 do not work or result in extremely dirty blotting profiles, therefore we used HA-tagged TRPML1 to visualize KD. Cellular inclusions have been previously shown to accumulate in the same TRPML1 KD model, further confirming that this model represents the early stages of MLIV (162). Electron micrographs of PPT1 KD cells also show large numbers of cellular inclusions. Therefore siRNA-mediated PPT1 KD is an effective model of lysosomal dysfunction (Fig 2.1C).

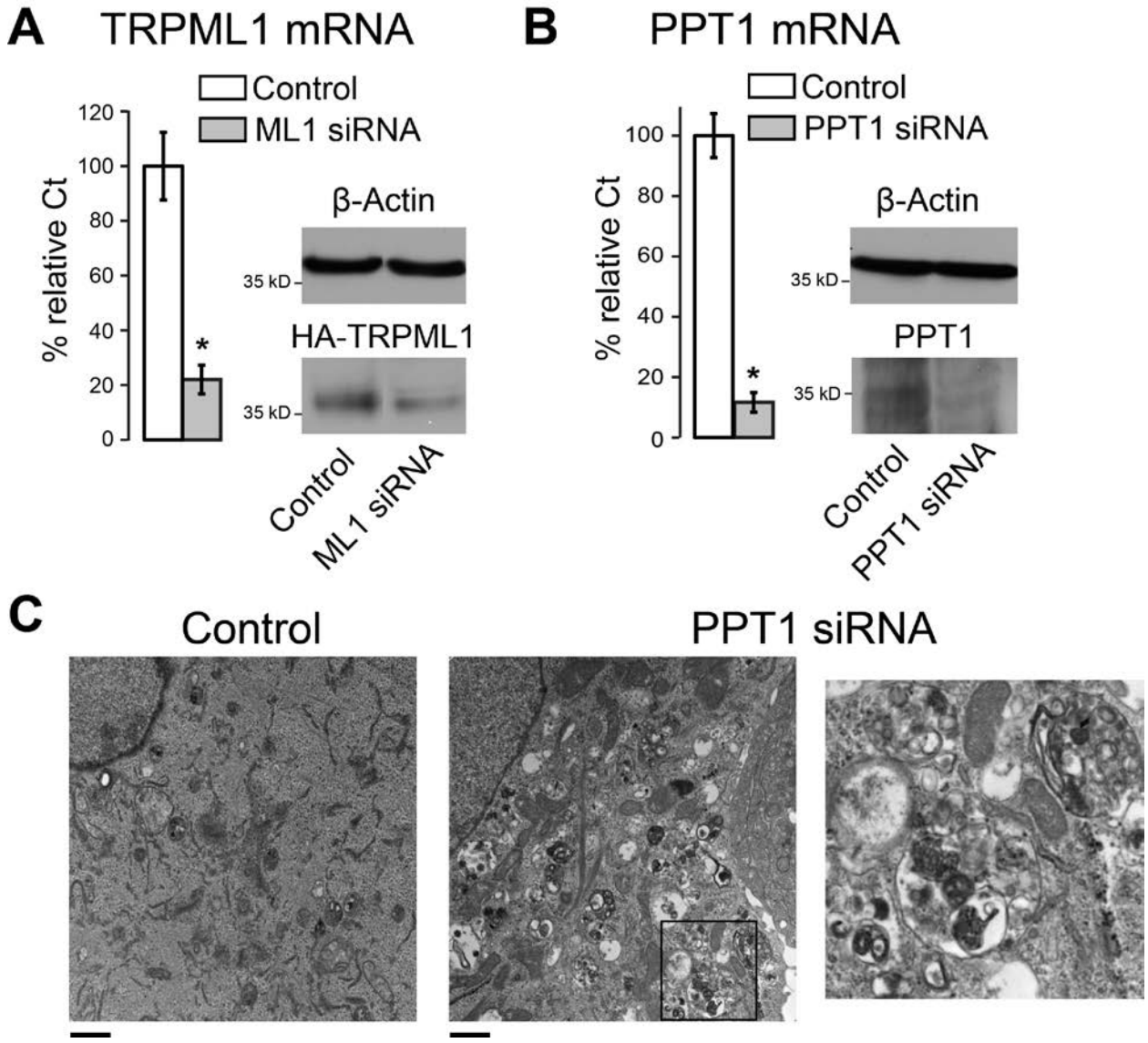


**Figure 2.1 siRNA-mediated downregulation of TRPML1 and PPT1 result in decreased mRNA and protein levels and recapitulate a storage defect phenotype.**

A) HeLa cells were transfected with TRPML1 siRNA 48 hr before collection. Total RNA was isolated and cDNA was synthesized and probed using TRPML1 specific exon-spanning primers. For protein detection, cells were transfected with N-terminally tagged HA-TRPML1 DNA 24 hr after siRNA transfection. Whole cell lysates were collected 24 hr later and subjected to Western blot analysis, probing for HA. The 37 kD band represents the N-terminal HA-tagged cleaved fraction of TRPML1. All protein and mRNA levels were normalized to β-actin. B) PPT1 mRNA and protein levels were measured 48 hr after siRNA transfection as described above. Arrow represents mature form of PPT1. C) Cells were collected and fixed for EM images 48 hr after siRNA transfection. Scale bar represents 1 μm. Right panel represents a zoom-in image of the area on the left panel indicated by the black square. *, $p<0.05$, $n=8$ for both A and B.

### 2.4.2 CatB buildup in TRPML1 KD cells

CatB is a ubiquitous lysosomal protease, which previously has been implicated in cell death upon lysosomal permeabilization. It has been shown that CatB released into the cytoplasm is active and promotes cleavage and activation of caspases involved in apoptosis (136, 137, 155, 228, 229). To determine whether TRPML1 KD had an effect on CatB levels, we performed Western blot analysis on control and TRPML KD HeLa cells using CatB antibodies. Cell lysates were collected 48 h after siRNA transfection. All protein levels were normalized to β-actin loading controls. Figs 2.2A,B show that TRPML1 KD results in a robust increase of pro- and mature CatB levels whereas intermediate CatB (Int. CatB) levels are unaltered. CatB is processed through the ER and Golgi (intracellular CatB intermediates are seen as multiple bands in Western blots) and enters the endocytic pathway as an inactive zymogen (proCatB), which is autocatalytically cleaved by the active enzyme into its mature form (144). ProCatB and mature CatB levels increased by 213.3%±9.2 and 81.0%±16.5 ($p<0.01$, $n=4$ each) respectively in TRPML1 KD cells.

In contrast to CatB, lysosomal acid lipase (LAL) levels decreased in TRPML1 KD cells (Fig. 2.2A,B; 32.5%±13.3 decrease, $p<0.05$, $n=7$), whereas LAMP-1 levels increased (72.4%±11.7 increase, $p<0.01$, $n=3$). The changes in LAMP1 levels are consistent with previous studies showing that lysosomal markers are increased in LSDs (13, 227). Cathepsin D (CatD) levels did not change in TRPML1 KD cells (Fig 2.2A,B) indicating that the effect of TRPML1 KD on CatB is specific.

The physiological significance of CatB upregulation in TRPML1 KD HeLa cells was evaluated using the Innozyne CatB Activity Assay. CatB activity was upregulated by 60.4%±15.6 ($p<0.05$, $n=5$) in TRPML1 KD whole cell lysates (Fig 2.2C), supporting the

upregulation of mature CatB seen in our Western blot results demonstrating that the mature, active form of CatB is upregulated as a consequence of TRPML1 loss.

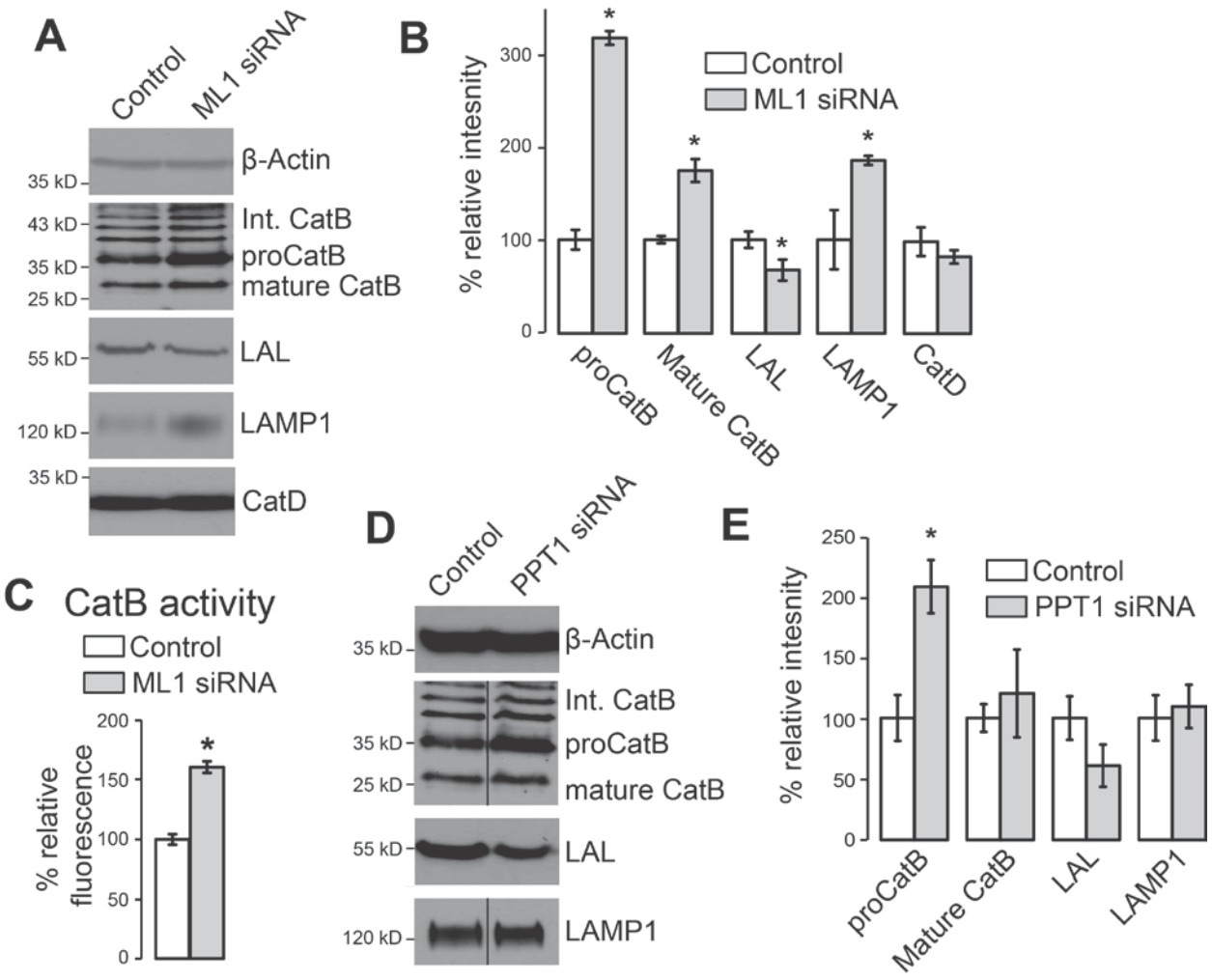


**Figure 2.2 TRPML1 KD and PPT1 KD specifically alter steady state protein levels of CatB, LAL, and LAMP-1.**

A, B) Representative Western blot (A) and blot density analysis (B) of HeLa whole cell lysates 48 hr after siRNA transfection show increased CatB and LAMP-1 levels, and decreased LAL levels in TRPML1 KD cells. CatD levels did not seem to change in TRPML1 KD cells. C) CatB activity was measured using the EMD Innozyme Cathepsin B detection kit. Precleaved AMC substrates were used to create a 6-point standard curve, μM AMC were determined using this curve. Values were normalized to total protein load. *$p<0.05$, $n=5$. D, E) Representative Western blot (D) and blot density analysis (E) of PPT1 KD cells shows an increase in proCatB not mature CatB, LAL, or LAMP-1. Lanes containing control and PPT1 KD samples were not run in continuous lanes, which is denoted by dividing line in CatB and LAMP-1 blots. *$p<0.05$, $n\geq3$.

To test whether TRPML1 KD induced changes of CatB and LAL levels were caused by general endocytic inhibition, HeLa cells were treated for 48 h with the lysosomal inhibitors BAPTA-AM (162), a $Ca^{2+}$ chelator which inhibits fission/fusion events and results in membrane trafficking defect; bafilomycin A1, an inhibitor of the lysosomal $H^{+}$ ATPase pump that blocks the acidification of lysosomes (61); or leupeptin, a serine/cysteine protease inhibitor which prevents degradation of protein substrates in the lysosome (230, 231). These inhibitors did not alter LAL levels and did not result in CatB increase (Figure 2.3), suggesting that these changes are TRPML1 KD specific.

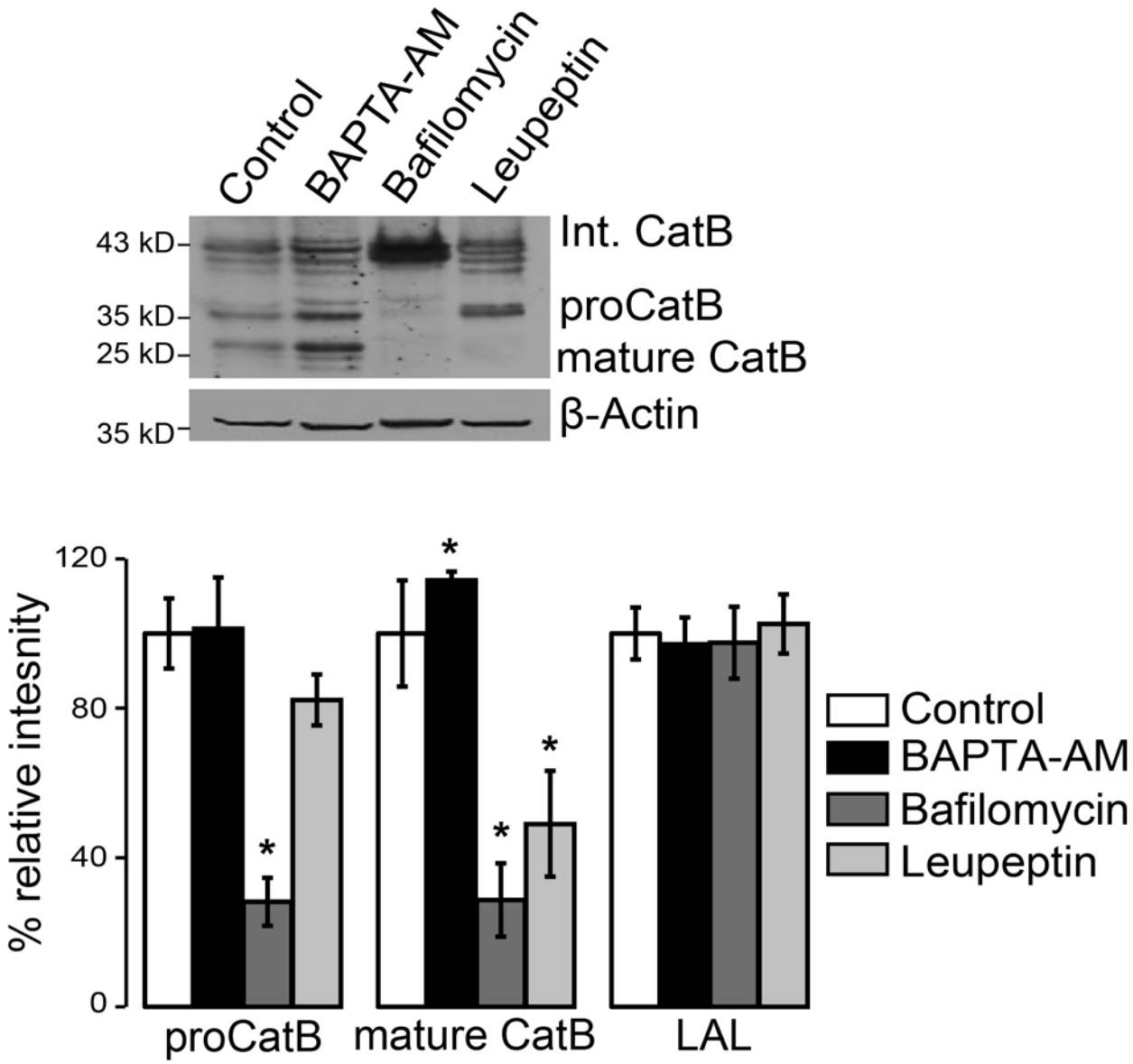


**Figure 2.3 Increased levels of CatB and decreases LAL levels are TRPML1 specific and not due to general endocytic disruption.**
HeLa cells were treated with the endocytic inhibitors BAPTA-AM (10 μM), bafilomycin A1 (10 nM), and leupeptin (10 μM) for 48 h. These inhibitors did not affect LAL levels and did not lead to a CatB increase. Therefore, general endocytic disruption does not cause protein changes similar to that of TRPML1 and PPT1 KD. *$p<0.05$. $n\geq5$.

Finally, we analyzed LAMP1, CatB, and LAL levels in PPT1 KD to determine if the changes we observe are specific to TRPML1 KD. LAL and LAMP-1 levels are unaffected in PPT1 KD cells (Figs 2.2D,E). We did observe a 107.8%±21.9 ($p<0.05$, $n=3$) increase in proCatB levels, however there was no significant increase in mature CatB levels in PPT1 KD cells. These

results suggest that PPT1 KD affects the automaturation of the inactive CatB zymogen. There was no significant change in LAMP1 (n=3, p=.4) or LAL (n=3, p=.1) levels in the PPT1 KD cells. Therefore, downregulation of the genes *MCOLN1* and *PPT1* affects protein levels of specific lysosomal components.

*CTSB*, the gene coding for CatB, is a member of the CLEAR gene network regulated by TFEB transcription factor, as are genes coding for LAL and LAMP-1. Genes in this network are upregulated upon increased TFEB expression and nuclear translocation (18). Although the CLEAR network was clearly shown to coordinate changes in genes coding for lysosomal proteins, input signals regulating it are currently unclear. To determine if the CLEAR network was activated in our system as well as inducing changes in gene expression, we measured mRNA levels of CatB, LAL, and LAMP1. There was no significant change in CatB, LAL, and LAMP1 mRNA levels in TRPML1 and PPT1 KD cells compared to control cells within 48 h of KD (Fig 2.4A). Values were normalized to β-actin mRNA levels. Western blotting and confocal microscopy show no change in TFEB protein levels or localization in TRPML1 KD cells (Figs 2.4B,C). Therefore, CatB upregulation in the acute KD model likely takes place at the post-transcriptional level and the TFEB driven lysosomal gene network is not activated in response to this KD.

To confirm that the TFEB gene network reports the functional status of lysosomes in our experimental system, we used protocols previously used to establish this paradigm. First, incubation of cells with 100 mM sucrose, previously shown to disrupt lysosomal traffic and stimulate the TFEB network (18), was performed and the transcriptional levels of CatB, LAL, and LAMP1 were analyzed using qRT-PCR. Fig 2.4D shows that 2 and 5 day sucrose treatments induce an increase in levels of these TFEB regulated genes, consistent with previous studies.

Prolonged (7 days) TRPML1 KD in HeLa cells is associated with an increased buildup of storage bodies (162). We reasoned that if the TFEB network reports the general disruption of the lysosomal function and/or buildup of storage bodies, then the genes belonging to the TFEB network would be upregulated after prolonged TRPML1 KD. Fig 2.4E shows that 7 day KD of TRPML1 or PPT1 results in upregulation of CatB and LAL mRNA (CatB levels respectively: 67.3%±14.2, 86.5%±12.1. LAL levels respectively: 63.7%±5.0, 66.1%±7.8. n=3, $p<0.01$). Since both genes belong to the TFEB network, we conclude that TFEB activation probably depends on general lysosomal cues such as storage bodies. It is interesting to note that LAMP1 mRNA is not changed in this model, suggesting that additional stimulation cues are necessary to change expression of this gene. The elevated level of LAMP1 expression in our sucrose treatment appears to be time dependent (Fig 2.4D), suggesting that increased lysosomal dysfunction may be required for increases in LAMP1 gene expression. These results indicate that the biochemical events leading to CatB upregulation precede the critical juncture in lysosomal dysfunction that is necessary for activation of the CLEAR network.

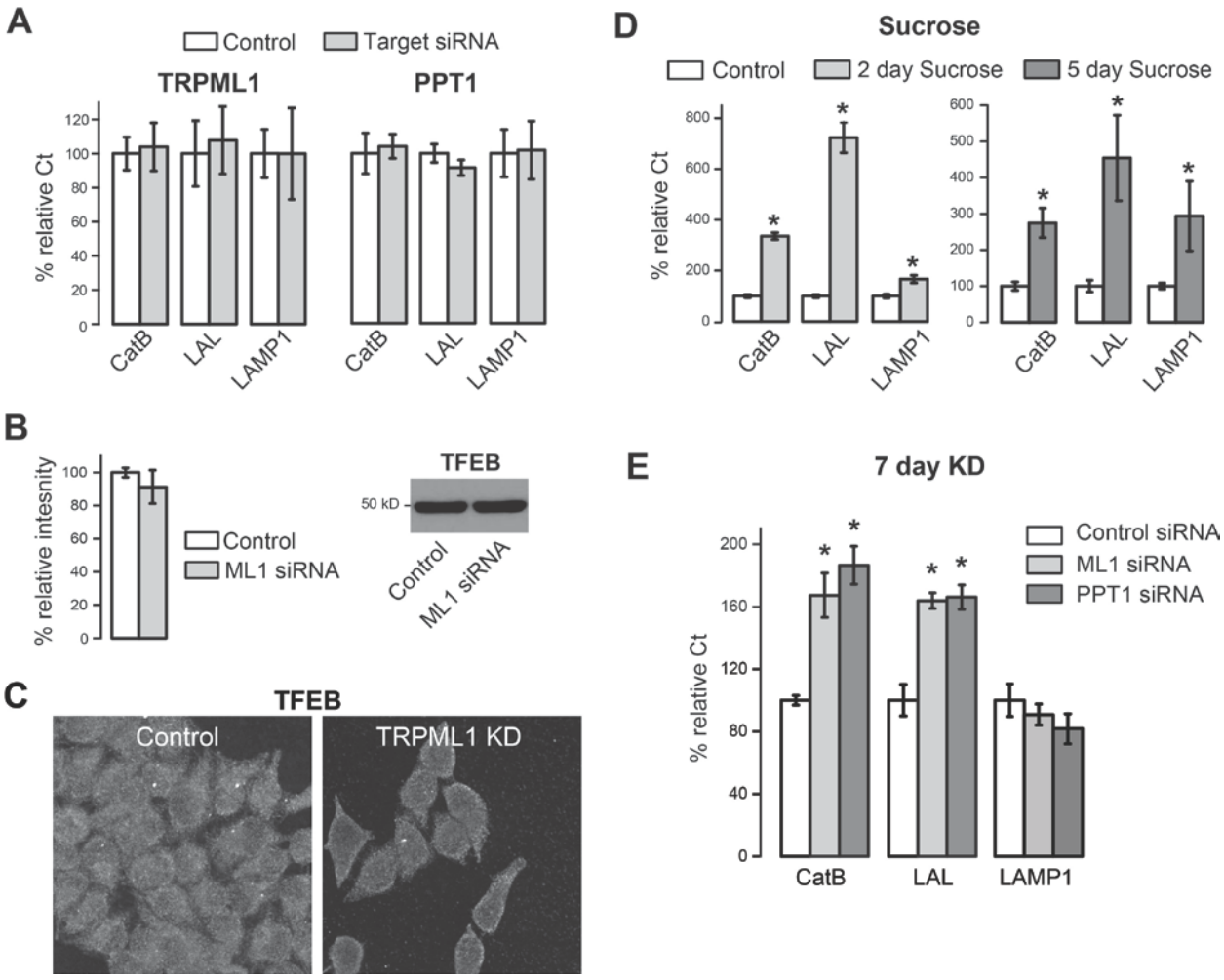


**Figure 2.4 TFEB regulated lysosomal genes and TFEB levels are unaltered in acute TRPML1 and PPT1 KD cells.**

A) mRNA levels were measured in TRPML1 and PPT1 KD cells using qRT-PCR using CatB, LAL, and LAMP-1 specific primers. n≥3. No significant change was seen in mRNA levels under either condition. B) TFEB protein levels were measured by Western blot analysis in TRPML1 KD cells. No difference was seen. C) TFEB cellular localization was analyzed by confocal microscopy. No change in localization occurs after 48 hr of TRPML1 KD. n=3. D) qRT-PCR analysis of CatB, LAL and LAMP1 mRNA in HeLa cells exposed to 100 mM sucrose for 2 or 5 days to induce general inhibition of the lysosomal function as described before. E) qRT-PCR analysis of the same genes in cells after 7-day KD of TRPML1 or PPT1. β-actin was used as a loading control. *$p<0.05$, n=3.

Taken together, the results described above show upregulation of proCatB and mature CatB shortly after TRPML1 KD. The buildup of proCatB in both TRPML1 and PPT1 KD cells can be explained by general lysosomal malfunction leading to delayed processing of CatB. However, upregulation of the mature form of CatB appears to be TRPML1 specific and, under the conditions of acute TRPML1 KD, it is not caused by changes in gene expression.

### 2.4.3 CatB release in TRPML1 KD cells

Lysosomal proteases have been implicated in cell death via the apoptosis program due to their release into the cytoplasm and activation of apoptotic caspases (136, 204, 232, 233). Several mechanisms of CatB release have been proposed. Some studies suggest general loss of lysosomal integrity, while in some studies lysosomes appear intact during the cytosolic CatB increase, suggesting a specific mechanism of CatB release. Since MLIV has a neurodegenerative profile, ostensibly due to neuronal loss, CatB changes in TRPML1 deficient cells may shed new light on cell death caused by MLIV. To elucidate the mechanism of CatB increase, we examined the degradation, synthesis, and cellular localization of CatB in TRPML1 KD cells.

To determine whether TRPML1 KD induced CatB upregulation is caused by increased protein synthesis or decreased degradation, cells were pulsed with $^{35}$S labeled cysteine-methionine for 2 h then chased with serum-free media for 0, 3, 6, 9, and 12 h. Whole cell lysates were collected at each time point and $^{35}$S-CatB was immunoprecipitated, and visualized on a SDS-PAGE gel. A small aliquot of lysate was collected and subjected to Western blot analysis to measure β-actin levels; all values were normalized to β-actin. There were no appreciable differences in CatB synthesis, as measured at the 0 hour time point (Fig 2.5A). Cell lysates were collected, immunoprecipited with CatB antibody, and subjected to Western blot analysis 30, 60, 90, and 120 min during labeling, to ensure that labeling is linear (data not shown). Furthermore, there was little difference between CatB degradation rates in control and TRPML1 KD cells (Fig 2.5B). Therefore, translation and degradation of CatB is unaffected in TRPML1 KD cells.

Concentrated proteins in the medium were subjected to Western blot analysis to measure CatB secretion. There was an 83.8%±18.2 ($p<0.01$, $n=3$) increase in extracellular Intermediate CatB in TRPML1 KD cells, normalized to extracellular β-actin (Fig 2.5C), however there was no difference in extracellular levels of proCatB. The increase in intracellular levels of proCatB, but the lack of increase in the extracellular media, suggests that proCatB secretion is impaired in TRPML1 KD cells and may contribute to the buildup of intracellular CatB.

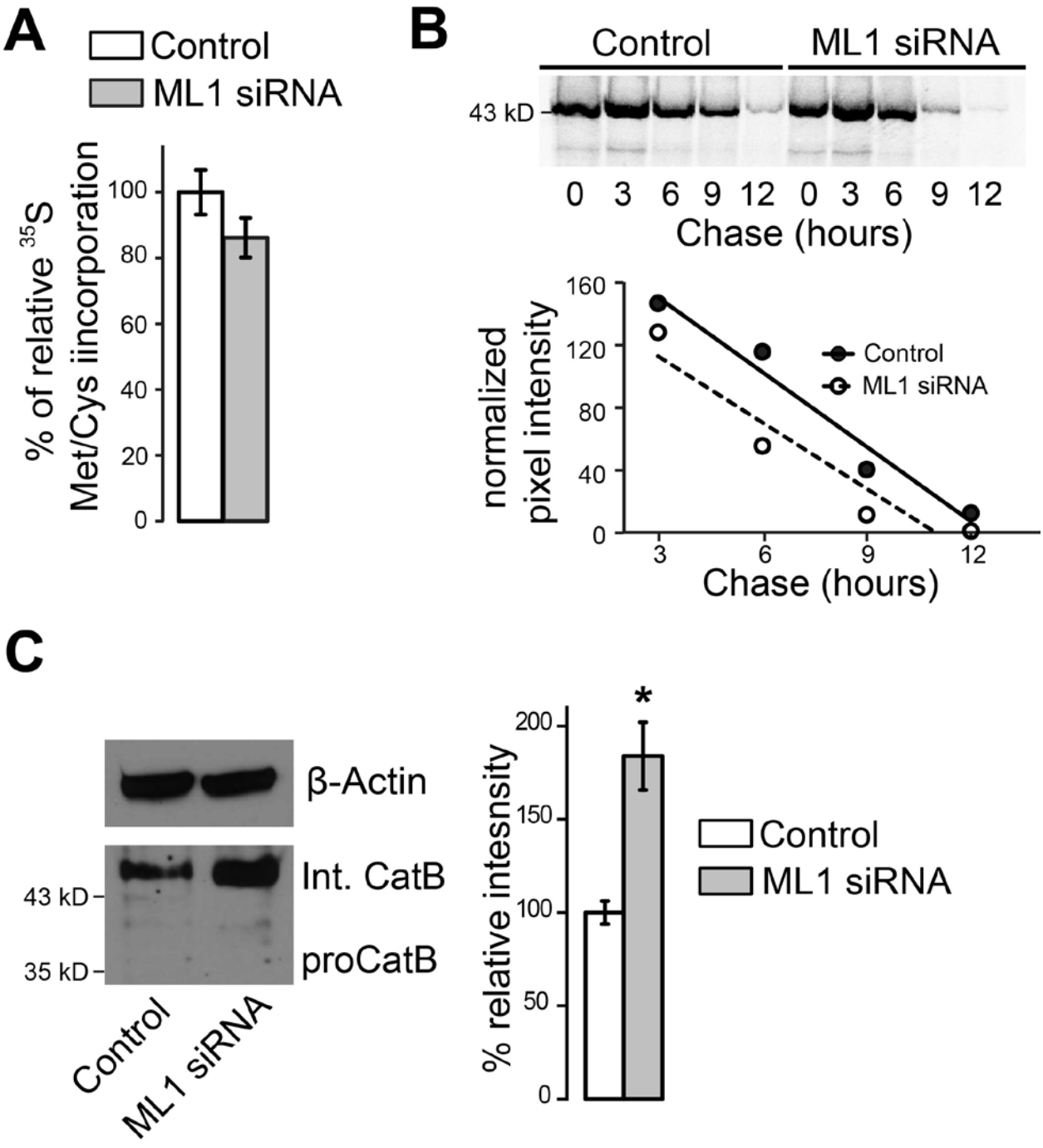


**Figure 2.5 Levels of CatB activity and secreted proCatB are elevated in TRPML1 KD cells.**
Degradation and synthesis is unaffected in these cells. A) Synthesis of $^{35}$S-CatB was measured beginning immediately after a 2 hr labeling period. Levels were normalized to β-actin. n=3. B) Degradation rates of CatB were measured over a 12 hr time course. $^{35}$S-CatB levels were normalized to β-actin and rates of degradation were determined using a linear fit curve. C) Levels of CatB secretion were measured by Western blot analysis. Higher levels of proCatB are detected in the media but are several fold less than intracellular proCatB levels. *$p<0.05$, n=3.

Cytosolic release of CatB has been demonstrated in several studies. Previous studies demonstrated CatB localization through the expression of GFP-CatB whereas others established endogenous CatB localization using fractionation assays (59, 136, 154, 234). Despite numerous attempts we were unable to clearly visualize endogenous CatB in HeLa cells. Since our data focuses on endogenous CatB dynamics we established CatB localization using cytosolic/membrane fractionation. Fractions from control and TRPML1 KD cells were isolated and CatB, LAMP-1, GAPDH, and β-actin were compared in these fractions. GAPDH was only detected in the cytosolic fractions while LAMP-1 was only detected in the membrane fraction (Fig 2.6A), confirming specificity of our preparation. β-actin was used to normalize CatB and LAMP-1 levels in our membrane fractions. GAPDH was used to normalize CatB in the cytosolic fractions. Our data show a significant increase of CatB in both fractions (Figs 2.6B,C) and increased LAMP-1 levels in membrane fractions (Fig 2.6C). These data are consistent with our whole cell analyses.

Interestingly, cytosolic proCatB levels increased 366.8%±31.6 ($p<0.01$, $n=3$) in TRPML1 KD cells, suggesting that a large amount of CatB is released into the cytosol. Overall, we suggest that decreased CatB secretion may result in high intracellular levels, combined with the release of CatB into the cytosol in TRPML1 KD cells.

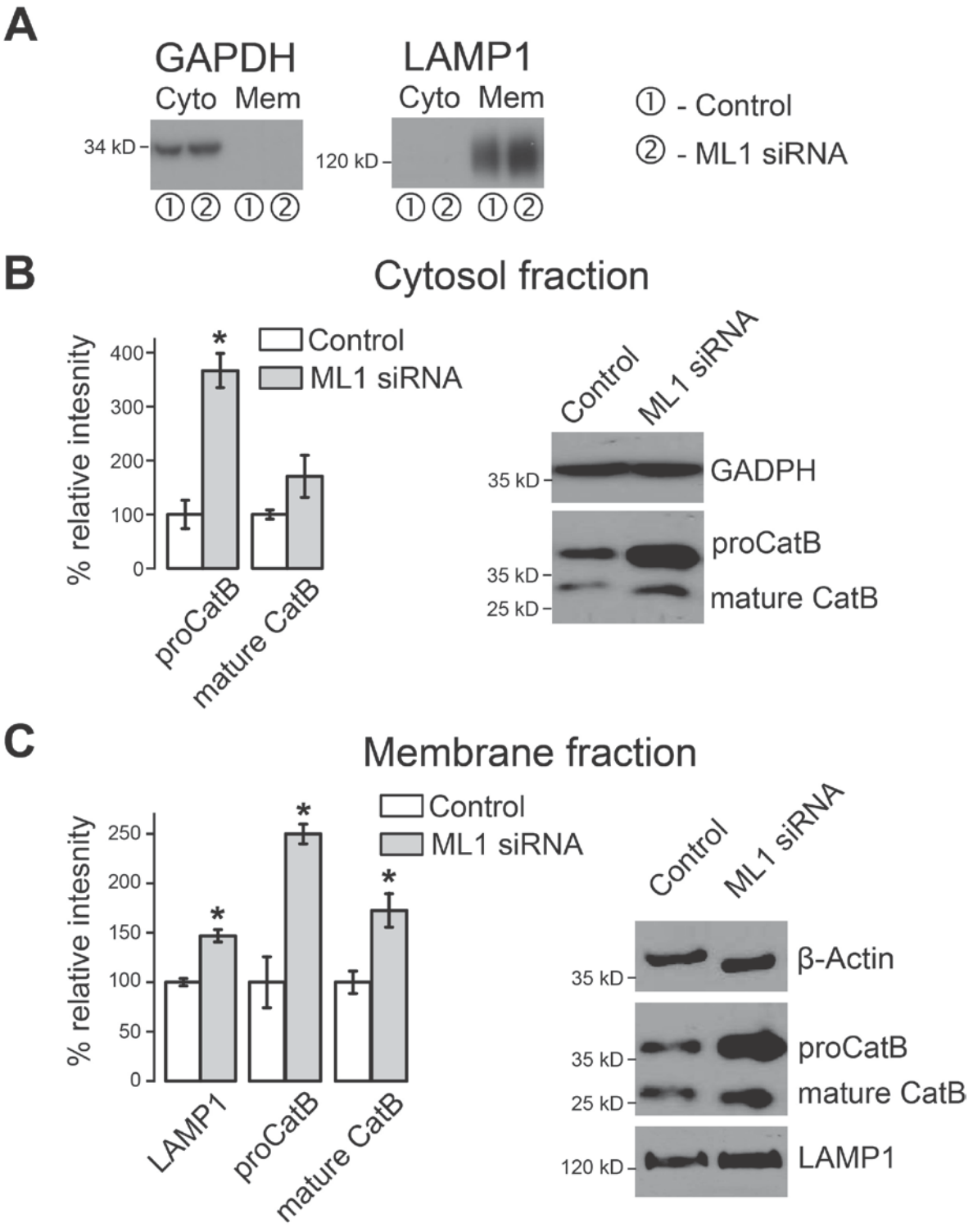


**Figure 2.6 TRPML1 KD results in high levels of cytosolic and membrane associated CatB.**
A) Cytosolic and membrane fractions were isolated from HeLa lysates through differential centrifugation 48 hr at TRPML1 KD and identified using GAPDH and LAMP-1 antibodies. B) Cytoplasmic fractions. CatB levels were measured by Western blot analysis and normalized to GAPDH. C) Membrane fractions show increases in CatB and LAMP-1 levels, consistent with whole cell lysate analyses. Due to changes in LAMP-1 levels, β-actin was used as a loading control for both CatB and LAMP-1 quantification. *$p<0.05$, n=3.

### 2.4.4 CatB and apoptosis in TRPML1 deficient cells

Leakage of CatB and other lysosomal proteases into the cytosol has been shown to lead to apoptosis (235-239). This phenomenon seems to take place in our system as well. Apoptosis levels were tested in control and in TRPML1 and PPT1 KD cells using a Caspase-3 (Cas3) fluorogenic substrate assay. Apoptosis was significantly upregulated in TRPML1, but not in PPT1 KD cells (Fig 2.7A). Western blot analysis revealed cytosolic cytochrome C release in these cells (Fig 2.7B), a positive marker of apoptosis. In TRPML1 KD cells, Cas3 activity averaged 162.9±9.3% of its value in control cells, while in PPT1 KD cells it averaged 107.31±4.7% of control values (n=3 for each set of conditions; $p<0.01$ for TRPML1 KD cells). 24 hour incubation of control and TRPML1 KD cells with the cell-permeable CatB inhibitor Ca-074Me (2.5 μM) resulted in decreased apoptosis in TRPML1 KD cells as compared with untreated control (67.9±7.2%, $p<.01$, n=3). Ca-074Me did not alter apoptosis in control treated cells as seen in Fig 2.7A. This suggests that apoptosis in TRPML1 KD cells is CatB dependent and that apoptosis is an early specific consequence of TRPML1 loss.

The proapoptotic protein Bax has been implicated in CatB release in several systems (136, 155, 240, 241). Fig 2.7B shows that 24 hour treatment with Bax inhibiting peptide (100 μM, Calbiochem) prevented apoptosis in TRPML1 KD cells without significantly affecting apoptosis rates in control cells, suggesting that this effect is specific to TRPML1 KD dependent apoptotic processes. Inhibition of Bax had varied results on cytoplasmic CatB levels, actually increasing CatB in control cells treated with the inhibitor. TRPML1 KD cells treated with the inhibitor had significantly elevated cytoplasmic CatB levels compared to both untreated and Bax

inhibited control cells as seen in Figure 2.7C (n=4, p<.01, p=.05 respectively). These data suggest that CatB release lies upstream of Bax. Confocal microscopy of TRPML1 cells showed punctate Bax staining (red) as compared to control cells, which did not overlap with the lysosomal marker LAMP1 (green) (Fig 2.7D) These observations are in agreement with previous studies, which indicate Bax translocation to punctate mitochondria and cytochrome release in Cathepsin/Bax-dependent apoptosis (58). Further studies will focus on elucidating these pathways and determining the sequence of events that leads to Bax activation, Caspase-3 activation, and apoptosis in these cells.

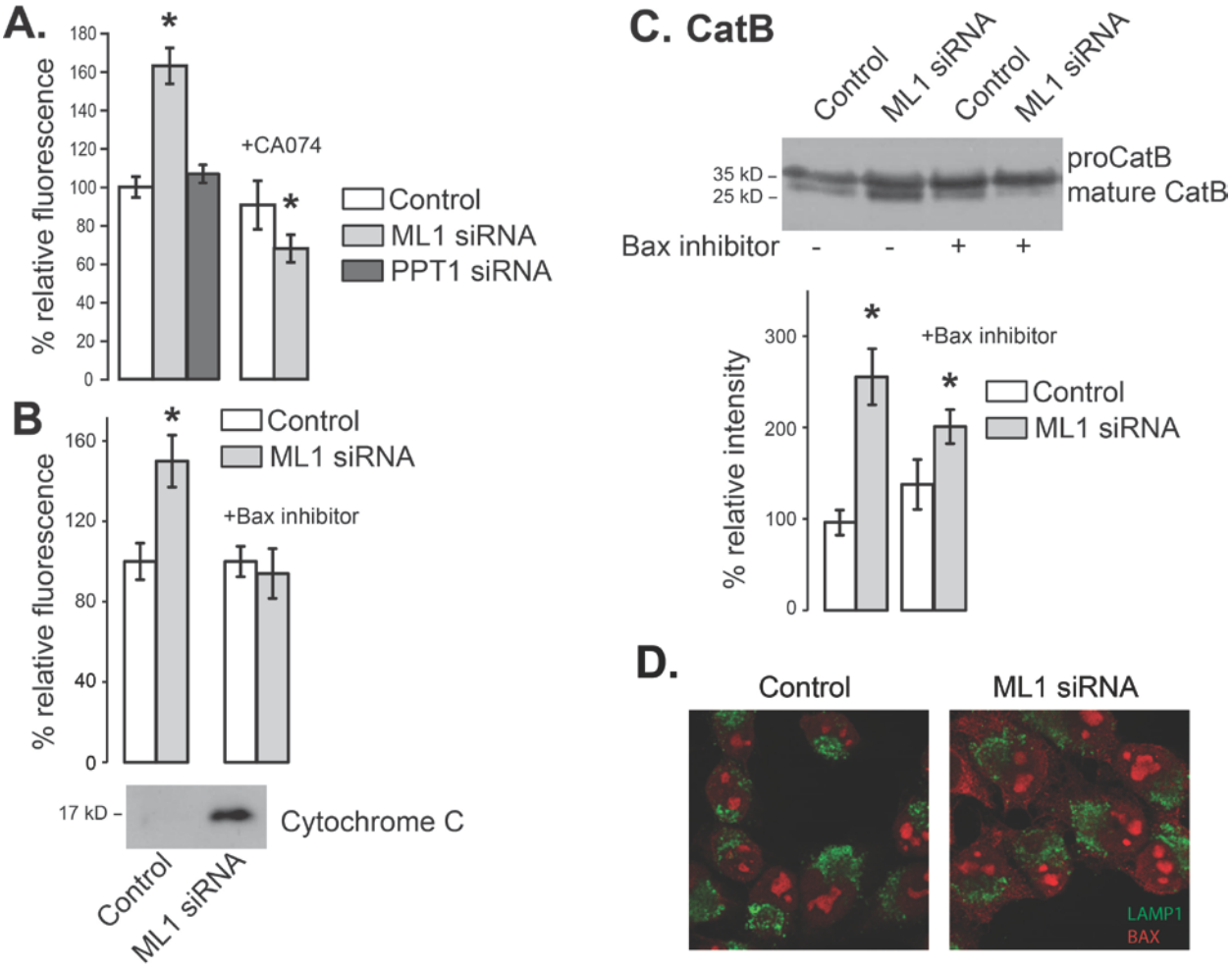


**Figure 2.7 TRPML1 KD results in cell death via Bax and CatB dependent mechanism.**
A) Apoptosis was measured using the EnzChek Caspase-3 Apoptotic assay 48 hr after TRPML1 and PPT1 KD. Ca-074Me (2.5 µM) was added 24 hr after KD. *$p<0.01$ of untreated control, n=3. B) Caspase-3 activity was measured in TRPML1 KD cells 48 hr after KD in the presence and absence of Bax inhibiting peptide (100 µM, added 24 hr after KD). *$p<0.05$, $n\geq3$. Western blot analysis of cytosolic fractions revealed an increase in the pro-apoptotic marker Cytochrome C in TRPML1 KD cells as compared with control. C) Western blot example and statistical analysis of CatB in 48 hr TRPML1 KD cells treated with Bax inhibiting peptide (100 µM, added 24 hr after KD). *$p<0.05$, $n\geq3$. D) Confocal microscopy of Bax localization reveals punctate localization in TRPML1 KD cells, which did not overlap with LAMP1 staining.

## 2.5 DISCUSSION

The present study shows that shortly after TRPML1 KD in HeLa cells, the lysosomal protease CatB is translocated into the cytoplasm where it triggers cell death through apoptosis.

Apoptosis is set in motion by a CatB dependent mechanism that involves the pro-apoptotic protein Bax. These data are in line with previous reports on lysosomal toxicity (136, 137, 155, 228, 229, 235-241). They do, however, raise several important questions relevant to lysosomal storage diseases and lysosomal function.

Cell death clearly underlies the key degenerative aspects of lysosomal storage diseases. Its mechanisms in lysosomal storage disorders, however, are not well understood. Some of the current models, including suppressed flow of key substrates or accumulation of effete organelles due to autophagy block, have been discussed (30, 209, 223). Here we showed that in addition to the "supply side" issues in lysosomal storage diseases, an active and early CatB release mechanism specifically caused by TRPML1 loss takes place soon after TRPML1 KD. Relative contribution of each of these mechanisms in cell death in specific tissues remains to be established. It is, however, likely that if the propensity for CatB release varies between different tissues, then the CatB release mechanism may explain tissue specific cell death in lysosomal storage diseases.

The mechanism of CatB release in TRPML1 KD cells remains to be identified. Cytosolic CatB release has been implicated in many instances of cellular toxicity, including those caused by cytoplasmic/ mitochondrial and by lysosomal events (235-239). Dissociation of lysosomal membrane by lysosomotropic agents has been proposed as one explanation for this phenomenon. It is important to note that nonselective physical damage to the lysosomal membrane is usually associated with a general loss of lysosomal integrity and release of a number of lysosomal components, including lysosomal dyes, into the cytoplasm. This has not been observed in our system; indeed the lysosomal component CatD does not appear to change in TRPML1 KD cells (Fig 2.2). We do not detect any measurable loss of lysosomal integrity using the lysosomal

marker lysotracker (not shown). These observations are in line with previous findings of CatB translocation into cytoplasm without detectable loss of lysosomal integrity. Bax is involved in permeability pore transition in mitochondria, which triggers apoptosis; however several studies clearly implicated it in lysosomal permeabilization by direct interaction with lysosomes or with another non-mitochondrial membrane fraction (232, 242-245). However, our results did not show a significant decrease in cytosolic CatB levels after Bax inhibition, suggesting that this protein lies downstream of CatB release. As TRPML1 KD does not seem to induce gross dissociation of lysosomal membrane, it is tempting to speculate that other pro-apoptotic molecules such as caspase-8 induce a specific CatB release route to assist or initiate apoptotic events. Elucidating these pathways will provide a clearer understanding of the consequences of TRPML1 KD that result in cell death.

It is important to remember that Bax has been implicated as a pro-apoptotic signal. The relation between TRPML1 KD, CatB release, apoptosis and Bax is a subject of future investigation. One possible mechanism could involve lysosomal deficiencies caused by TRPML1 KD inducing pathways that activate Bax, which initiates CatB release followed by caspase cleavage. Alternatively, CatB release could be a “cleanup” event, taking place downstream or in parallel with apoptosis caused by Bax activation.

One interesting observation is that TRPML1 has been shown to be cleaved by CatB in the lysosome (1). If the cell monitors the loss of TRPML1 activity, it could be that CatB cleavage of TRPML1 mediates this activity and is therefore a direct cellular response to TRPML1 loss, which results in downstream off-target effects such as apoptosis. Future studies will be conducted to determine if CatB mediated TRPML1 cleavage modulates the activity of the channel and whether loss of TRPML1 activity itself is enough to potentiate CatB upregulation.

## 2.6 ACKNOWLEDGEMENTS

This work was supported by the National Institutes of Health grants HD058577 and ES01678 to Kirill Kiselyov. Mark T. Miedel's work, which includes the design of *MCOLN1*-specific siRNA and the preliminary discovery of changes in lysosomal protein levels in TRPML1 KD cells, was supported by a National Institutes of Health predoctoral CTSI fellowship (NIH 5TL1RR 024155). I would like to thank the Center for Biologic Imaging at the University of Pittsburgh and Tom Harper in the Department of Biological Sciences, University of Pittsburgh for invaluable help with electron microscopy, which was prepared and imaged by James Quinn. I would also like to thank Neel Andharia for help in confocal imaging. Finally, I would like to thank Dr. Gustavo Maegawa for fruitful discussion, which helped guide the present direction of this project.

# 3.0 ACUTE DOWNREGULATION OF LYSOSOMAL GENES SPECIFICALLY AFFECTS TRANSCRIPTION OF GENES OUTSIDE THE "CLEAR" NETWORK

## 3.1 ABSTRACT

Lysosomal storage diseases (LSDs) are rare disorders caused by mutations in the genes coding for components of the endocytic pathway. Their defects result in the buildup of inclusions containing undigested substrates and in cell death, manifesting clinically as a range of conditions that include developmental delays, loss of motor function, retinal degeneration and corneal opacity. It is becoming increasingly clear that the effects of LSDs reach beyond the accumulation of undigested substrates and involve gene and protein networks. It is thus possible that the pathogenesis of LSDs may involve processes not directly related to the root cause of the disease but rather the changes induced by the downstream cellular responses, such as transcriptional changes. To elucidate the early transcriptional responses set in motion by LSDs, we induced acute downregulation by siRNA-mediated KD of proteins linked to LSDs such as the ion channel mucolipin-1 (TRPML1) and the enzyme palmitoyl-protein thioesterase 1 (PPT1), which are defective in mucolipidosis type IV and infantile neuronal ceroid lipofuscinosis 1, respectively. We analyzed changes in transcription 48 h after KD using microarray analyses. We found that specific subsets of genes are affected by TRPML1 and PPT1 KD and these genes appear to be regulated by a small set of transcription factors. In TRPML1 KD a high percentage of genes

altered are associated with the transcription factor NFκB, which is upregulated upon TRPML1 loss. These findings suggest that loss of lysosomal proteins activate specific transcriptional pathways. Further elucidation of the transcription factors and pathways activated by TRPML1 and PPT1 loss may shed light on the early consequences of losing these proteins as well as explain the downstream cellular responses.

## 3.2 INTRODUCTION

How do cells assess the functional status of their endocytic pathway and do they actively respond to the changes in its function? Is it possible that cellular responses to LSDs reach beyond the endocytic pathway and factor in to the pathogenesis of LSDs? To address these questions, we have examined alterations in gene expression upon loss of genes implicated in LSDs, measuring the immediate cellular response to loss of endocytic components. Recently published evidence suggests existence of a lysosomal gene network driven by the transcription factor (TF) TFEB, which regulates the expression of genes whose regulatory elements contained a well-defined "CLEAR" sequence (18). It was suggested that TFEB orchestrates the expression of lysosomal proteins for lysosomal biogenesis and perhaps in response to disturbances in the endocytic pathway, including chronic cell models of LSDs (18). This attractive model and the previous reports on changes in gene expression in LSDs suggest active cellular monitoring of endocytic integrity (220, 246).

It is not clear whether TFEB is the only means of coordinating the expression of lysosomal proteins or whether the TFEB regulated lysosomal network interacts with other cellular regulatory circuits. It is possible, and, indeed, likely that the cellular program of

endocytic monitoring involves processes both directly involved and unrelated to lysosomal function. It is also possible that some of the cellular changes induced in response to endocytic deficiencies may contribute to disease pathogenesis. Towards delineating such responses, we performed gene expression analyses in cells with acute deficiencies of the important endocytic components TRPML1 and PPT1. The loss of either protein results in LSDs however their function in the lysosome is unrelated, allowing us to compare how cells respond to the loss of different types of endocytic components (1, 7, 186). We performed microarray analyses 48 h after siRNA-mediated KD of TRPML1 and PPT1 in HeLa cells to separate changes induced directly by the loss of these proteins from those induced by the buildup of the undigested material, which occurs in chronic LSD cell models (247, 248).

TRPML1 is an ion channel coded by the gene *MCOLN1* (2). TRPML1 is a member of the TRP family of ion channels and is localized in lysosomes and late endosomes (1, 2). Physiological readings demonstrate that TRPML1 is permeable to mono- and divalent cations and that permeation through a constitutively active form of TRPML1 is stimulated by low pH (1, 7, 8). Recently, TRPML1 was shown to be activated by $PI(3,5)P_2$ and previous reports demonstrating its ability to conduct $Ca^{2+}$, supports its role in $Ca^{2+}$-driven, SNARE-dependent membrane fusion in the endocytic pathway (7, 10). Another model for TRPML1 function suggests a role in the modulation of lysosomal ion homeostasis and, therefore, digestive function, by regulating the lysosomal $Fe^{2+}$ load or pH (162, 188).

Neuronal ceroid lipofuscinoses (NCL) are a class of diseases collectively referred to as Batten disease. Each NCL is caused by the loss of a specific lysosomal enzyme. The loss of PPT1 results in infantile neuronal ceroid lipofuscinosis (INCL) and is the most severe NCL (249). PPT1 is responsible for the cleavage of fatty acids from lysosomal protein substrates and

the buildup of undigested substrates in PPT1 deficient cells is associated with stunted growth, cognitive dysfunction, blindness and an abbreviated lifespan. The amount of PPT1 activity lost in INCL correlates with the severity of the disease, directly linking the activity of this enzyme with the disease pathogenesis (250). Studies have suggested both lysosomal as well as synaptic vesicle localization of PPT1, suggesting that it may play a role both in the endocytic pathway and extracellularly (251, 252). The differences between protein function and localization of PPT1 and TRPML1 allow us to answer whether the cell can distinguish between specific endocytic components and respond accordingly or whether lysosomal malfunction will trigger a generalized response.

Our results show that genes outside of the TFEB network are altered upon TRPML1 KD, and that these same genes are not affected by PPT1 loss. The genes affected in TRPML1 and PPT1 KD cells seem to share regulatory elements for a select subset of transcription factors. A large percentage of genes affected in TRPML1 KD are associated with the transcription factor NFκB, which, is itself, upregulated upon TRPML1 loss. The genes altered in this study are not part of the "CLEAR" network. This suggests that specific gene pathways are being altered upon TRPML1 and PPT1 loss and that these pathways are independent of the reported lysosomal gene network. Interestingly, the "CLEAR" network genes *LAMP1*, *LIPA*, and *CTSB*, which are unaltered 48 h after TRPML1 and PPT1 KD, are upregulated after 7 days of downregulation. These genes are also upregulated 48 h and 5 days after sucrosome formation. This differential activation of "CLEAR" network genes suggests that higher degrees of lysosomal dysfunction may be driving the activation of this network. This also suggests that there are different cues that activate the specific transcriptional changes we see in acute, "mild" lysosomal dysfunction compared to more robust dysfunction and demonstrates crosstalk between the endocytic pathway

and nucleus, through TF activity. Further work into dissecting these pathways and understanding the cascades that lead to transcriptional and lysosomal changes will help to elucidate how the cell monitors and responds to endocytic disruption and whether these responses directly affect disease pathogenesis.

## 3.3 EXPERIMENTAL PROCEDURES

*Cell Culture:* Cells were maintained as described in 2.3. Antibiotic free media supplemented with 100mM sucrose was used for sucrose treatments.

*siRNA-mediated KD*: KDs were performed as described in 2.3. All KDs were confirmed before microarray analyses and confirmed using microarray readout of *MCOLN1* and *PPT1* respectively.

*Microarray*: Microarrays were performed using Illumina BeadChip® Human Whole Genome (WG-6) arrays for the TRPML1 analyses and Illumina HumanHT-12 v4 Expression BeadChip for the PPT1 analyses. The microarrays and normalization was performed by the Genomic Core Laboratories at the University of Pittsburgh. 4 sets of control siRNA and PPT1 siRNA samples were run in triplicate. 2 sets of TRPML1 siRNA samples were run in triplicate for this analysis. Data was normalized using the cubic spline method by the Core Laboratories. Cy3 emission values were normalized to control values to obtain changes in gene expression.

*RNA isolation, Reverse Transcriptase, and Quantitative qPCR*: All methods and primers used are described in section 2.3.

*Western blot analysis*: Performed as described in section 2.3. Monoclonal NFκB p105/p50 (Abcam, ab7971) at 1:250, and monoclonal β-actin (AC-15 clone, Abcam) at 1:5000

were used for protein detection. HRP conjugated goat anti-mouse or anti-rabbit secondary antibodies (Amersham, Piscataway, NJ) were used at 1:20,000 and 1:1,500 dilutions respectively. Nuclear fractions were isolated using the Millipore Nuclear Extraction kit.

*Confocal Microscopy*: As described in 2.3. The following primary antibodies were used: polyclonal NFκB p105/p50 (clone E381, Abcam), monoclonal anti-NPM (Invitrogen, 187288), polyclonal anti-Lamin B1 (Sigma, SAB2101352). For indirect detection, a goat anti-mouse and goat anti-rabbit secondary antibodies from Invitrogen were used.

Statistical significance was calculated using a one-tailed, unpaired t-test with $p \leq 0.05$ considered significant. Data are presented as mean±S.E.M.

## 3.4 RESULTS

### 3.4.1 Microarrays show specific gene changes in TRPML1 and PPT1 KD

Limited proteomic and gene expression analyses of cell lines from LSD patients including an MLIV line have previously been performed (253, 254). However, these models are not well suited for studying the initial regulatory networks set in motion by the loss of endocytic components, as the chronic buildup of undigested material in these models may cause secondary effects, which may convolute, override, or mask the initial cellular responses. Therefore, acute KD models give us a unique opportunity to test the immediate effects of downregulating lysosomal components on gene expression. As shown in section 2.4.2., several TFEB driven "CLEAR" network genes seem to be activated by high levels of endocytic disruption but not after acute downregulation of single lysosomal components. Therefore, we suggest that

microarray analyses of TRPML1 and PPT1 acute KD cells will demonstrate transcriptional changes outside of the TFEB network. siRNA-mediated TRPML1 and PPT1 KD in HeLa cells was confirmed using quantitative real-time PCR (qRT-PCR) as described in section 2.4.2. Verified KD samples were sent for microarray analysis to the Genomic Core Laboratories at the University of Pittsburgh. TRPML1 KD mRNA levels were between 30-50% of control cells, PPT1 KD mRNA levels were ~10-30% of control cells.

In our microarray assays, TRPML1 mRNA expression was decreased to between 29 and 50% of control levels and PPT1 was decreased ~20% of control levels in all samples, consistent with the preliminary qRT-PCR results. Our microarray analysis identified close to 100 genes that were unidirectionally altered in two biological replicates. The genes altered in our TRPML1 and PPT1 KDs were not associated with the TFEB network, confirming that acute downregulation of lysosomal components does not put enough stress on the endocytic pathway to activate this response. In addition, the level of differential expression of these genes correlated with the efficiency of the knockdown, providing further evidence that these changes were a direct effect of TRPML1 or PPT1 KD. For further analyses, we focused on genes that were decreased to less than 50% or increased to more than 150% of control levels in all samples. Tables A.1,2 (Appendix A) list the 32 genes altered in our TRPML1 KD and 71 genes altered in our PPT1 KD using this cutoff criteria.

To further confirm our microarray analyses, we more closely examined two genes selected in the TRPML1 KD microarray using qRT-PCR. The genes, *LYPLA1* and *CD83*, are downregulated upon TRPML1 KD, but remain unaltered in PPT1 KD samples. These genes were selected because their products have been shown to either play a role in substrate degradation (LYPLA1) or be processed in the lysosome (CD83) (255, 256). qRT-PCR results

confirmed our microarray data, showing a 50.3%±23.5 decrease in LYPLA1 mRNA and a 54.9%±11.3 decrease in CD83 ($p<0.05$, $n=4$, Fig 3.1A). There was no significant difference in *LYPLA1* and *CD83* mRNA between our control and PPT1 KD cells (Fig 3.1C). In addition, the measured mRNA resulted in similar protein changes. As seen in Figs 3.1B,D CD83 and LYPLA1 protein levels were decreased in TRPML1 but not PPT1 KD cells. Therefore, the loss of lysosomal components results in specific changes in gene expression.

### 3.4.2 Regulatory analysis of TRPML1 KD suggests that changes in gene expression may be regulated by specific transcription factors

As a preliminary analysis of our microarray data, we sought to determine if genes altered in the microarrays share common regulatory elements. To do this, we used TF predictions made by SABiosciences' Text Mining Application and the UCSC Genome Browser (panel of over 200 TF). Using this database we found that our candidate genes are associated with at least 1 of 5 TFs (ARNT, NRSF, CUTL1, NFκB, and PPAR-γ2 Fig 3.2A), suggesting that these TFs may play a major role in the regulation of our candidate genes in response to TRPML1 KD. NFκB is the most commonly associated TF in our panel (Fig 3.2A).

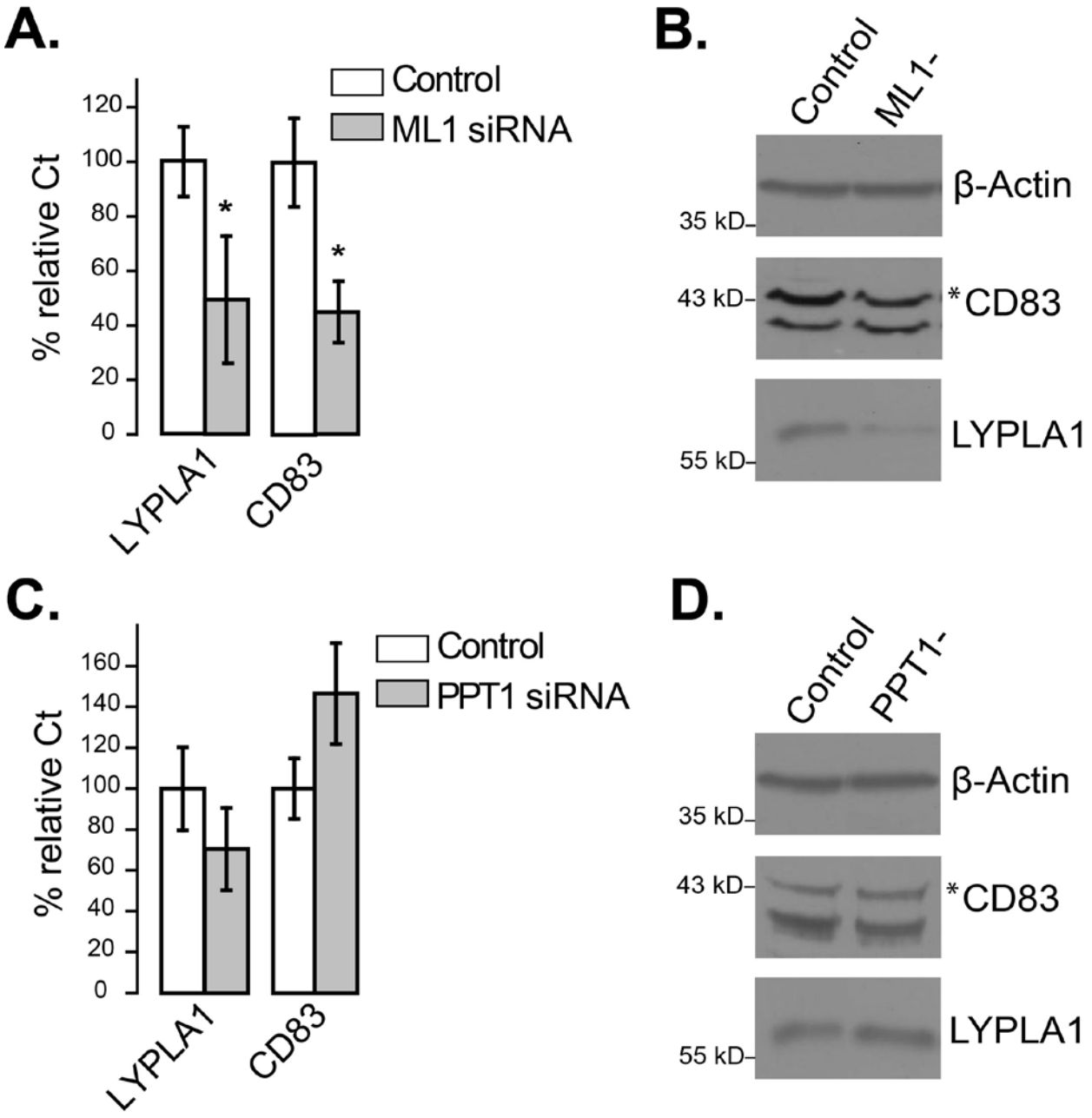


**Figure 3.1 Candidate genes *CD83* and *LYPLA1* are downregulated in TRPML1 but not PPT1 KD cells.**
Candidate genes *CD83* and *LYPLA1* are downregulated in TRPML1 KD but not PPT1 KD cells. A,C) Total RNA was isolated from cells 48 h after siRNA transfection. cDNA was synthesized and subjected to SYBR green based real-time PCR using β-actin, *CD83*, and *LYPLA1* primers. mRNA levels of both *CD83* and *LYPLA1* are downregulated in TRPML1 KD cells. There was no significant difference between PPT1 and control siRNA gene levels. B,D) Downregulation of *CD83* and *LYPLA1* mRNA levels resulted in decreased protein levels in TRPML1 cells as assayed by Western blot analysis. *, $p<0.05$.

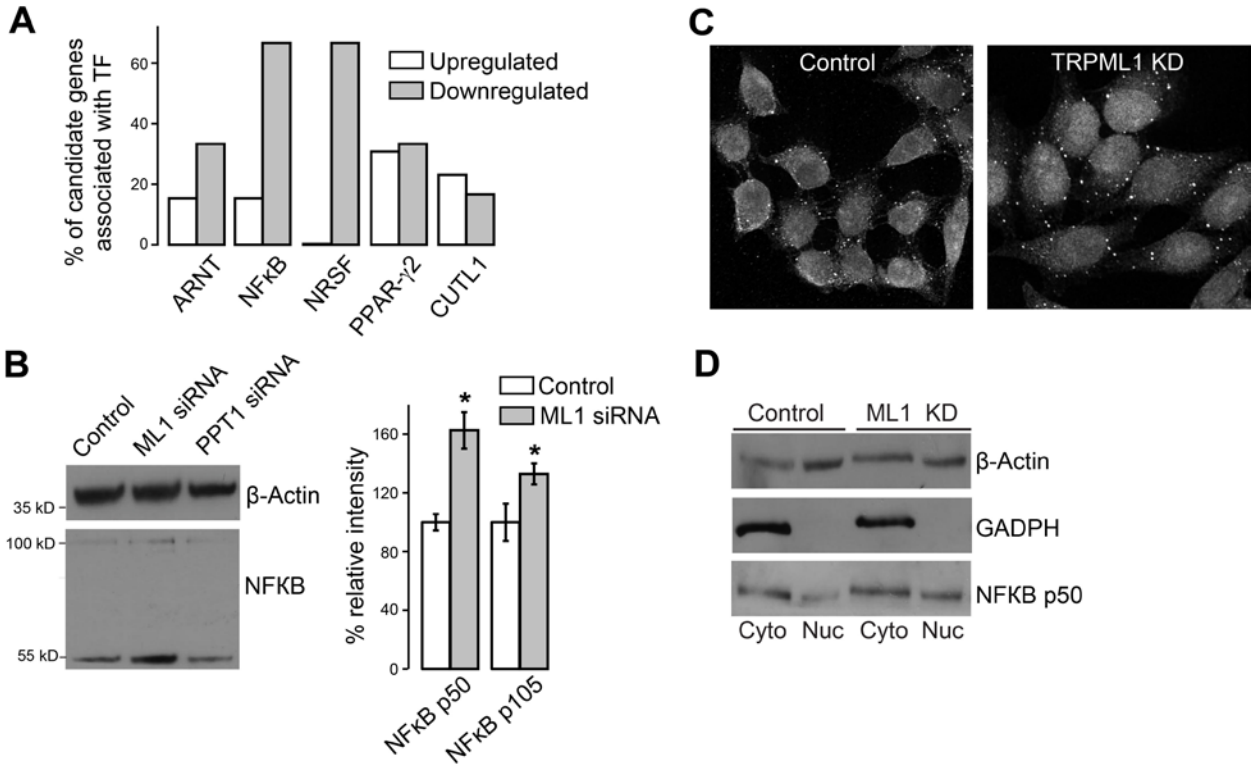


**Figure 3.2 Analysis of TRPML1 KD candidate genes reveals common subset of TFs which may regulate candidate gene expression, including NFκB.**
A) Identification of SABiosciences' regulatory TF binding sites on genes downregulated by 50% or upregulated by 150% or more in TRPML1 KD cells revealed 5 TFs that associate with these genes. B) p105/p50 NFκB which is associated with over 60% of these genes is upregulated in TRPML1 KD cells. *$p<0.05$, n=3. C,D) Confocal analysis reveals increased p105/p50 NFκB levels and nuclear translocation in TRPML1 KD cells. Western blot analysis of nuclear and cytoplasmic extracts show increased nuclear translocation of NFκB in TRPML1 KD cells.

### 3.4.3 NFκB is upregulated in TRPML1 KD cells and may regulate transcriptional changes

Since NFκB is associated with the highest percentage of candidate genes in TRPML1 KD cells, we decided to look at transcriptional levels of this TF from our microarray. We found that NFκB p105/p50 mRNA levels were elevated in TRPML1 KD cells (167% and 142% of control levels in each microarray). Western blot analysis revealed an upregulation of the p105/50 isoforms 48 hr after TRPML1 KD (Fig 3.2B). Confocal analysis and nuclear extraction assays

blotting with p105/p50 NFκB-specific antibodies showed upregulation and nuclear translocation of NFκB in TRPML1 KD cells (Figs 3.2C), suggesting that NFκB plays a role in TRPML1 KD induced gene expression changes. NFκB was unaltered in PPT1 KD cells (Fig 3.2B).

### 3.4.4 Comparison of TRPML1 and PPT1 KD reveals common TFs associated with altered genes.

In order to study regulatory networks controlling genes altered in our microarray analyses, we compared the TFs associated with our candidate genes from each analysis. Since we do not see an overlap in the genes that are altered in these KDs, we wanted to determine if any common TF pathways may be activated, although their ultimate effect would be different. We find that there are several specific TFs associated with our candidate genes in each KD condition, however, we find that CUTL1, c-jun, GATA-1, and AP-1 are associated with a fair percentage of candidate genes from both microarrays (Fig 3.3). This may suggest that these TFs are activated or repressed in both KD conditions. Further work will have to be conducted to determine whether or not these TFs are regulating the altered genes, and whether common pathways are being activated in the KD conditions.

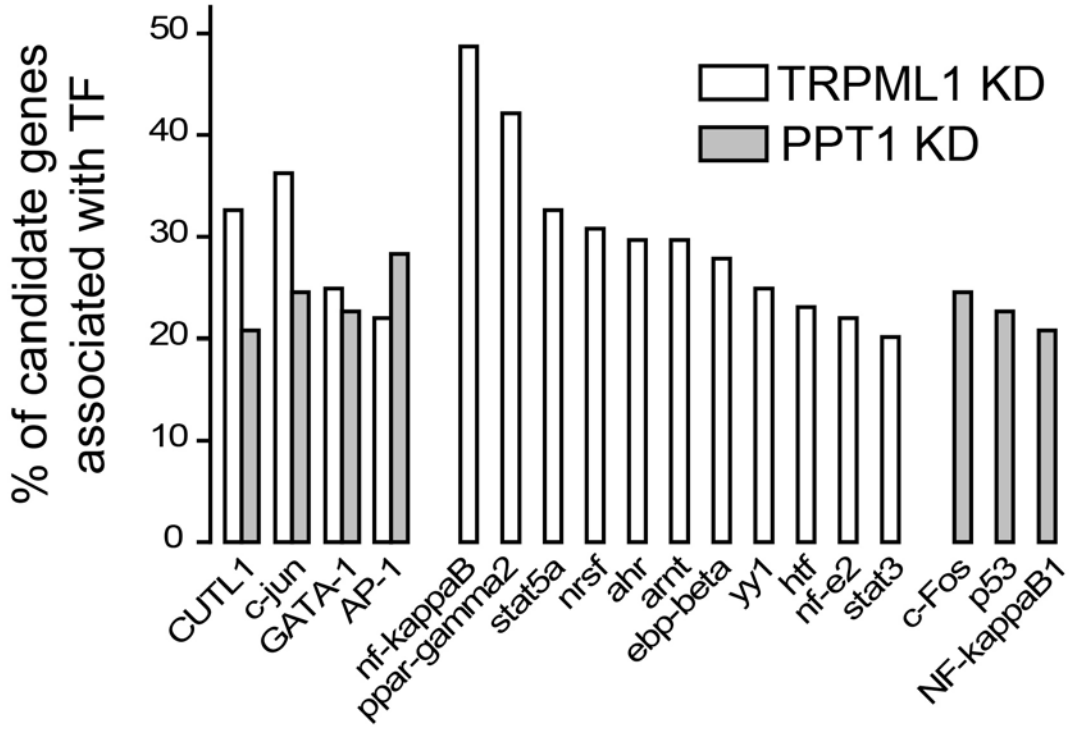


**Figure 3.3 Comparison of TFs associated with candidate genes in TRPML1 and PPT1 KD**
Using the SABiosciences' Text Mining Application and the UCSC Genome Browser, we compiled a list of TFs associated with 20% or more of our candidate genes. We then compared our results in the TRPML1 and PPT1 KD cells.

## 3.5 DISCUSSION

We previously tested whether the length or degree of lysosomal dysfunction is driving "CLEAR" network changes through 2 and 5 day sucrosome formation as well as 2 and 7 day TRPML1 KD, as discussed in section 2.4.2. We found that sucrosome formation led to upregulation of the "CLEAR" network genes *LAMP1*, *LIPA*, and *CTSB* and that 7 day TRPML1 KD was able to induce upregulation of *LIPA* and *CTSB.* These findings suggest that the degree of lysosomal dysfunction drives these transcriptional changes, rather than the length of the dysfunction. This is supported by our current microarray results, which showed changes in

several genes, none of which belong to the "CLEAR" network in either KD condition. This preliminary analysis of the microarray data shows that several specific as well as common TFs are associated with genes altered in both TRPML1 and PPT1 KDs. Interestingly, using this approach we have been able to identify that NFκB p50/p105 is transcriptionally upregulated and translocates to the nucleus after TRPML1 KD. Understanding the pathway that regulates this change will be the focus of future studies in the lab. Interestingly, Cathepsin B has been shown to cleave Caspase-1, which has been linked to the activation of NFκB and NFκB-inducing pathways (257, 258). Therefore, it will be interesting to address whether Cathepsin B and subsequent Caspase-1 cleavage activates this pathway. Preliminary data (not shown) suggested that NFκB upregulation may be Cathepsin B dependent, however there was some variation suggesting that optimization of Cathepsin B inhibition may be required to get a clear readout.

It will be interesting to further analyze other TFs selected using this approach, such as c-jun, which is associated with a large percentage of candidate genes from both microarrays and which, is itself, transcriptionally upregulated in both TRPML1 and PPT1 KDs (28% and 88% increase, respectively, data not shown). Future work will include altering our "target" TFs, such as NFκB using chemical and siRNA downregulation and measuring changes in gene expression in our KD conditions. If we can identify which TFs are modulating these genes, we can then begin to dissect the pathways which may be activated upon TRPML1 and PPT1 loss. Future studies will hopefully give a clearer understanding of how the endocytic pathway functions and responses to changes.

## 3.6 ACKNOWLEDGEMENTS

This work was supported by the National Institutes of Health grants HD058577 and ES01678 to Kirill Kiselyov. I would like to thank the University of Pittsburgh's Genomic and Proteomic Facility for their efficient microarray analysis. I would also like to thank Paula Grabowski and Jon Boyle at the University of Pittsburgh for discussion about these microarray data.

# 4.0 TRPML3 BLOCK BY TRANSITION METALS

## 4.1 ABSTRACT

Chronic and acute exposures to transition metals cause a range of conditions such as liver and brain damage (201, 259). Transition metals enter cells through plasma membrane transporters and through endocytosis of extracellular medium, which includes free and bound forms of transition metals (65, 66, 196, 197). Toxic effects of transition metals are usually attributed to their ability to catalyze production of reactive oxygen species, leading to degeneration of organellar membranes and buildup of misprocessed material within the endocytic tract (201, 203, 260-266). Whether or not transition metals directly affect components of the endocytic machinery is not well understood. The recent identification of TRPML channels as critically important endocytic components responsible for ion fluxes through endocytic membranes suggests a new target for transition metal toxicity. Here we report that micromolar concentrations of $Co^{2+}$, $Cu^{2+}$, $Ni^{2+}$ and $Zn^{2+}$ block TRPML3, while $Fe^{2+}$ is significantly less effective in blocking TRPML3. Treatment of cells with 100 uM concentrations of transition metals leads to the formation of inclusion bodies, suggesting that endocytic function is impaired by these treatments. The *varitint-waddler* (*Va*) TRPML3 mutant and the homologous $TRPML1^{V432P}$ are insensitive to transition metal block. A cysteine residue near the channel pore contributes to TRPML3 sensitivity to transition metals and is conserved in TRPML1. These data

suggest that TRPML1 and TRPML3 may be blocked by transition metals, which could lead to cell toxicity if cells are exposed to high levels of transition metals.

## 4.2 INTRODUCTION

Transition metals are a group of elements comprising, among others, Co, Cu, Fe, Ni and Zn. They play major roles in key cellular processes such as respiration and therefore, they are indispensable for proper cell function. At the same time, transition metal overdose is a well-documented environmental hazard associated with food, water and air pollution caused by industry or by improper food storage and handling techniques (193, 261, 267-269). Acute and chronic exposure to high levels of transition metals induces degenerative processes in brain, liver and other tissues, manifesting as cirrhosis, gastroenteritis and dementia (201, 259).

Studies of transition metal toxicity have, primarily, focused on their effects in the cytoplasm (260, 261). Upon entering the cytoplasm through dedicated plasma membrane transporters such as Ctr1 (Slc31a1) (196, 197), or via the lysosomal route discussed below, transition metals catalyze production of reactive oxygen species (ROS), particularly in the mitochondria. The ROS destabilize mitochondrial membranes, resulting in release of cytochrome C, followed by cell death (260, 261). Hence, the wide use of metal chelation and neutralization of ROSs as treatments for metal toxicity.

In a majority of tissues, transition metals first enter cells through endocytosis of metal binding proteins such as ceruloplasmin and transferrin. Liberation of transition metals from the binding proteins in lysosomes is followed by metal absorption in the cytoplasm via transporters such as Slc11a2 (also called DMT1, NRAMP2) (65, 66) and, perhaps, other ion channels and

transporters. In the lysosomal lumen, transition metals catalyze Fenton reactions, resulting in the buildup of ROS, which in turn, facilitate production of indigestible material such as lipofuscin. Lipofuscin buildup in the lysosomes has been linked to autophagic and mitochondrial abnormalities in aging cells (262-264).

When the metal uptake exceeds the clearing capacity, lysosomes become overloaded with transition metals. The overload can occur due to abnormally high dietary metal uptake or genetic disorders of metal handling. It is important to note that metal overload frequently manifests as a buildup of undigested material captured during endocytoisis and retained in cytoplasmic storage bodies, a condition known as lysosomal storage disease. For example, liver samples of human and mouse $Cu^{2+}$ overload models showed inclusions similar to those in lysosomal storage diseases (201, 203). It is unlikely that the storage phenotype in transition metal toxicity models is exclusively a function of lipofuscin buildup. Indeed, a multitude of factors including ion channels and transporters coordinate the endocytic function. Among the lysosomal components whose inhibition by transition metals may lead to this storage phenotype are TRPML ion channels (270-272).

Several aspects of endocytic function depend on ion channel activity. They include regulation of lysosomal acidity, $Ca^{2+}$ release driving organellar fusion and, quite likely, absorption of metal ions across the lysosomal membrane (30, 32). This list is likely incomplete, as demonstrated by the relatively recent identification and characterization of the ion channels TRPML1 and TRPML3. The gene *MCOLN1* coding for TRPML1 is mutated in the lysosomal storage disease mucolipidosis type IV (MLIV) (273, 274). MLIV is a major lysosomal deficiency associated with cytoplasmic buildup of storage bodies, developmental delays and motor retardation. Due to its lysosomal localization, TRPML1 is assumed to have a role in the

lysosomal function, presumably in regulation of lysosomal ion homeostasis (pH, $Fe^{2+}$ or $Zn^{2+}$ content) and/or the release of $Ca^{2+}$ from the endocytic compartments that drives the organellar fusion (161, 186, 214, 221, 270, 275). The recent characterization of TRPML1 activation by $PI(3,5)P_2$ raised the possibility that this ion channel is activated by delivery to the $PI(3,5)P_2$ rich lower portions of the endocytic pathway or that it is a proximity sensor for endocytic organelles (9, 270).

TRPML3 is a close TRPML1 relative, which appears to be expressed in multiple endocytic vesicles including early endosomes and late endosomes. It is primarily expressed in the inner ear; the Varitint-waddler (*Va)* gain of function mutant of TRPML3 leads to massive degeneration of the hair cells causing deafness and a circling behavior phenotype (8, 20, 24-26, 271, 276). TRPML1 and TRPML3 are contradirectionally regulated by pH (8, 23, 26), which is consistent with their proposed site of function: TRPML3 is inhibited by low pH typically present in the lower portion of the endocytic pathway. While acute deletion (or overexpression) of TRPML1 or TRPML3 has been shown to inhibit various aspects of endocytic function including autophagy (14, 162, 277-279), clear demarcation of their roles in endocytosis has not been established.

TRPMLs are members of the TRP superfamily of ion channels, with which they share a 6 transmembrane domain architecture, with a putative pore region located in between the 5th and 6th transmembrane domains. TRPML1 contains a set of lysosomal targeting motifs whose deletion was shown to retain TRPML1 in the plasma membrane (271, 280). No localization signals have been shown for TRPML3 yet. Keeping in mind that transition metals have been shown to accumulate in the deeper portions of the endocytic pathway, we set out to establish whether or not they inhibit TRPMLs and whether this inhibition is a contributing factor to the

transition metal effect on lysosomes. Here we report that some transition metals block the TRPML3 channel and that the block depends on cysteine residues in the vicinity of the channel's pore. An "activating" mutation in TRPML3 and TRPML1, TRPML3$^{A419P}$ and TRPML1$^{V432P}$, is insensitive to transition metal blockage. Metal toxicity appears to cause endocytic malfunction, indicated by the buildup of storage bodies. However, the inhibition of TRPMLs by transition metals does not seem to be the sole factor responsible for the lysosomal storage defects observed in these cells as inclusion profiles differ between these treatment.

## 4.3 EXPERIMENTAL PROCEDURES

*Cell Culture:* HeLa and HEK293 cells were maintained in DMEM (Sigma-Aldrich, St Louis, MO) supplemented with 7% FBS, 100 µg/mL penicillin/streptomycin, and 5 µg/mL Plasmocin prophylactic (Invivogen, San Diego, CA). For siRNA KD, antibiotic free media was used. Metals were added directly to the DMEM.

*siRNA-mediated KD*: ON-TARGET plus siRNA were designed as described previously (162) and custom synthesized by Dharmacon (Lafayette, CO). The TRPML1 siRNA probe targeting the sequence 5'-CCCACATCCAGGAGTGTAA-3' in *MCOLN1* was used for all TRPML1 KD. The TRPML3 siRNA probe targeting the sequence 5'-CCAAUGGAUGACACAUAU-3' in *MCOLN3* was used for TRPML3 KD. Non-targeting control siRNA#1 (Sigma) was used as a negative control. 6-well plates were transfected using Lipofectamine 2000 (Invitrogen, Carlsbag, CA). Transfections were performed as described by manufacturer's protocol using 600 nM siRNA per well. All KDs were confirmed using SYBR-green based quantitative real-time RT-PCR.

*Clones and mutagenesis.* GFP-tagged TRPML1 and TRPML3 were obtained by cloning human TRPML1 and TRPML3 cDNA into pEGFP-N1 or pEGFP-C1 clones from Clontech (Mountain View, CA). TRPML3 clone was a gift from Shmuel Muallem (NIH, NIDCR). HA-tagged constructs were obtained by cloning into pCMV-HA vector from Clontech. All clones were verified by sequencing through GENEWIZ (South Plainfield, NJ) using primers designed by Grace Colletti. Site-directed mutagenesis was performed using the Gene Tailor$^{TM}$ Site-Directed Mutagenesis System from Invitrogen according to the manufacturer's protocol.

*Electrophysiology:* For conventional whole cell recording, cells were resuspended in DMEM and allowed to attach to a coverslip inside perfusion chamber. Transfected cells were identified by GFP fluorescence. Transmembrane currents were recorded using an HEKA EPC-10 amplifier (HEKA Instruments, Southboro, MA), stored in a PC and analyzed using Patchmaster and Origin software. Currents were digitized at 1 kHz and filtered through low-bandpass filter set at 5 kHz cutoff frequency. In whole cell mode, the pipette solution contained (in mm) 140 Cs-aspartate (to cancel endogenous $K^+$ and $Cl^-$ conductances), 5 Na-ATP, 5 $MgCl_2$, 10 HEPES, 10 BAPTA, pH 7.2. The standard bath solution contained (in mm): 150 NaCl, 5 KCl, 1 CaCl2, 1 MgCl2, 10 HEPES, pH 7.4. In some experiments, NaCl was replaced with NMDG-glutamate and 0 or 10 mm divalent metals were included in the bath solutions. The experiments were performed at room temperature. The solutions were applied by bath perfusion with ten volumes of the perfusion chamber. Pipette resistance was in the 2-8 MOhm range, and seal resistance was always over 1 GOhm. Series resistance and capacitance were compensated using the proprietary protocol included with Patchmaster.

*Electron Microscopy*: Electron microscopy was performed as previously described (162). In brief, cells were fixed using 2.5% glutaraldehyde in 0.1M Na-cacodylate, washed with 0.1M

Na-cacodylate, postfixed with a solution containing 1% OsO4, washed with PBS, and stained *en bloc* for uranyl acetate. After dehydration in ethanol, the samples were resin embedded, mounted on grids and analyzed with a transmission electron microscope (100CX; JEOL Ltd). For colloidal gold uptake experiments, 10-nm gold particles were coated with gelatin and BSA. The particles were washed and added to the cells for 1 hr and chased for 6 hr to load the endocytic pathway and then fixed for conventional electron microscopy. The images were analysed and inclusions were counted using ImageJ.

Statistical significance was calculated using a one-tailed, unpaired t-test with $p \leq 0.05$ considered significant. Data are presented as mean±S.E.M.

## 4.4 RESULTS

### 4.4.1 TRPML3 is activated by $PI(3,5)P_2$

TRPML3 was previously shown to reside in the plasma membrane in overexpression systems (8, 20-26), therefore we performed whole cell patch clamp analysis to determine the dynamics of this channel. For these studies, we expressed GFP-fused human TRPML3 in HEK 293 cells by transient cDNA transfection and tested its activity using whole cell patch clamp. In our system, we detected a fairly high rate of spontaneous wildtype TRPML3 activity: over 30% of cells (n=135) showed large inwardly rectifying currents characteristic of TRPML3 (Fig 4.1 B). C- and N-terminal GFP fusion constructs showed the same tendency. Currents were recorded with $Na^+$ and $Ca^{2+}$ as main charge carriers, at pH 7.4. Mock transfected cells did not show this activity (data not shown, n=8). The incidence and amplitude of TRPML3 activity was

dramatically increased when 5 or 20 μM $PI(3,5)P_2$ was included in the pipette solution (Fig 4.1). Some cells showed delayed activation of TRPML3 in the presence of $PI(3,5)P_2$; the delay likely representing $PI(3,5)P_2$ diffusion from the patch pipette into the cytoplasm (Fig 4.1C). The TRPML3 activation by $PI(3,5)P_2$ is not entirely surprising since the putative $PI(3,5)P_2$ binding motif previously identified in TRPML1 (9) is present in TRPML3 (TRPML1: $^{42}$RRR, $^{55}$KFRAKGRK, TRPML3: $^{39}$RR, $^{52}$KFWARGRK).

The functional significance of TRPML3 activation by $PI(3,5)P_2$ is unclear. $PI(3,5)P_2$ is believed to be restricted to the lower portions of the endocytic pathway, which is, ostensibly, outside or on the border of the TRPML3 functional range and localization. This is supported by the fact that wild type (WT) TRPML3, both spontaneously active and $PI(3,5)P_2$ activated, is inhibited by low pH (Fig 4.1A). It's possible that $PI(3,5)P_2$ activation of TRPML3 via an increase in local concentration or proximity sensing could result in a calcium efflux that in turn initiates SNARE mediated fusion, as was suggested for TRPML1. Fairly recent evolutionary separation between TRPML1 and TRPML3 (*C elegans* and *Drosophila* have only one mucolipin gene) could also suggest that at the present point of evolution, the functional specialization of these channels is at the stage of spatial segregation and may not (yet) involve specialization of signaling inputs.

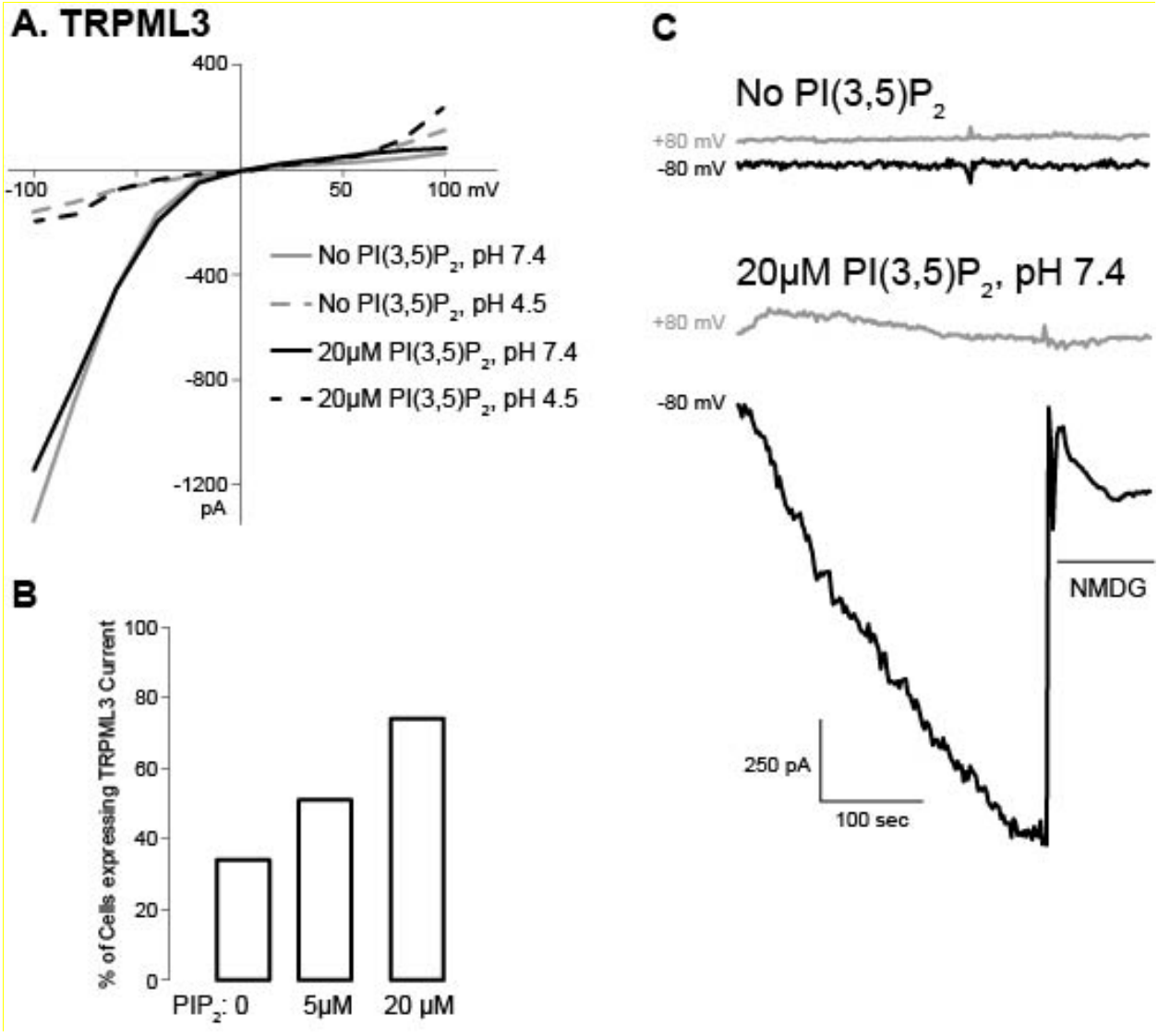


**Figure 4.1 TRPML3 activation by PI(3,5)P2.**
HEK 293 cells transfected with YFP-TRPML3 were analyzed using whole cell patch clamp with $Na^+$ and $Ca^{2+}$ as main charge carriers in the outside solution and $Cs^+$ - in the pipette solution. A) Current voltage curve of TRPML3 at different pH and presence/absence of $PI(3,5)P_2$. Data represent 2 to 35 experiments. B) Bar graph representing probability of detecting TRPML3 activity in the presence and absence of $PI(3,5)P_2$. Data represent 55 to 135 experiments. C) Current recording illustrating development of TRPML3 current in cells perfused with $PI(3,5)P_2$. Panel represents 10 to 14 experiments.

Transfected HA- or GFP-tagged human TRPML1 did not produce currents in the presence or absence of $PI(3,5)P_2$, at normal or low (4.5) pH (data not shown, n=13 and 31 respectively). Furthermore, deletion of the putative TRPML1 localization signals ($^{15}$LL and $^{577}$LL), previously shown to result in retention of the channel in the plasma membrane (5, 6) did

not result in spontaneous or $PI(3,5)P_2$ activated current activity under conditions of normal or low pH (data not shown, n=11 and 14 respectively). Since previous studies had observed WT TRPML1 current with lysosomal patches under the same conditions, we suggest that additional factors are involved in TRPML1 activation by $PI(3,5)P_2$ in the lysosomal context.

### 4.4.2 TRPML3 is blocked by transition metals

With the discovery of $PI(3,5)P_2$ activation of TRPML3, our lab performed further analysis on transition metal block of TRPML3. Addition of 1 to 100 µM of $Co^{2+}$, $Cu^{2+}$, $Ni^{2+}$, $Fe^{2+}$ and $Zn^{2+}$ to the bath solution (corresponding to the lumen of endocytic organelles) inhibited both spontaneous and $PI(3,5)P_2$ induced TRPML3 activity. The extent of inhibition varied between metals. Addition of 10-100uM of $Cu^{2+}$ and $Zn^{2+}$ consistently blocked the channel resulting in 70-90% inhibition at pH 7.4. The same concentrations of $Co^{2+}$ and $Ni^{2+}$ also had a strong inhibitory effect, ~60-75% channel block, although the extent of this block varied between experiments (Fig 4.2A, B). $Fe^{2+}$ was much less effective in blocking TRPML3 currents (Fig 4.2A, B).

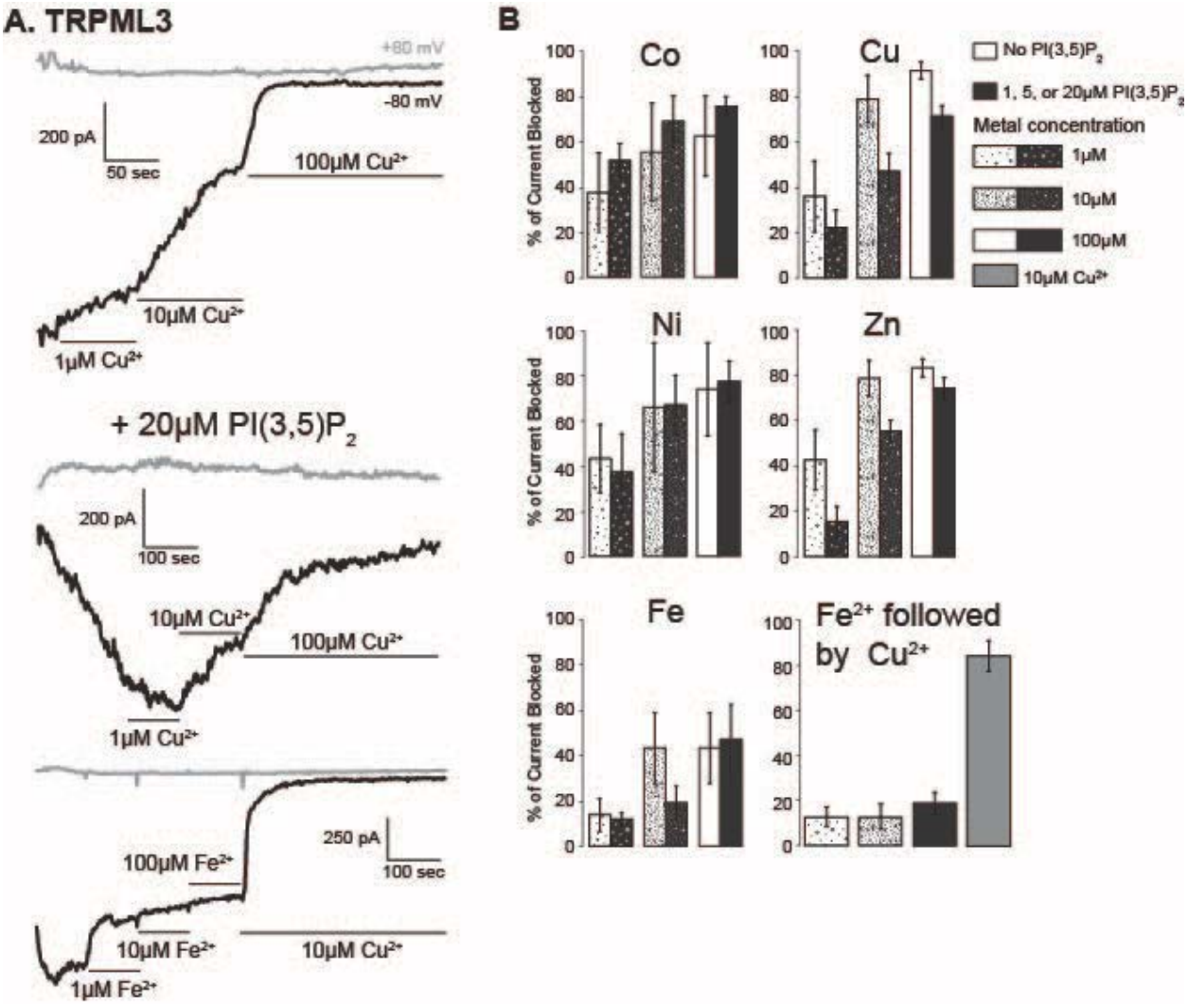


**Figure 4.2 TRPML3 block by transition metals.**
HEK 293 cells transfected with YFP-TRPML3 were analyzed using whole cell patch clamp with $Na^+$ and $Ca^{2+}$ as main change carriers in the outside solution and $Cs^+$ - in the pipette solution. A) Representative current traces. B) Bar graph representing relative efficacy of each metal tested in blocking TRPML3. Data are expressed as percentage of total current lost after application of the given metal concentration. Data represent 3 to 10 experiments.

The *Va* TRPML3 mutant A419P ($TRPML3^{Va}$) was previously shown to be spontaneously active and to have reduced sensitivity to pH (8, 20, 24-26, 271). Fig 4.3A shows that this remained true in our system. The vast majority of cells expressing $TRPML3^{Va}$ (n=18/24) showed spontaneously active currents; the current development in the presence of $PI(3,5)P_2$ described above for WT TRPML3 has not been detected in $TRPML3^{Va}$ expressing cells. $TRPML3^{Va}$ showed significantly reduced sensitivity to $Co^{2+}$ and $Cu^{2+}$; the efficacy of block fell to

approximately 20% (n=6 and 4 respectively, Fig 4.3A,B,D). This is consistent with large structural changes introduced to these mutants by the helix-breaking proline residue, as suggested previously (8).

The TRPML1 *Va* analogue, the V432P mutant, resulted in $PI(3,5)P_2$ insensitive spontaneously active current which was potentiated by low pH and by removal of divalent cations (Fig 4.2C). It also showed little sensitivity to transition metals (Fig 4.2D).

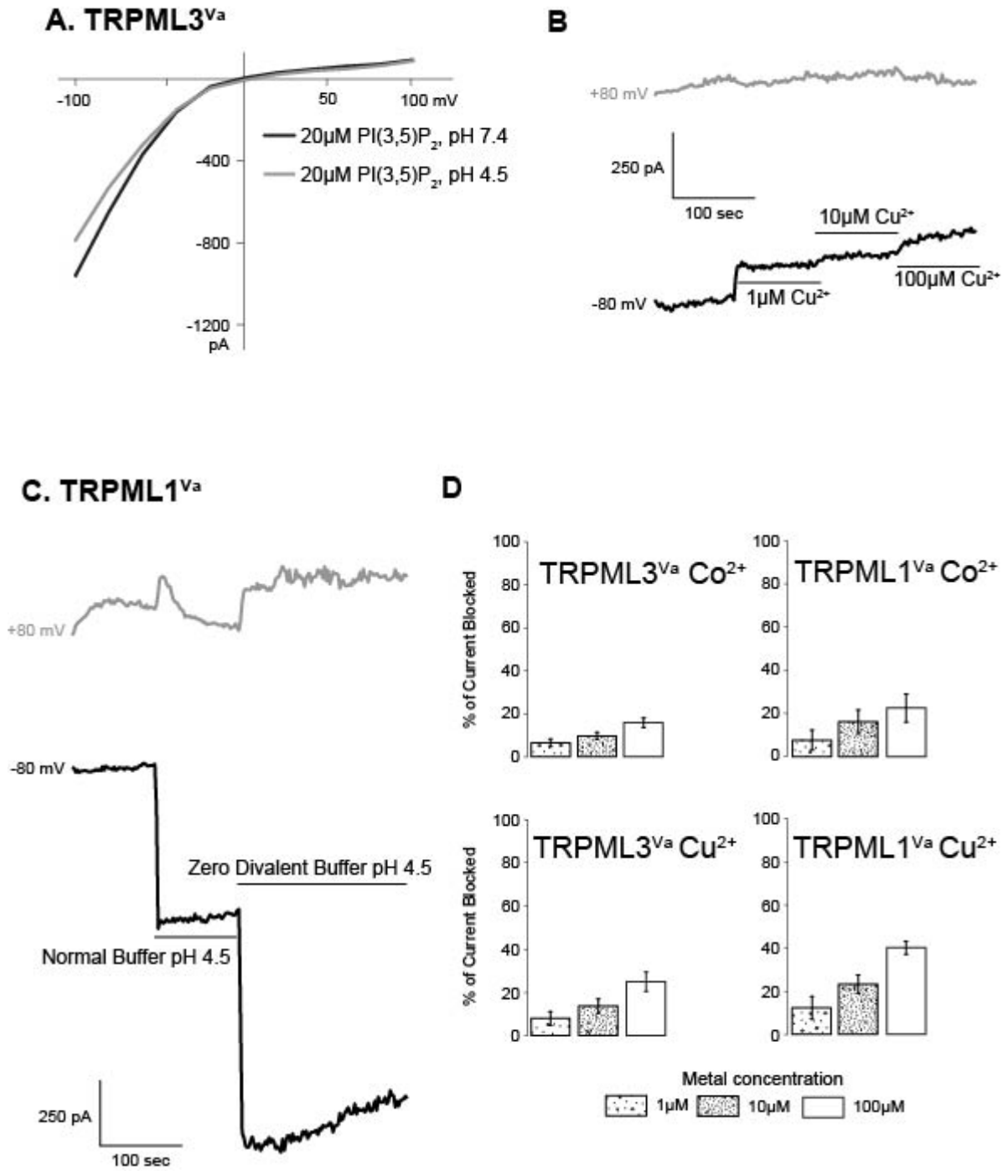


**Figure 4.3 The Va mutants and transition metals.**
HEK 293 cells transfected with YFP-TRPML3 were analyzed using whole cell patch clamp with $Na^+$ and $Ca^{2+}$ as main change carriers in the outside solution and $Cs^+$ - in the pipette solution. A,B) Current voltage relationship and current traces demonstrating insensitivity of the Va TRPML3 mutant (A419P, $TRPML3^{Va}$) to transition metals. C) Current trace showing potentiation of the Va TRPML1 (V432P, $TRPML1^{Va}$) current by low pH and divalent free external buffer. Data on panels A-C represent 3 to 10 experiments. D) Bar graphs representing the efficacy of $Co^{2+}$ and $Cu^{2+}$ in blocking the $TRPML1^{Va}$ and the $TRPML3^{Va}$. Please note significant loss of blocking efficacy compared to data on WT TRPML3 shown in Fig 2B. The loss of blocking efficiency in Va mutants was statistically significant (at $p<0.05$ level, when compared with WT) under all conditions. Data represent 4 to 6 experiments.

Cysteine residues were previously implicated in metallothionesins and their transcription factors to reduce metal toxicity and oxidative stress (281)**.** In order to explore their role in TRPML3 block by transition metals, we substituted a cysteine near the pore of TRPML3 for serine: C450S. This mutation did not affect the TRPML3 current voltage curve (Fig 4.4A) and did not preclude TRPML3 gating by 20μM $PI(3,5)P_2$ (75% activation n=32) (Fig 4.4B). However, it did significantly suppress the ability of $Co^{2+}$ and $Cu^{2+}$ to block TRPML3 (Fig 4.4B,C). We conclude that C450 in TRPML3 is at least partially responsible for the block of TRPML3 by transition metals. No detectable activity was observed with the TRPML1 C436S mutant (n=6) suggesting that this mutant preserves the functional regulation of the WT TRPML1.

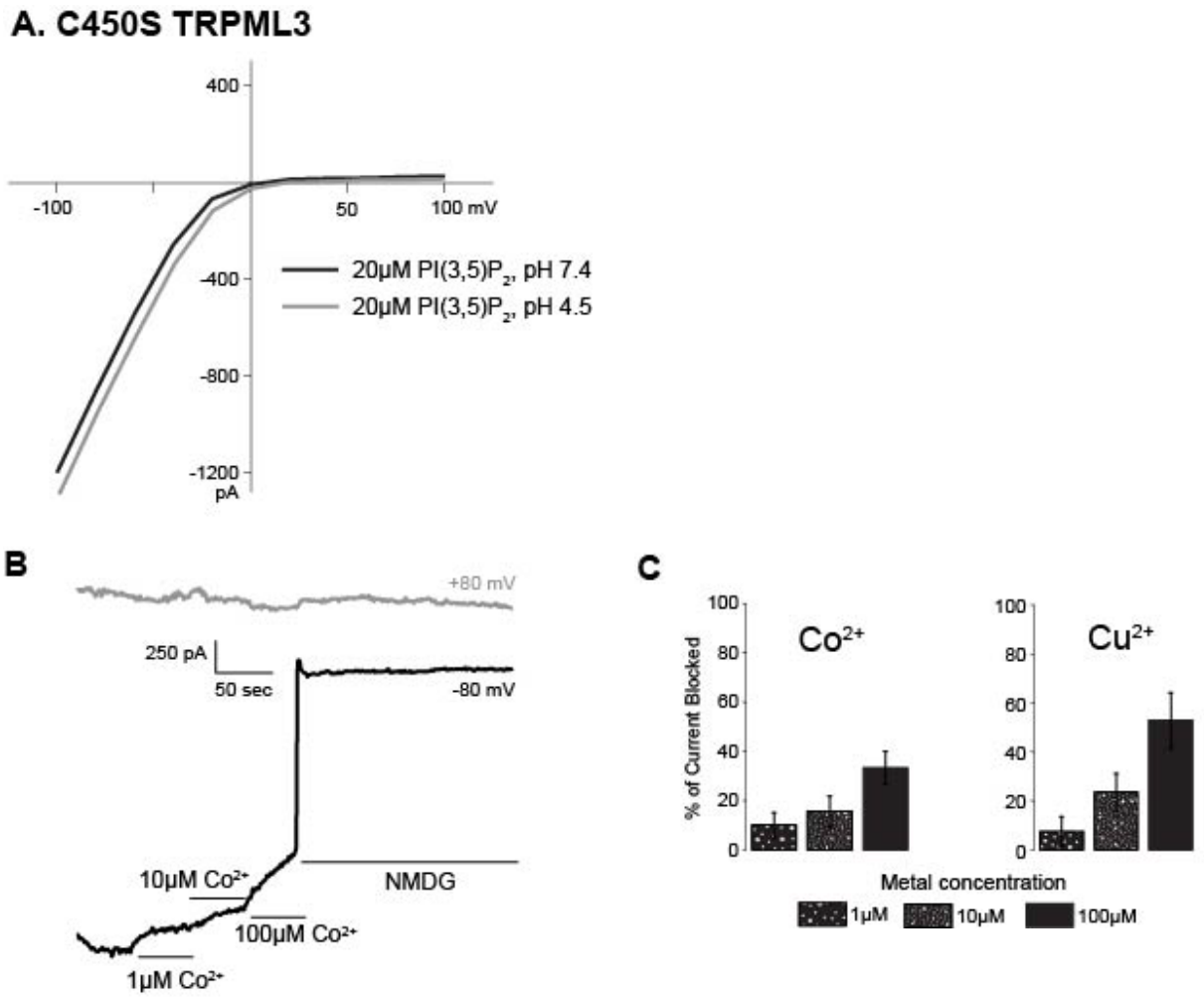


**Figure 4.4 Cysteine residues in TRPML3 and block by transition metals.**
HEK 293 cells transfected with YFP-TRPML3 were analyzed using whole cell patch clamp with $Na^+$ and $Ca^{2+}$ as main change carriers in the outside solution and $Cs^+$ - in the pipette solution. A) Current voltage relation of C450S TRPML3 current at normal and low pH. Note the loss of pH dependent TRPML3 inhibition with the cysteine mutant. B, C) Current traces and bar graph demonstrating decreased sensitivity of C450S TRPML3 to transition metals compared to WT TRPML3 (Fig 2). The loss of blocking efficiency in C450S mutants was statistically significant (at $p<0.05$ level, when compared with WT) under all conditions, except 100 μM $Cu^{2+}$ ($p=0.12$). Data represent 2 to 10 experiments. $PI(3,5)P_2$ was present in the pipette solution in these experiments.

### 4.4.3 Significance of TRPML block by transition metals.

TRPMLs are among many ion channels, transporters and enzymes active in the endocytic pathway. The biochemistry of transition metals in this pathway is far from being completely

understood. In order to delineate the impact of TRPML block on lysosomal function, we compared the types of storage bodies that accumulate in cells shortly after acute KD of TRPML1 and TRPML3 and in cells treated with transition metals. If TRPML1 and TRPML3 block by transition metals is the sole cause of early lysosomal abnormalities induced by transition metals, then a) the ability of a metal to block TRPML would correlate with its ability to induce inclusions, and b) the types of storage bodies accumulating in metal treated and TRPML deficient cells would be the same.

To test these assumptions, HeLa cells were treated with TRPML1 and TRPML3 specific siRNA for 24 to 72 h and TRPML1 and TRPML3 KD were verified by RT-PCR (Fig 4.5A). In a separate set of experiments utilizing microarray technology we observed little change in TRPML3 mRNA under the conditions of TRPML1 KD (116% and 107% of control levels; n=2). Previous reports estimated TRPML1 half-life in lysosomes to be several hours (6) and our previous experiments show that under the same conditions, TRPML1 protein is almost completely eliminated within 6 hours of transfection (162). Fig 4.5B shows that TRPML1 and TRPML3 KD resulted in a buildup of storage bodies similar to those seen in MLIV. Within 24 hours of treatment, storage bodies began to accumulate in cells exposed to transition metals (Fig 4.5C). Metal treated cells contained types of inclusion profiles that were scarcely observed in TRPML knockdown cells (Fig 4.5D). Therefore, the block of TRPML channels by transition metals is not the sole cause of inclusion body formation in these cells. However, that is not to say that block of these channels does not contribute to the formation of cellular inclusions and endocytic malfunction. Preliminary data in our lab suggests that treatment of cells with transition metals or TRPML3 KD both lead to similar trafficking defects. These findings further suggest that transition metal overload inhibits TRPML function, driving these endocytic defects.

Therefore, the differences we observe in storage bodies between TRPML KD and metal treated cells may be due to the fact that transition metals produce additional and compounding effects in addition to TRPML block, resulting in morphologically different inclusion profiles.

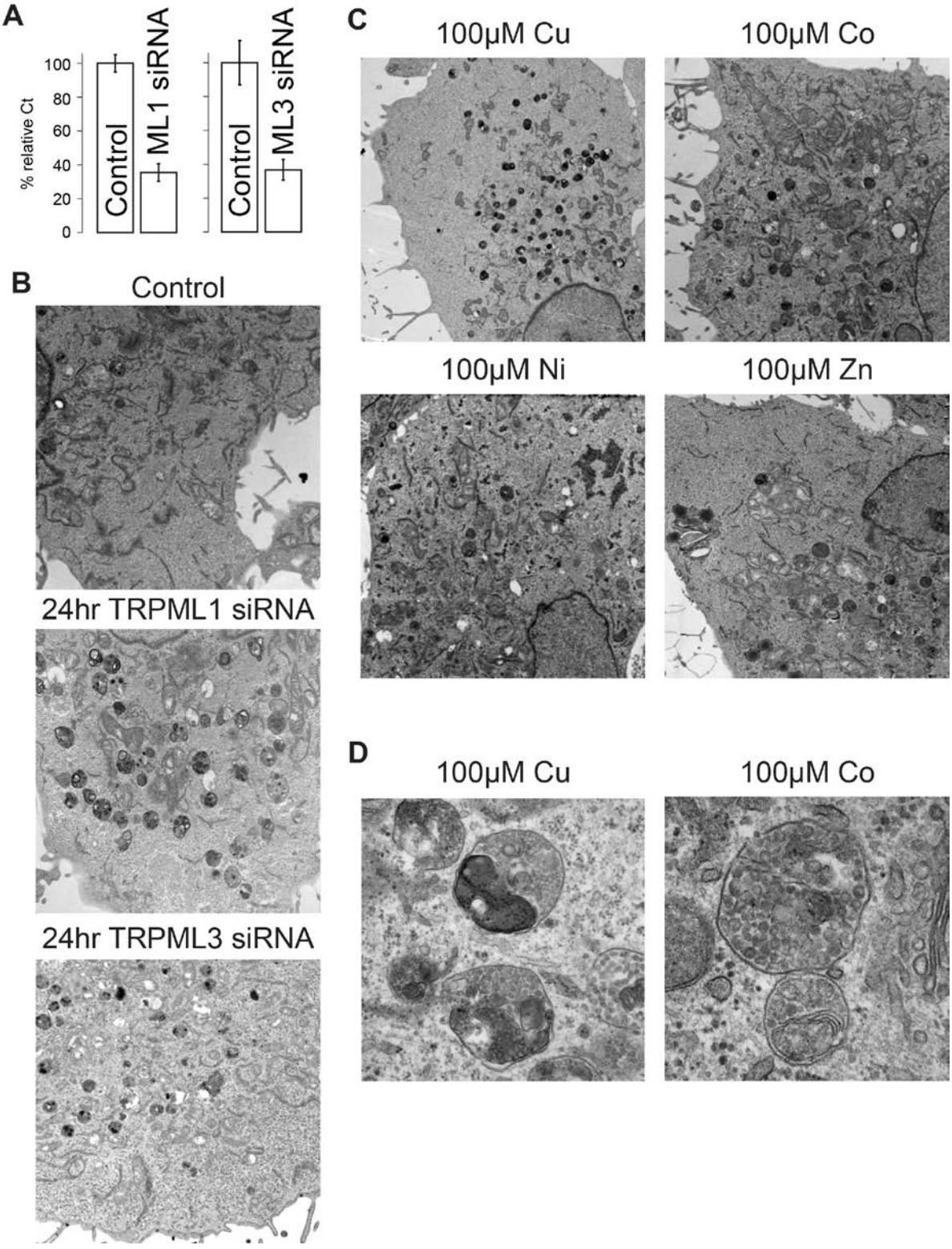


**Figure 4.5 Ultrastructural comparison of TRPML KD and metal treated cells.**
A) Bar graph demonstrating siRNA efficacy of TRPML1 and TRPML3 KD in HeLa cells. B,C) Electron micrographs of HeLa cells treated for 24 hr with TRPML1 and TRPML3 siRNA (B) or with transition metals (C). Note accumulation of storage bodies under these conditions. D. Zoom in images of inclusions.

Close examination of storage bodies suggested 10 distinct types illustrated in Fig 4.6A. The inclusions are (or once were) parts of the endocytic pathway, since they could be loaded by the fluid phase marker BSA-conjugated colloidal gold (Fig 4.6B). Classifying the storage body types allowed us to calculate and compare inclusion indexes under various conditions.

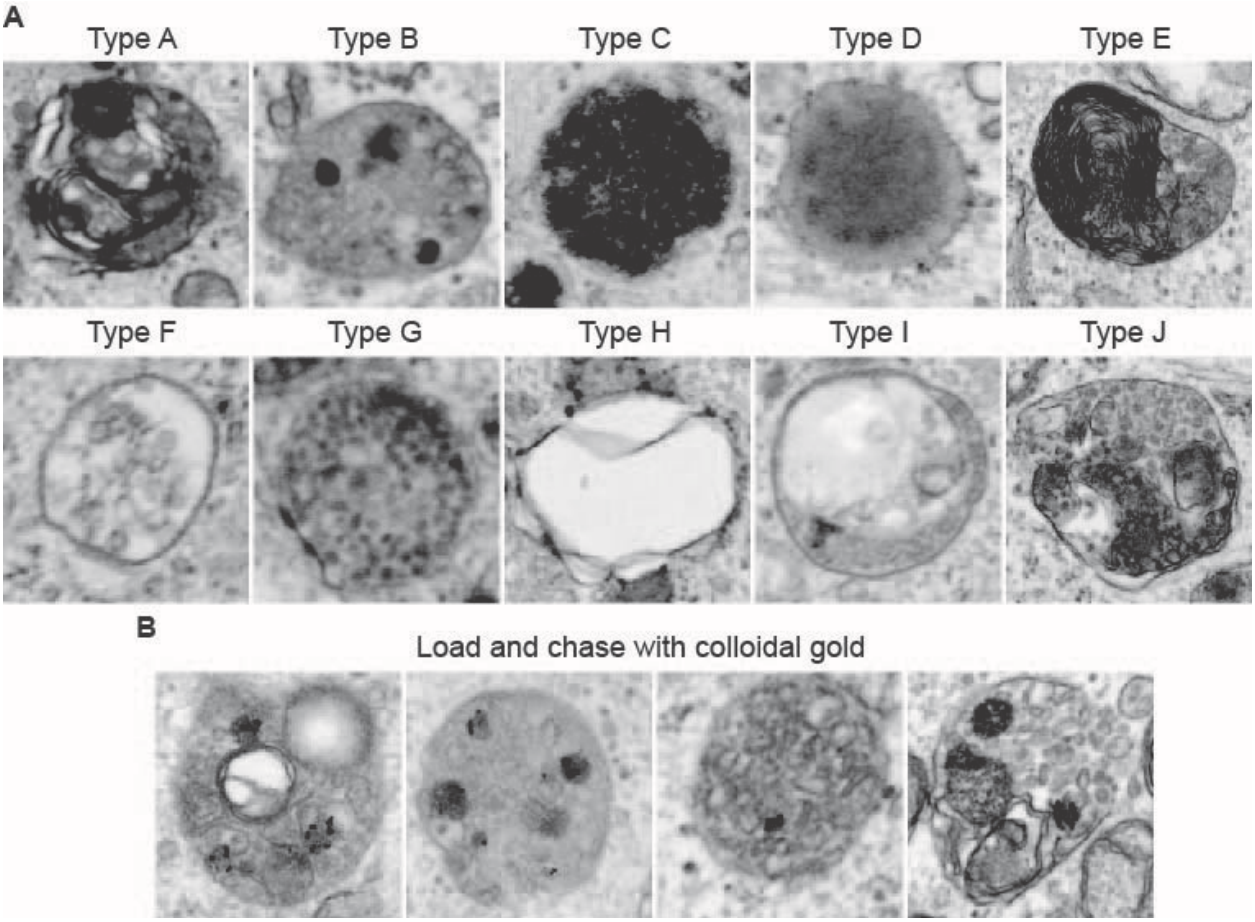


**Figure 4.6 Inclusion types in metal treated and siRNA transfected HeLa cells.**
A) Representative inclusions of the 10 different cellular inclusion profiles observed in HeLa cells. B) Examples of inclusions loaded with colloidal gold.

TRPML1 and TRPML3 KD resulted in accumulation of cytoplasmic inclusions in a time dependent manner, displaying essentially the same profiles of inclusions (Fig 4.7A,B). This result suggests that while TRPML1 and TRPML3 are likely distinct in their specific functions,

their loss has similar downstream targets and effects. Fig 4.7A shows that the total amount of inclusions accumulated in metal treated cells did not correlate with the severity of TRPML3 block by these metals. Fig 4.2B shows that while $Cu^{2+}$ and $Zn^{2+}$ are similarly efficient in blocking TRPML3, $Cu^{2+}$ is more effective than $Zn^{2+}$ in causing inclusions. Furthermore, the inclusion profiles observed in metal treated and TRPML1/TRPML3 siRNA treated cells differed: the predominant type of inclusions in TRPML1 and TRPML3 KD cells was scarcely observed in metal treated cells (Fig 4.7B). We conclude that TRPML inhibition by transition metals is not the sole defining factor in the lysosomal aspects of transition metal toxicity.

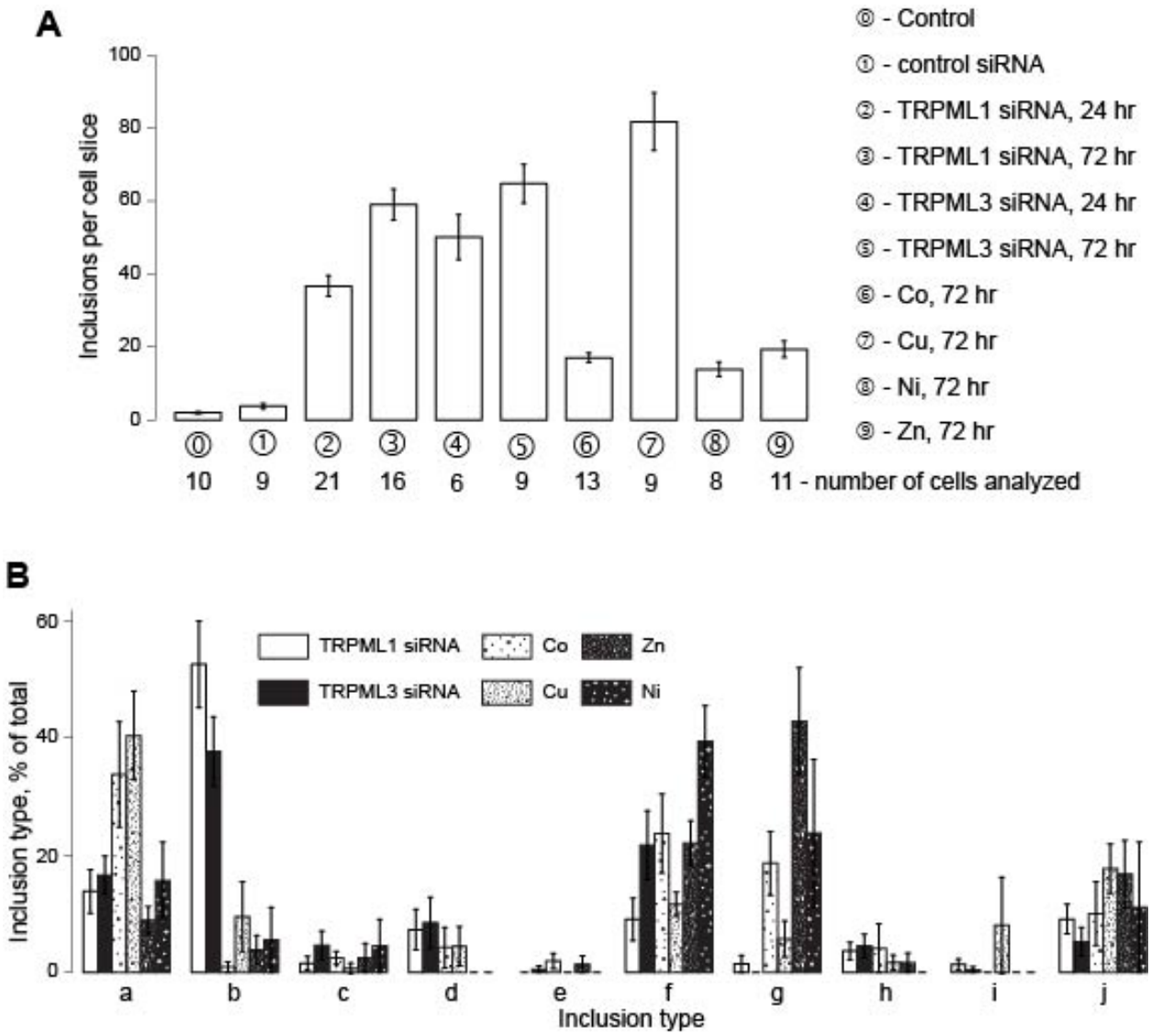


**Figure 4.7 Inclusion profiles in metal treated and TRPML siRNA transfected HeLa cells.**
A) The total number of inclusions per cell slice under different conditions. Metals were used at 100μM. Numbers below the bars represent conditions and number of cell slices used for analysis. Note that the number of inclusions in $Cu^{2+}$ treated cells is much higher than the number of inclusion in $Zn^{2+}$ treated cells, while $Zn^{2+}$ and $Cu^{2+}$ efficiency in blocking TRPML1 is about the same (Fig 2) B) Bar graph representing percentile value of each inclusion type in total number of inclusions per cell slice under different experimental conditions. Note that TRPML KD and metal treatments result in accumulation of different types of inclusions.

## 4.5 DISCUSSION

Lysosomal digestive machinery is very complex in content and function. Its activity depends on a plethora of factors coordinating fusion and fission events, digestive enzymes and supporting proteins, metabolite transporters as well as ion channels, carriers and pumps responsible for proper ion balance and transmembrane ion release events. Here we have shown that one of the important components of the endocytic machinery – ion permeation through TRPML channels, is inhibited by transition metals. The inhibition seems to depend on a cysteine residue near the putative pore of the channels.

Our data is in agreement with previously published studies that utilized the *Va* mutations in TRPML1 and TRPML3 but indicates that WT TRPML1 activity may depend on additional lysosomal factors for activation (8). The spontaneous, constitutive activity of the *Va* mutant channels and the role of the cysteine pore residue in transition metal permeability suggests that the *Va* mutation places the pore in an open state that blocks the full interaction of transition metals with the cysteine residue.

The functional significance of TRPML block by transition metals remains to be established. Here we proposed that comparative analysis of storage bodies in TRPML deficient and metal treated cells as a test of whether or not the functional consequences of TRPML loss and metal treatment are the same. The fact that different inclusion profiles are seen in TRPML KD and metal treated cells suggests, especially since the profiles vary between metals, that, in addition to TRPML, transition metals affect other components of the endocytic pathway. Comparison of the inclusion profiles in TRPML KD cells and in cells treated with transition metals indicates that both treatments result in the buildup of storage bodies, however their composition varies. Also, these data suggest that although transition metal buildup in TRPML

KD cells may contribute to disease pathology or substrate buildup, it is not the sole cause of inclusion body formation in these cells. A detailed investigation of the effects of transition metals on specific components of lysosomal digestive machinery, including TRPML channels will help elucidate their place in the lysosomal aspects of transition metal toxicity.

## 4.6 ACKNOWLEDGEMENTS

This work was supported by the National Institutes of Health grants HD058577 and ES01678 to Kirill Kiselyov. I'd like to thank several members of the lab for their specific contributions. First, Austen Terwillinger and Jeffrey Lee for their contribution in measuring TRPML3 activity. For the electron microscopy and inclusion profiling work, I'd like to thank Youssef Rbaibi, Christopher Lyons, and James Quinn. This work would not be possible without the help of the Center for Biologic Imaging at the University of Pittsburgh and Tom Harper at Department of Biological Science, University of Pittsburgh for invaluable help with electron microscopy. We thank Dr. Haoxing Xu for fruitful discussion.

# 5.0 CONCLUSIONS AND FUTURE DIRECTIONS

This work spans several aspects of TRPML1 function. The major focus of my work has been to understand the protein and transcriptional changes caused by TRPML1 loss in order to delineate cell death and inflammatory pathways that may be activated in MLIV. Such studies may provide valuable information for understanding the primary downstream effects caused by TRPML1 loss, as well as providing insight into properly treating this disorder. Below is a summary of this work, illustrated in Figure 5.1.

TRPML1 loss leads to both protein and transcriptional changes. At the lysosomal level, TRPML1 loss specifically results in CatB and LAMP1 increase, as well as a decrease in LAL. The increase in CatB seems to be caused by decreased secretion (Fig 5.1.1.), and was not altered at the transcriptional or translational levels. Whether these are the only lysosomal changes will need to be further evaluated. One method to do this would be to compare lysosomal protein profiles using a 2-D DIGE analysis, comparing control and TRPML1 KD cells. I attempted this method, successfully isolating and analyzing lysosomal fractions; however, the analysis identified several non-lysosomal components. Therefore, this method will need to be revised in the future, possibly by using a more stringent lysosomal isolation protocol as well as collecting cells grown in low-serum media, in order to limit the amount of background substrates.

From our protein analysis, we found that CatB is released into the cytosol of TRPML1 KD cells as seen in Figure 5.1.2. This leak is accompanied by an increase in CatB and Bax

dependent apoptosis (Fig 5.1.4, 5). Furthermore, inhibition of Bax did not significantly decrease cytosolic CatB levels suggesting that Bax activation is downstream of CatB release. Apoptosis was measured using a Caspase-3 activity assay. Future work will focus on elucidating these cell death pathways. Preliminary Western blot and fluorogenic data (not shown) suggests that Caspase-9 and Caspase-8 are not activated by TRPML1 KD, while cytochrome C is released from the mitochondria. Previous studies have shown that during the induction of apoptosis, Bid can translocate from the cytoplasm to the mitochondria and bind Bax, resulting in a conformation change which induces insertion of Bax into the outer mitochondrial membrane and release of cytochrome C. This process has been shown to be caspase independent and cathepsin dependent (158, 282). It has also been shown that Bax can activate p53-driven cell death pathways independent of caspase activity. In this study, Caspase-3 was still activated but was not contributing to p53-driven cell death, demonstrating that multiple cell death pathways can occur simultaneously (283). Therefore identifying whether Caspase-3 is activated downstream of Bax activation and cytochrome C release will help clarify TRPML1 mediated apoptosis. For example, we will test whether CatB inhibition blots Bax activation and whether Bax inhibition prevents cytochrome C release in TRPML1 KD cells. Since we see Caspase-3 activation in our cells, which appears to be independent of Caspase-8 and Caspase-9, we can also test whether p53 is activated in these cells. Another possibility, is that Bax and Cathepsin B are functioning in separate pathways. One study found that Cathepsin driven apoptosis functioned independently of Bid, suggesting that the Bid/Bax pathway and Cathepsin-mediated apoptosis may play a role in two separate pathways (284). Therefore, we will also evaluate alternative routes of cell death in our TRPML1 KD, such as necrosis. It may be possible that multiple pathways are simultaneously being activated in these cells. One interestingly possibility, given that TRPML1

is suggested to be an $Fe^{2+}$ release channel (161), is that a buildup of $Fe^{2+}$, which has been shown to drive lysosomal ROS production and cause lysosomal permeabilization (285), could be driving this pathway.

The changes we observe in CatB, LAMP1, and LAL (members of the "CLEAR" network of lysosomal genes) in our TRPML1 KD are independent of transcriptional changes. This suggests that the "CLEAR" network may be activated by greater amounts of endocytic stress, not seen in the early stages of TRPML1 loss. Interestingly, through our microarray analyses, we saw consistent changes in non-lysosomal genes outside of the "CLEAR" network. Preliminary analysis showed that the p50/p105 subunit of NFκB was associated with a large percentage of these genes and was upregulated (~20-40%) after TRPML1 KD. Further analysis showed that these changes resulted in increased p50 protein levels as well as nuclear translocation of this transcription factor as modeled in Figure 5.1.7. These changes appear to be independent of CatB release. An interesting observation made in previous studies links NFκB to pro-inflammatory responses, such as those seen in MLIV and other LSDs. This suggests that NFκB upregulation in response to TRPML1 loss may drive these inflammatory responses (Fig 5.1.8), which may modulate the pathogenesis of MLIV (Fig 5.1.9). Further work will need to be done to determine if NFκB is contributing to the inflammatory responses seen in this disease.

Delineating the p50 NFκB pathway in TRPML1 KD cells will be the focus of future work in the lab. Analysis of candidate genes after NFκB modulation will confirm whether this transcription factor is suppressing or activating these genes. Furthermore, elucidating the pathways that result in NFκB upregulation may help us dissect the early steps of TRPML1 KD. Preliminary results suggest that CatB release may be linked to NFκB upregulation, as CatB KD inhibited NFκB increase (data not shown). Caspase-1, a known substrate of CatB and an

activator of the NFκB pathway, was not activated in our KD cells. However, NFκB regulation is a complex pathway, which can be modulated by several inputs; therefore a more detailed analysis of its activation as well as downstream effects will be the target of future work in the lab.

These data demonstrate that the immediate effects of TRPML1 loss result in dynamic and complex cellular changes, which may modulate cell death. These studies are the first to address the early stages of TRPML1 loss, in the context of cell death. Studies focused on these early events will hopefully clarify the primary defects of MLIV, driving a better understanding of both endocytic function and how to treat lysosomal disorders arising from non-enzymatic protein loss.

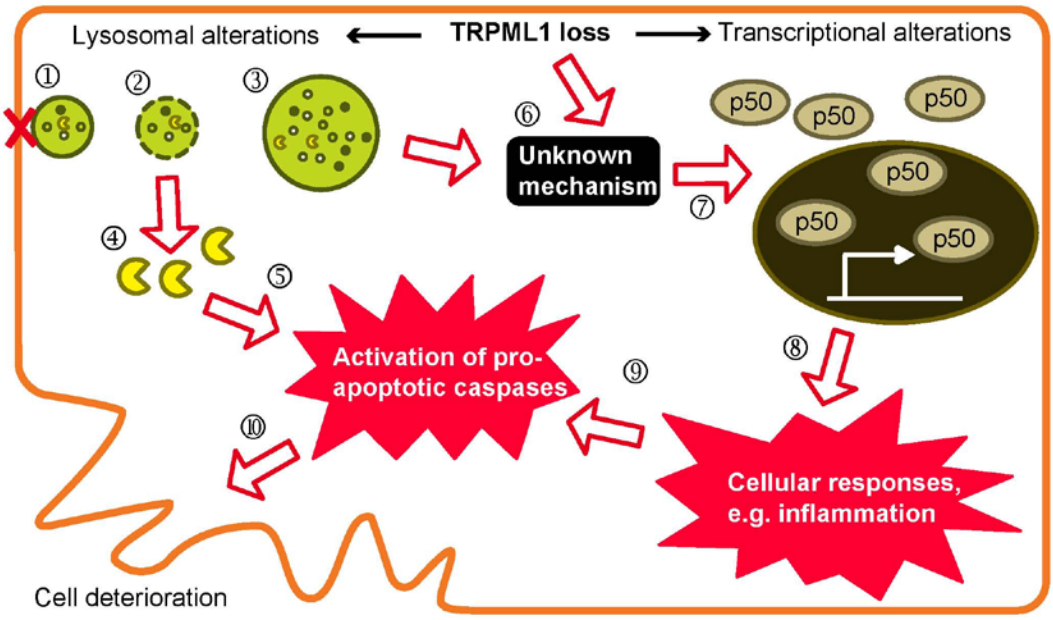


**Figure 5.1 Model representing changes in TRPML1 KD cells and how these may contribute to cellular malfunction.**
TRPML1 KD or loss of another lysosomal component results in lysosomal alterations (1) such as impaired secretion, fusion or enzymatic activity, leading to the appearance of storage bodies (3). The buildup and release of lysosomal enzymes such as CatB into the cytosol due to lysosomal permeabilization (2) results in cleavage of proapoptotic factors (4-5). In response to TRPML1 KD, NFκB levels are upregulated (7) by an unknown mechanism either in direct response to TRPML1 KD or in response to altered lysosomal integrity (6). Changes in TF activity and levels may result in cellular changes such as activation of inflammatory responses (8) and could contribute, alleviate, or exacerbate apoptotic activation (9) leading to cell death (10).

The remainder of my work was focused on characterizing the function and activity of TRPML channels. Due to the lack of TRPML1 expression at the plasma membrane, even under overexpressing conditions, we focused our work on TRPML3, the closely related relative. I performed the preliminary work using patch clamp analysis, studying TRPML3 block by transition metals, activity of the constitutively active TRPML$^{Va}$ mutants, and analyzing the activity of TRPML3 mutants in order to identify key residues that regulate TRPML3 activity (discussed in Appendix B). This project was taken over by several members of the lab, who completed the patch clamp analysis and electron microscopy profiling of TRPML3. Our work is in agreement with previously published papers, which analyzed TRPML function, and provide a unique profiling of transition metal blockage of these channels.

Interestingly, our patch clamp analysis as well as similarities between TRPML1 and TRPML3 KD (discussed in Appendix B), suggest that there may be similarities shared between these channels. However, the localization of these channels suggests that they may function in mutually exclusive cellular compartments. In support of this, TRPML1 does not localize to the plasma membrane, as does TRPML3. Furthermore, a dileucine mutation, which targets TRPML1 to the plasma membrane, is not active in our system, suggesting that it requires localization to the lysosome (likely due to $PI(3,5)P_2$ and possibly other adaptor proteins present at the lysosome) for proper function. Taken together, our data suggest that TRPML channels share similar activity profiles; however they have evolved to work in specific environments, which likely drive their specific cellular functions.

My work will add a new level of understanding to MLIV research, providing a clearer depiction of cell death caused by TRPML1 loss as well as characterizing TRPML1 function and its relationship to TRPML3. These studies also leave several questions unanswered, which will

be addressed in the future by the Kiselyov Lab. For example: what is the role of NFκB in TRPML1 loss, do the changes we see modulate disease pathology, and do TRPML1 and TRPML3 play redundant roles in the endocytic pathway? These few examples point, I think, to the major direction of this project, which will be dissecting the pathways activated by TRPML1 loss in order to elucidate the context of TRPML1 function and how the cell senses/responds to its loss. It is clear that our knowledge of the endocytic pathway and its complexity is ever growing; therefore, using defects in this pathway as a tool to study its function is a major driving force to understanding the pathway. This novel approach to studying the immediate effects of LSD pathogenesis may open a new system to study the endocytic pathway and reveal cellular dynamics that we were previously unaware of.

# APPENDIX A

## A.1 MICROARRAY GENE CANDIDATES

**Table.A.1 Gene candidates from TRPML1 KD microarray**

| | Gene | Description |
|---|---|---|
| Downregulated genes | ANAPC13 | Homo sapiens anaphase promoting complex subunit 13 (ANAPC13). |
| | CIRBP | Homo sapiens cold inducible RNA binding protein (CIRBP). |
| | HNRPH2 | Homo sapiens heterogeneous nuclear ribonucleoprotein H2 (H') (HNRPH2), transcript variant 1. |
| | MGC24039 | Homo sapiens hypothetical protein MGC24039 (MGC24039). |
| | RDH10 | Homo sapiens retinol dehydrogenase 10 (all-trans) (RDH10). |
| | RPL15 | Homo sapiens ribosomal protein L15 (RPL15). |
| | SNCG | Homo sapiens synuclein, gamma (breast cancer-specific protein 1) (SNCG). |
| Upregulated genes | BCAR3 | Homo sapiens breast cancer anti-estrogen resistance 3 (BCAR3). |
| | BIVM | Homo sapiens basic, immunoglobulin-like variable motif containing (BIVM). |
| | CAP2 | Homo sapiens CAP, adenylate cyclase-associated protein, 2 (yeast) (CAP2). |
| | CPLX1 | Homo sapiens complexin 1 (CPLX1). |
| | ERO1L | Homo sapiens ERO1-like (S. cerevisiae) (ERO1L). |
| | GDAP1 | Homo sapiens ganglioside-induced differentiation-associated protein 1 (GDAP1), transcript variant 1. |
| | HCN3 | Homo sapiens hyperpolarization activated cyclic nucleotide-gated potassium channel 3 (HCN3). |
| | IRAK2 | Homo sapiens interleukin-1 receptor-associated kinase 2 (IRAK2). |
| | KRT17 | Homo sapiens keratin 17 (KRT17). |
| | KRT80 | Homo sapiens keratin 80 (KRT80), transcript variant 1. |
| | MAL2 | Homo sapiens mal, T-cell differentiation protein 2 (MAL2). |
| | PAQR4 | Homo sapiens progestin and adipoQ receptor family member IV (PAQR4). |
| | PTBP2 | Homo sapiens polypyrimidine tract binding protein 2 (PTBP2). |
| | PTPLB | Homo sapiens protein tyrosine phosphatase-like (proline instead of catalytic arginine), member b (PTPLB). |
| | QSOX2 | Homo sapiens quiescin Q6 sulfhydryl oxidase 2 (QSOX2). |
| | RAI14 | Homo sapiens retinoic acid induced 14 (RAI14). |
| | SCG2 | Homo sapiens secretogranin II (chromogranin C) (SCG2). |

| | | |
|---|---|---|
| | SIX4 | Homo sapiens SIX homeobox 4 (SIX4). |
| | SLC2A3 | Homo sapiens solute carrier family 2 (facilitated glucose transporter), member 3 (SLC2A3). |
| | SLC25A19 | Homo sapiens solute carrier family 25, member 19, nuclear gene encoding mitochondrial protein. |
| | SNAP25 | Homo sapiens synaptosomal-associated protein, 25kDa (SNAP25), transcript variant 2. |
| | SOCS2 | Homo sapiens suppressor of cytokine signaling 2 (SOCS2). |
| | TMEM145 | Homo sapiens transmembrane protein 145 (TMEM145). |
| | VGF | Homo sapiens VGF nerve growth factor inducible (VGF). |
| | WDR22 | Homo sapiens WD repeat domain 22 (WDR22). |

**Table A.2 Gene candidates for PPT1 KD microarray**

| Gene | Description | Gene | Description |
|---|---|---|---|
| LOC100129882 | PREDICTED: Homo sapiens similar to mCG49427 (LOC100129882) | KRT17 | Homo sapiens keratin 17 (KRT17). |
| MORF4L1 | Homo sapiens mortality factor 4 like 1 (MORF4L1), transcript variant 2. | KRT17P3 | PREDICTED: Homo sapiens misc_RNA (KRT17P3), miscRNA. |
| ALS2CR4 | Amyotrophic lateral sclerosis 2 chromosome region, candidate 4, variant 1. | KRTCAP2 | Homo sapiens keratinocyte associated protein 2 (KRTCAP2). |
| ANG | Homo sapiens angiogenin, ribonuclease, RNase A family, 5 (ANG), variant 2. | LOC100132377 | PREDICTED: Homo sapiens hypothetical protein LOC100132377. |
| ANXA2 | Homo sapiens annexin A2 (ANXA2), transcript variant 1. | LOC645638 | PREDICTED: Homo sapiens misc_RNA (LOC645638), miscRNA. |
| ANXA2P1 | Homo sapiens annexin A2 pseudogene 1 (ANXA2P1) on chromosome 4. | LOX | Homo sapiens lysyl oxidase (LOX). |
| ANXA3 | Homo sapiens annexin A3 (ANXA3). | LPP | Homo sapiens LIM domain containing preferred translocation partner in lipoma (LPP). |
| ARMET | Homo sapiens arginine-rich, mutated in early stage tumors (ARMET). | MGC4677 | Homo sapiens oxidized low density lipoprotein (lectin-like) receptor 1 (OLR1). |
| ARNT2 | Homo sapiens aryl-hydrocarbon receptor nuclear translocator 2 (ARNT2). | MRLC2 | Homo sapiens protein disulfide isomerase family A, member 5 (PDIA5). |
| ARPC1A | Homo sapiens actin related protein 2/3 complex, subunit 1A, 41kDa (ARPC1A). | NAMPT | Homo sapiens protein disulfide isomerase family A, member 6 (PDIA6). |
| ASNS | Homo sapiens asparagine synthetase (ASNS), transcript variant 1. | NFIB | Homo sapiens SCO cytochrome oxidase deficient homolog 1 (yeast) (SCO1), nuclear gene encoding mitochondrial protein. |
| C1GALT1C1 | C1GALT1-specific chaperone 1 (C1GALT1C1), transcript variant 1. | NIPA1 | Homo sapiens stromal cell-derived factor 2-like 1 (SDF2L1). |

| | | | |
|---|---|---|---|
| C1ORF218 | Homo sapiens chromosome 1 open reading frame 218 (C1orf218). | NPC1 | Homo sapiens SEC11 homolog C (S. cerevisiae) (SEC11C). |
| CAV2 | Homo sapiens caveolin 2 (CAV2), transcript variant 1. | NT5E | Homo sapiens sel-1 suppressor of lin-12-like 3 (C. elegans) (SEL1L3). |
| CCL5 | Homo sapiens chemokine (C-C motif) ligand 5 (CCL5). | OLR1 | Homo sapiens hypothetical protein MGC4677 (MGC4677). |
| CD46 | CD46 molecule, complement regulatory protein (CD46), transcript variant m. | PDIA5 | Homo sapiens myosin regulatory light chain MRLC2 (MRLC2). |
| CFB | Homo sapiens complement factor B (CFB). | PDIA6 | Homo sapiens nicotinamide phosphoribosyltransferase (NAMPT). |
| CLDN12 | Homo sapiens claudin 12 (CLDN12). | SCO1 | Homo sapiens nuclear factor I/B (NFIB). |
| CPOX | Homo sapiens coproporphyrinogen oxidase (CPOX). | SDF2L1 | Homo sapiens non imprinted in Prader-Willi/Angelman syndrome 1 (NIPA1). |
| CREG1 | Homo sapiens cellular repressor of E1A-stimulated genes 1 (CREG1). | SEC11C | Homo sapiens Niemann-Pick disease, type C1 (NPC1). |
| CRELD2 | Homo sapiens cysteine-rich with EGF-like domains 2 (CRELD2). | SEL1L3 | Homo sapiens 5'-nucleotidase, ecto (CD73) (NT5E). |
| CXORF61 | Homo sapiens chromosome X open reading frame 61 (CXorf61). | SLC2A3 | Homo sapiens oxidized low density lipoprotein (lectin-like) receptor 1 (OLR1). |
| CYR61 | Homo sapiens cysteine-rich, angiogenic inducer, 61 (CYR61). | SLCO4A1 | Homo sapiens protein disulfide isomerase family A, member 5 (PDIA5). |
| DNAJB11 | Homo sapiens DnaJ (Hsp40) homolog, subfamily B, member 11 (DNAJB11). | SOD2 | Homo sapiens protein disulfide isomerase family A, member 6 (PDIA6). |
| DUSP1 | Homo sapiens dual specificity phosphatase 1 (DUSP1). | SPCS3 | Homo sapiens SCO cytochrome oxidase deficient homolog 1 (yeast) (SCO1), nuclear gene encoding mitochondrial protein. |
| EFEMP1 | EGF-containing fibulin-like extracellular matrix protein 1 (EFEMP1), variant 2. | SRGN | Homo sapiens stromal cell-derived factor 2-like 1 (SDF2L1). |
| EFHD2 | Homo sapiens EF-hand domain family, member D2 (EFHD2). | SSR1 | Homo sapiens SEC11 homolog C (S. cerevisiae) (SEC11C). |
| EFR3A | Homo sapiens EFR3 homolog A (S. cerevisiae) (EFR3A). | TMBIM6 | Homo sapiens sel-1 suppressor of lin-12-like 3 (C. elegans) (SEL1L3). |
| FAM46A | Homo sapiens family with sequence similarity 46, member A (FAM46A). | TNFRSF12A | Homo sapiens solute carrier family 2 (facilitated glucose transporter), member 3 (SLC2A3). |
| GOLT1B | Homo sapiens golgi transport 1 homolog B (S. cerevisiae) (GOLT1B). | TROVE2 | Homo sapiens solute carrier organic anion transporter family, member 4A1 (SLCO4A1). |
| HS.127310 | Homo sapiens cDNA DKFZp434C1613 (from clone DKFZp434C1613) | TXNDC12 | Superoxide dismutase 2, mitochondrial (SOD2), nuclear gene encoding mitochondrial protein, transcript variant 1. |

| | | | |
|---|---|---|---|
| HS.570988 | Homo sapiens primary neuroblastoma cDNA, clone:Nbla10111, full insert sequence | UBE2V2 | Homo sapiens signal peptidase complex subunit 3 homolog (S. cerevisiae) (SPCS3). |
| HS.5724 | Homo sapiens cDNA DKFZp779O0231 | VTN | Homo sapiens serglycin (SRGN). |
| IER3 | Homo sapiens immediate early response 3 (IER3). | WFDC1 | Homo sapiens signal sequence receptor, alpha (translocon-associated protein alpha) (SSR1). |
| JUN | Homo sapiens jun oncogene (JUN). | ZFP36 | Homo sapiens transmembrane BAX inhibitor motif containing 6 (TMBIM6), transcript variant 1. |

# APPENDIX B

## B.1 PRELIMINARY ANALYSIS OF THE CLOSELY RELATED ENDOSOMAL CHANNEL TRPML3

TRPML3 is a closely related homologue of TRPML1, with similar proposed topology and localization to late endocytic vesicles. A mutation in the gene *MCOLN3,* coding for TRPML3, results in the *varitint-waddler* phenotype in mice, characterized by pigmentation, hearing and behavioral defects (8, 276, 286, 287). The equivalent mutation in TRPML1 results in a constitutively active channel with the same activity and ion selectivity as TRPML3, suggesting that these channels may function similarly (8). Furthermore, localization studies of these channels also suggest that TRPML1, TRPML2, and TRPML3 colocalize in vesicles in the later portion of the endocytic pathway and were shown to homo- and heterotetramize (288). Although little is known about the role and regulation of TRPML3, it has been suggested to play a role in endocytic trafficking, $Ca^{2+}$ conductance from the endocytic organelles (289), and to be a regulator of late endocytic pH (290). Therefore, we believe TRPML3 could a useful tool for comparative analysis with TRPML1 and suggest that if these channels share similar function or activity, that loss of either mucolipin could result in similar phenotypes and cellular responses. To test the similarity between TRPML1 and TRPML3, we performed structure/function analysis

of TRPML3 using site-directed mutagenesis followed by patch clamp analysis. We found that, consistent with other reports, TRPML3 seems to share an activity profile similar to TRPML1, although it is inhibited by low pH, unlike TRPML1 (Fig 4.1A). Furthermore, 48 hour KD of TRPML3 resulted in a similar cellular inclusion phenotype and lysosomal protein changes seen in TRPML1. This preliminary work suggests that these channels not only share similar activity and inhibition profiles, but also that the loss of these channels shares similar pathologies. This may lead to a better understanding as to the celular role of these channels as well as the consequence of their downregulation.

### B.1.1 Mutation of conserved TRPML residues result in inactivation of TRPML3

The following sections include patch clamp analysis, to determine the activity of TRPML3 and its block by transition metals. The structure/function analysis consisted of site-directed mutagenesis of key residues that may play a role in the activity and regulation of this channel followed by analysis of mutant channel activity. During these studies several of these mutations were concurrently identified by another group, verifying our results. However we also identified other key residues which may contribute to the activity of TRPML channels. The activating mutations discussed in section 4.4 were also published during these studies, and therefore we made these mutants to test pore selectivity of these mutants to $Cu^{2+}$. The following section describes the outcomes of these experiments.

Structure/functional analyses performed on the Shaker family of $K^+$ channels identified critical residues in the voltage sensing domains of these channels (transmembrane domains) which control the opening and closing of the pore through interaction with key residues in linker

regions of the channel (291, 292). Using these studies as a guide, we targeted several charged residues in the pore, linker regions, and 4$^{th}$ transmembrane domain of TRPML channels. By aligning the highly homologous TRPML1 and TRPML3, we identified several conserved residues in these regions. Using site-directed mutagenesis, we negated or reversed the charge of the pore residues D458 and D459 as well as the S3/TM4 residues E336/N339, and E349. These mutants were screened for proper lysosomal localization in HeLa cells. Properly localized mutants were then transfected in HEK293 cells and activity was measured using whole-cell patch clamp analysis as described in section 4. Several additional pore, C-terminal, and S4 residues were also screened, but they either resulted in ER retention or did not alter TRPML3 activity (data not shown).

Negating the charge of D458 and D459 resulted in a small, linear current as seen in Figure B.1.A. This current remained unaltered after the addition of $Cu^{2+}$. This suggests that these pore residues play a critical role in regulating the activity of the channel and may coordinate the movement of cations ions through the channel. A study published in 2007 demonstrates that switching these acidic amino acids to basic residues (DD→KK) eliminates the inwardly rectifying current of TRPML3, confirming our results (8).

Further analysis outside of the pore region suggests that residues in the S3 and TM4 domain of TRPML3 regulate the activity of the pore region. Switching the charge in residues E446/N339 and E469 resulting in the loss of an inwardly rectifying current. This may suggest that these residues coordinate the opening and closing of the pore, as seen in Figure B.1.B. The residues targeted in both regions are conserved between TRPML1 and TRPML3, suggesting that these residues may play a similar function between these channels. This evidence points to the similarity between TRPML channels.

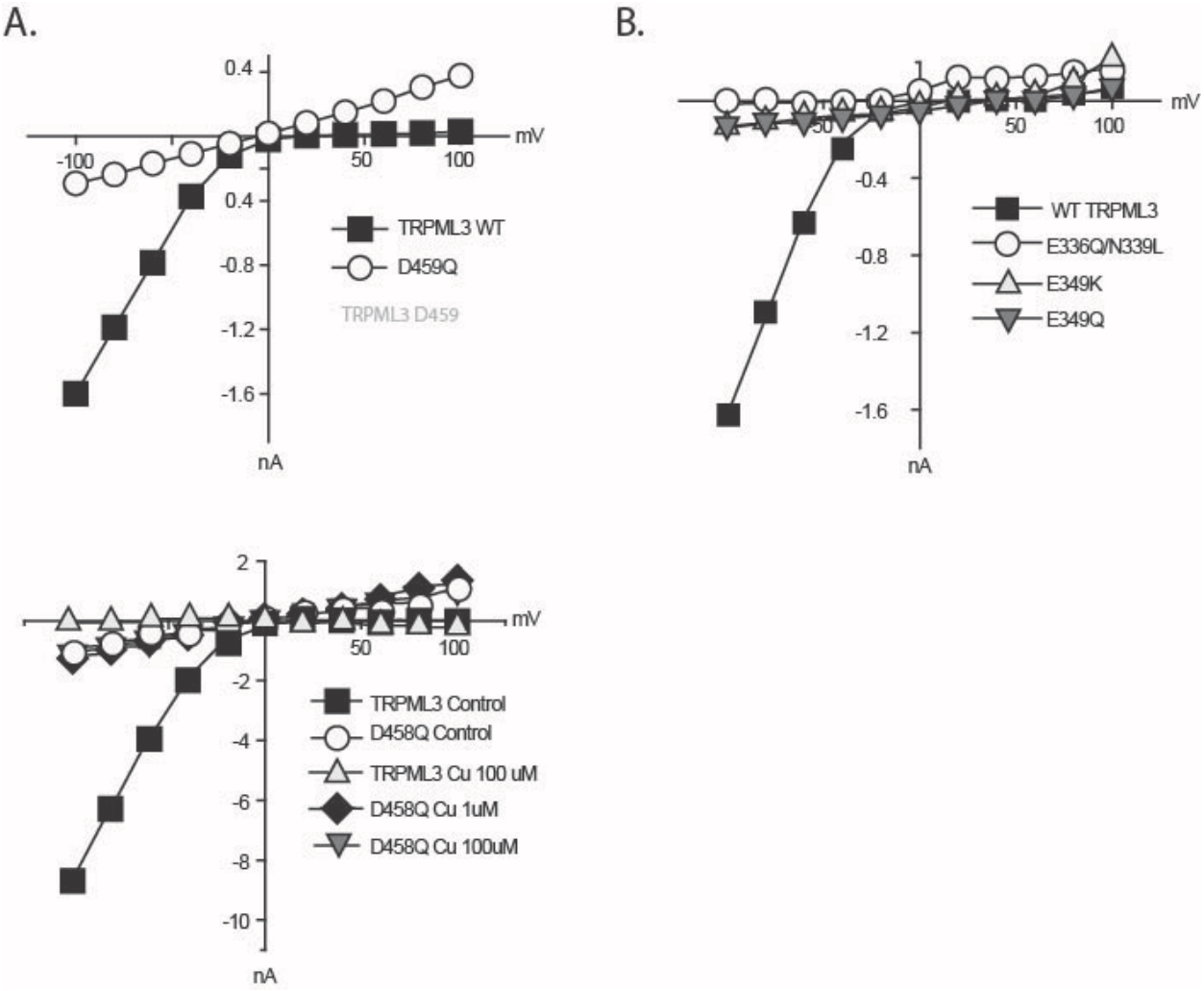


**Figure B.1 Analysis of mutants reveals inactivating mutations in the pore and S3 domains of TRPML3.**
HEK293 cells were transfected with GFP-TRPML3 and analyzed using whole cell patch clamp with $Na^+$ and $Ca^{2+}$ as main charge carriers in the outside solution and $Cs^+$ in the pipette solution. A) Mutations made in the pore domain of TRPML3 result in small, linear currents. Ablating the charge of residues D458 and D459 both resulted in inactivation of the inwardly rectifying current. B) Current voltage relationship demonstrating the loss of inward current by changing or ablating the charge of E349 or double mutants E336/N339 in the TM4/S3 domain of the TRPML3.

### B.1.2 Activating mutations in the S3 domain of TRPML1 and TRPML3 are not sensitive to $Cu^{2+}$ block.

When the activating mutation in the S3 domain of TRPML3 and TRPML1 was identified in 2007, it provided a useful tool for studying these channels. First, it allowed us to determine if "fixing" the channel in an open state allowed the passage of transition metals. Furthermore, it was shown that this TRPML1 mutant localized to the plasma membrane and produced spontaneous activity, allowing us to analyze it using patch clamp analysis. The following data is the preliminary work from section 4.

$TRPML3^{A419P}$ resulted in spontaneous channel activity (100% of patches resulted in large inward rectifying current). Furthermore, addition of various concentrations of $Cu^{2+}$, previously shown to robustly inhibit TRPML3 activity, did not inhibit the channel as seen in Figure B.2.A. Analysis of $TRPML1^{V432P}$ also resulted in spontaneous inward rectifying current. Addition of $Cu^{2+}$ did not inhibit this channel, suggesting that these channels have similar inwardly rectifying currents and that the coordination of transition metal block may be shared between these channels. Another study demonstrated that patching enlarged lysosomes, transfected with wildtype TRPML1, resulted in inwardly rectifying current, further supporting that this is the endogenous activity of this channel (9). The similar activity profiles of these channels, combined with the effects of mutating conserved residues suggests that these channels may have similar activity profiles, while functioning in separate components of the endocytic pathway.

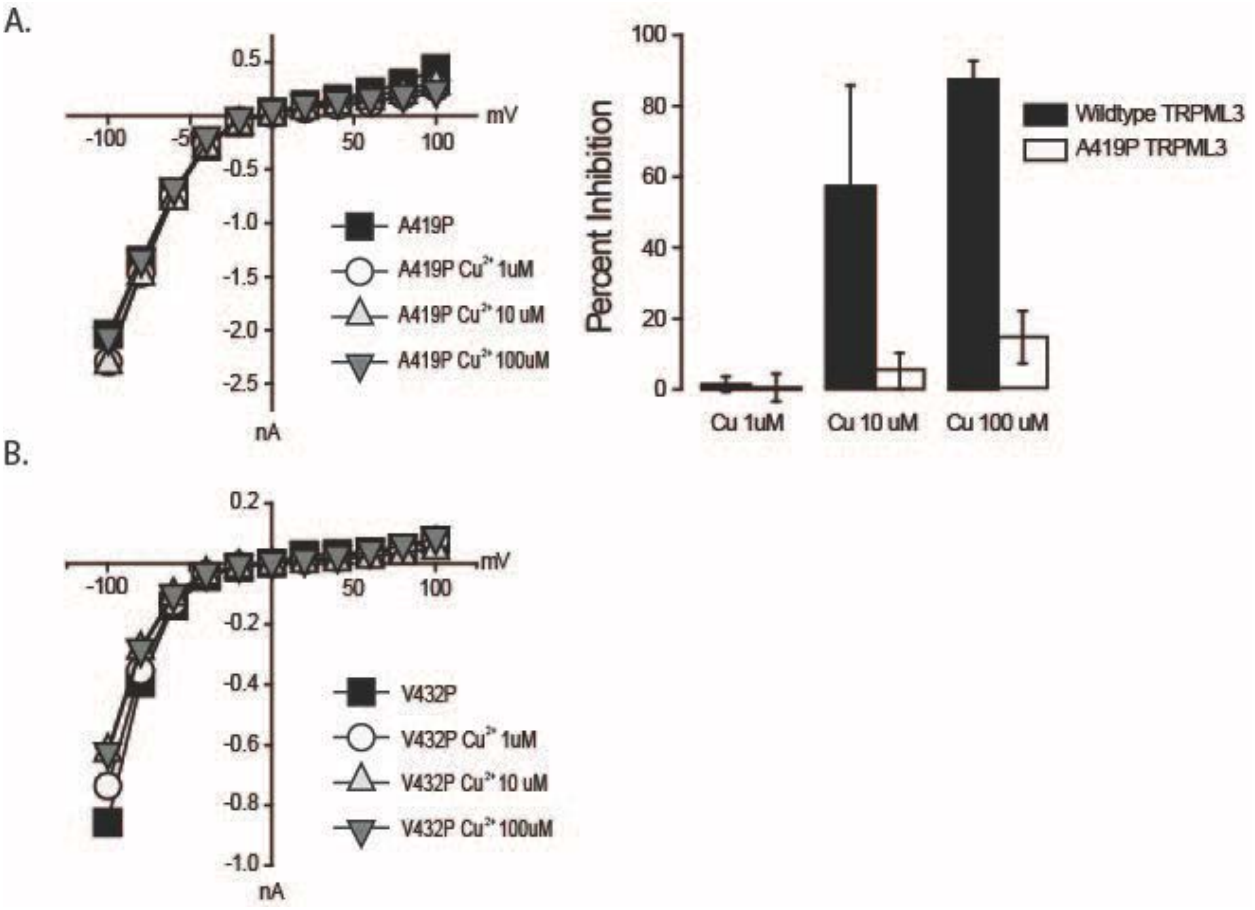


**Figure B.2 Sensitivity of Va TRPML3 and TRPML1 mutants to $Cu^{2+}$**
HEK293 cells were transfected with GFP-TRPML3 and analyzed using whole cell patch clamp with $Na^{+}$ and $Ca^{2+}$ as main charge carriers in the outside solution and $Cs^{+}$ in the pipette solution. A) Current voltage relationship demonstrating insensitivity of the *Va* $TRPML3^{A419}$ mutant to transition metals. Inhibition of wildtype TRPML3 and $TRPML3^{A419}$ is graphed (n=4) B) Current voltage relationship demonstrating inward current and insensitivity of the *Va* $TRPML1^{V432P}$ mutant to transition metals.

### B.1.3 TRPML3 KD leads to similar cellular pathologies as TRPML1 KD

In order to compare the effects of TRPML3 KD to TRPML1 KD, we performed a 48 hour KD using transient transfection with TRPML3 targeting siRNA. We verified KD using qRT-PCR as described in section 2. As seen in Figure B.3.A, KD resulted in a 63.3%±9.2 decrease in *MCOLN3* mRNA levels compared to control cells (n=3, p<.01). To determine if

TRPML3 KD had the same effects on lysosomal components as TRPML1 KD, we used Western blot analysis to measure mature CatB and LAL levels in these KD cells. As seen in Figure B.3.B, TRPML3 KD leads to a similar increase in CatB and decrease in LAL, as seen in TRPML1 KD cells. This suggests that although these proteins may function in separate compartments of the cell, that loss of these proteins may activate similar responses.

Finally, we analyzed cellular inclusion formation in TRPML3 KD cells using electron microscopy. As seen in Figure B.3.C., TRPML3 lead to a similar increase in inclusion formation as TRPML1, suggesting that loss of this protein results in endocytic malfunction. A further profiling of these inclusions will elucidate whether these bodies share similar phenotypes.

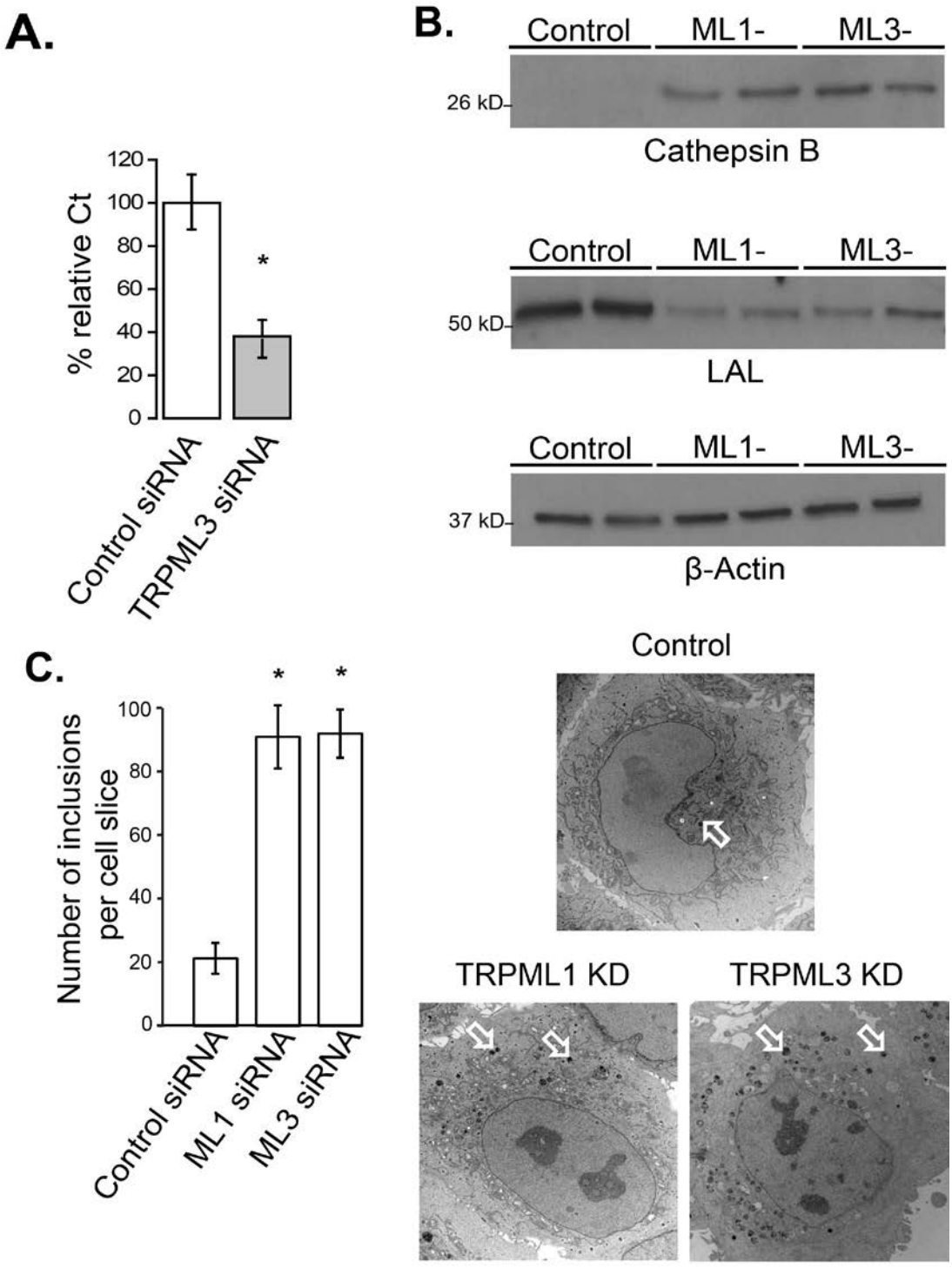


**Figure B.3. TRPML3 KD results in similar cellular changes as TRPML1 KD**
A) 48 hour siRNA mediated KD of TRPML3 resulted in decreased *MCOLN3* mRNA levels (n=3, *p<.01). B) Western blot analysis shows an elevation of mature CatB and a decrease in LAL 48 hours after TRPML1 and TRPML3 KD. C) Electron microscopy shows a similar buildup of storage inclusions 48 hours after TRPML1 and TRPML3 KD.

### B.1.4 Conclusions and acknowledgements

Our data strongly support the hypothesis that TRPML1 and TRPML3 function similarly, although in different cellular compartments. It is interesting that loss of either channel results in similar cellular changes. It is important to note an observation as well about the activating *Va* mutants of each channel: under overexpression conditions, these activating channels lead to severe cell death and thus were difficult to patch. This suggests that the regulation of channel activity is critical for cell survival, and may suggest why no gain of function mutations have been linked to disease.

Whether these channels play redundant roles in the cell or whether the loss of one can be compensated to some extent by the other will still need to be evaluated. It seems that these channels do share similarities, but it may be their spatial differences that lead to their specific cellular functions. In the future it will be interesting to test whether overexpression of either channel can rescue the downregulation of the other. Furthermore, understanding the localization differences between these channels and further elucidating their roles in endocytic compartments will be critical for clarifying the role of these channels in endocytic function.

For these studies I would like to thank Christopher Lyons for imaging and counting the cellular inclusions in TRPML1 and TRPML3 cells compared to control cells. I would also like to thank my undergraduate Emina Hodzic for help in creating and screening TRPML3 mutant channels.

## BIBLIOGRAPHY


1. Kiselyov, K., Chen, J., Rbaibi, Y., Oberdick, D., Tjon-Kon-Sang, S., Shcheynikov, N., Muallem, S., and Soyombo, A. 2005. TRP-ML1 is a lysosomal monovalent cation channel that undergoes proteolytic cleavage. *J Biol Chem* 280:43218-43223.
2. Sun, M., Goldin, E., Stahl, S., Falardeau, J.L., Kennedy, J.C., Acierno, J.S., Jr., Bove, C., Kaneski, C.R., Nagle, J., Bromley, M.C., et al. 2000. Mucolipidosis type IV is caused by mutations in a gene encoding a novel transient receptor potential channel. *Hum Mol Genet* 9:2471-2478.
3. LaPlante, J.M., Falardeau, J., Sun, M., Kanazirska, M., Brown, E.M., Slaugenhaupt, S.A., and Vassilev, P.M. 2002. Identification and characterization of the single channel function of human mucolipin-1 implicated in mucolipidosis type IV, a disorder affecting the lysosomal pathway. *FEBS Lett* 532:183-187.
4. Hersh, B.M., Hartwieg, E., and Horvitz, H.R. 2002. The Caenorhabditis elegans mucolipin-like gene cup-5 is essential for viability and regulates lysosomes in multiple cell types. *Proc Natl Acad Sci U S A* 99:4355-4360.
5. Vergarajauregui, S., and Puertollano, R. 2006. Two di-leucine motifs regulate trafficking of mucolipin-1 to lysosomes. *Traffic* 7:337-353.
6. Miedel, M.T., Weixel, K.M., Bruns, J.R., Traub, L.M., and Weisz, O.A. 2006. Posttranslational cleavage and adaptor protein complex-dependent trafficking of mucolipin-1. *J Biol Chem* 281:12751-12759.
7. Zhang, F., Jin, S., Yi, F., and Li, P.L. 2008. TRP-ML1 Functions as a Lysosomal NAADP-Sensitive Ca(2+) Release Channel in Coronary Arterial Myocytes. *Journal of Cellular and Molecular Medicine* 13:3174-3185.
8. Xu, H., Delling, M., Li, L., Dong, X., and Clapham, D.E. 2007. Activating mutation in a mucolipin transient receptor potential channel leads to melanocyte loss in varitint-waddler mice. *Proc Natl Acad Sci U S A* 104:18321-18326.
9. Dong, X.P., Shen, D., Wang, X., Dawson, T., Li, X., Zhang, Q., Cheng, X., Zhang, Y., Weisman, L.S., Delling, M., et al. 2010. PI(3,5)P(2) controls membrane trafficking by direct activation of mucolipin Ca(2+) release channels in the endolysosome. *Nat Commun* 1:38.
10. Cantiello, H.F., Montalbetti, N., Goldmann, W.H., Raychowdhury, M.K., Gonzalez-Perrett, S., Timpanaro, G.A., and Chasan, B. 2005. Cation channel activity of mucolipin-1: the effect of calcium. *Pflugers Arch* 451:304-312.
11. Bassi, M.T., Manzoni, M., Monti, E., Pizzo, M.T., Ballabio, A., and Borsani, G. 2000. Cloning of the gene encoding a novel integral membrane protein, mucolipidin-and identification of the two major founder mutations causing mucolipidosis type IV. *Am J Hum Genet* 67:1110-1120.

12. Micsenyi, M.C., Dobrenis, K., Stephney, G., Pickel, J., Vanier, M.T., Slaugenhaupt, S.A., Walkley, S.U. 2009. Neuropathology of the Mcoln1-/- Knockout Mouse Model of Mucolipidosis Type IV. *J Neuropathol Exp Neurol* 68:125-135.
13. Venugopal B, B.M., Curcio-Morelli C, Varro A, Michaud N, Nanthakumar N, Walkley SU, Pickel J, Slaugenhaupt SA. 2007. Neurologic, gastric, and opthalmologic pathologies in a murine model of mucolipidosis type IV. *Am J Hum Gen* 81:1070-1083.
14. Jennings, J.J., Jr., Zhu, J.H., Rbaibi, Y., Luo, X., Chu, C.T., and Kiselyov, K. 2006. Mitochondrial aberrations in mucolipidosis Type IV. *J Biol Chem* 281:39041-39050.
15. Venkatachalam, K., Long, A.A., Elsaesser, R., Nikolaeva, D., Broadie, K., Montell C. . 2008. Motor deficit in a Drosophila model of mucolipidosis type IV due to defective clearance of apoptotic cells. *Cell* 135:838-851.
16. Vesa, J., Hellsten, E., Verkruyse, L.A., Camp, L.A., Rapola, J., Santavuori, P., Hofmann, S.L., and Peltonen, L. 1995. Mutations in the palmitoyl protein thioesterase gene causing infantile neuronal ceroid lipofuscinosis. *Nature* 376:584-587.
17. Weimer, J.M., Kriscenski-Perry, E., Elshatory, Y., and Pearce, D.A. 2002. The Neuronal Ceroid Lipofuscinoses. *NeuroMolecular Medicine* 1:111-124.
18. Sardiello, M., Palmieri, M., di Ronza, A., Medina, D.L., Valenza, M., Gennarino, V.A., Di Malta, C., Donaudy, F., Embrione, V., Polishchuk, R.S., Banfi, S., Parenti, G., Cattaneo, E., Ballabio.A. 2009. A gene network regulating lysosomal biogenesis and function. *Science* 325:473-477.
19. Manzoni, M., Monti, E., Bresciani, R., Bozzato, A., Barlati, S., Bassi, M.T., and Borsani, G. 2004. Overexpression of wild-type and mutant mucolipin proteins in mammalian cells: effects on the late endocytic compartment organization. *FEBS Lett* 567:219-224.
20. Kim, H.J., Yamaguchi, S., Li, Q., So, I., and Muallem, S. 2010. Properties of the TRPML3 channel pore and its stable expansion by the Varitint-Waddler-causing mutation. *J Biol Chem* 285:16513-16520.
21. van Aken, A.F., Atiba-Davies, M., Marcotti, W., Goodyear, R.J., Bryant, J.E., Richardson, G.P., Noben-Trauth, K., and Kros, C.J. 2008. TRPML3 mutations cause impaired mechano-electrical transduction and depolarization by an inward-rectifier cation current in auditory hair cells of varitint-waddler mice. *J Physiol* 586:5403-5418.
22. Nagata, K., Zheng, L., Madathany, T., Castiglioni, A.J., Bartles, J.R., and Garcia-Anoveros, J. 2008. The varitint-waddler (Va) deafness mutation in TRPML3 generates constitutive, inward rectifying currents and causes cell degeneration. *Proc Natl Acad Sci U S A* 105:353-358.
23. Kim, H.J., Li, Q., Tjon-Kon-Sang, S., So, I., Kiselyov, K., Soyombo, A.A., and Muallem, S. 2008. A novel mode of TRPML3 regulation by extracytosolic pH absent in the varitint-waddler phenotype. *Embo J* 27:1197-1205.
24. Cuajungco, M.P., and Samie, M.A. 2008. The varitint-waddler mouse phenotypes and the TRPML3 ion channel mutation: cause and consequence. *Pflugers Arch* 457:463-473.
25. Kim, H.J., Li, Q., Tjon-Kon-Sang, S., So, I., Kiselyov, K., and Muallem, S. 2007. Gain-of-function mutation in TRPML3 causes the mouse Varitint-Waddler phenotype. *J Biol Chem* 282:36138-36142.
26. Grimm, C., Cuajungco, M.P., van Aken, A.F., Schnee, M., Jors, S., Kros, C.J., Ricci, A.J., and Heller, S. 2007. A helix-breaking mutation in TRPML3 leads to constitutive activity underlying deafness in the varitint-waddler mouse. *Proc Natl Acad Sci U S A* 104:19583-19588.

27. Berthet, J.a.D.D.C. 1951. Tissue Fractionation Studies 1. The Existence of a Mitochondrial-linked, Enzymatically Inactive Form of Acid Phosphatase in Rat-Liver Tissue. *Biochem J* 50:174-181.
28. Appelmans, F., Wattiaux, R., De Duve, C. 1955. Tissue fractionation studies. 5. The association of acid phosphatase with a special class of cytoplasmic granules in rat liver. *Biochem J* 59:438-445.
29. De Duve, C., Pressman, B.C., Gianetto, R., Wattiaux, R., and Appelmans, F. 1955. Tissue fractionation studies. 6. Intracellular distribution patterns of enzymes in rat-liver tissue. *Biochem J* 60:604-617.
30. Ruivo, R., Anne, C., Sagne, C., and Gasnier, B. 2009. Molecular and cellular basis of lysosomal transmembrane protein dysfunction. *Biochim Biophys Acta* 1793:636-649.
31. Jentsch, T.J. 2007. Chloride and the endosomal-lysosomal pathway: emerging roles of CLC chloride transporters. *J Physiol* 578:633-640.
32. Luzio, J.P., Pryor, P.R., Gray, S.R., Gratian, M.J., Piper, R.C., and Bright, N.A. 2005. Membrane traffic to and from lysosomes. *Biochem Soc Symp*:77-86.
33. Codogno, P., and Meijer, A.J. 2005. Autophagy and signaling: their role in cell survival and cell death. *Cell Death Differ* 12 Suppl 2:1509-1518.
34. Cuervo, A.M. 2004. Autophagy: in sickness and in health. *Trends Cell Biol* 14:70-77.
35. Eskelinen, E.L., and Saftig, P. 2009. Autophagy: a lysosomal degradation pathway with a central role in health and disease. *Biochim Biophys Acta* 1793:664-673.
36. Jahreiss, L., Menzies, F.M., and Rubinsztein, D.C. 2008. The Itinerary of Autophagosomes: From Peripheral Formation to Kiss-and-Run Fusion with Lysosomes. *Traffic* 9:574-587.
37. Nakamura, N., Matsuura, A., Wada, Y., and Ohsumi, Y. 1997. Acidification of vacuoles is required for autophagic degradation in the yeast, Saccharomyces cerevisiae. *J Biochem* 121:338-344.
38. Bright, N.A., Gratian, M.J., and Luzio, J.P. 2005. Endocytic delivery to lysosomes mediated by concurrent fusion and kissing events in living cells. *Curr Biol* 15:360-365.
39. Aravanis, A.M., Pyle, J.L., Harata, N.C., and Tsien, R.W. 2003. Imaging single synaptic vesicles undergoing repeated fusion events: kissing, running, and kissing again. *Neuropharmacology* 45:797-813.
40. Mullock, B.M., Bright, N.A., Fearon, C.W., Gray, S.R., Luzio, J.P. 1998. Fusion of Lysosomes with Late Endosomes Produces a Hybrid Organelle of Intermediate Density and Is NSF Dependent. *Journal of Cell Biology* 140:591-601.
41. Jordens, I., Fernandez-Borja, M., Marsman, M., Dusseljee, S., Janssen, L., Calafat, J., Janssen, H., Wubbolts, R., and Neefjes, J. 2001. The Rab7 effector protein RILP controls lysosomal transport by inducing the recruitment of dynein-dynactin motors. *Curr Biol* 11:1680-1685.
42. Jager, S., Bucci, C., Tanida, I., Takashi, U., Kominami, E., Saftig, P., and Eskelinen, E. 2004. Role for Rab7 in maturation of late autophagic vacuoles. *Journal of Cell Science* 117:4837-4848.
43. Gutierrez, M.G., Munafo, D.B., Beron, W., and Colombo, M.I. 2004. Rab7 is required for the normal progression of the autophagic pathway in mammalian cells. *J Cell Sci* 117:2687-2697.
44. Bucci, C., Thomsen, P., Nicoziani, P., McCarthy, J., and van Deurs, B. 2000. Rab7: a key to lysosome biogenesis. *Mol Biol Cell* 11:467-480.

45. Wurmser, A.E., Sato, T.K., and Emr, S.D. 2000. New component of the vacuolar class C-Vps complex couples nucleotide exchange on the Ypt7 GTPase to SNARE-dependent docking and fusion. *J Cell Biol* 151:551-562.
46. Rink, J., Ghigo, E., Kalaidzidis, Y., and Zerial, M. 2005. Rab conversion as a mechanism of progression from early to late endosomes. *Cell* 122:735-749.
47. Cantalupo, G., Alifano, P., Roberti, V., Bruni, C.B., and Bucci, C. 2001. Rab-interacting lysosomal protein (RILP): the Rab7 effector required for transport to lysosomes. *EMBO J* 20:683-693.
48. Johansson, M., Lehto, M., Tanhuanpaa, K., Cover, T.L., and Olkkonen, V.M. 2005. The oxysterol-binding protein homologue ORP1L interacts with Rab7 and alters functional properties of late endocytic compartments. *Mol Biol Cell* 16:5480-5492.
49. Brett, C.L., Plemel, R.L., Lobinger, B.T., Vignali, M., Fields, S., and Merz, A.J. 2008. Efficient termination of vacuolar Rab GTPase signaling requires coordinated action by a GAP and a protein kinase. *J Cell Biol* 182:1141-1151.
50. Collins, K.M., Thorngren, N.L., Fratti, R.A., and Wickner, W.T. 2005. Sec17p and HOPS, in distinct SNARE complexes, mediate SNARE complex disruption or assembly for fusion. *EMBO J* 24:1775-1786.
51. Pryor, P.R., Mullock, B.M., Bright, N.A., Lindsay, M.R., Gray, S.R., Richardson, S.C., Stewart, A., James, D.E., Piper, R.C., and Luzio, J.P. 2004. Combinatorial SNARE complexes with VAMP7 or VAMP8 define different late endocytic fusion events. *EMBO Rep* 5:590-595.
52. Luzio, J.P., Gray, S.R., and Bright, N.A. 2010. Endosome-lysosome fusion. *Biochem Soc Trans* 38:1413-1416.
53. Furuta, N., and Amano, A. 2010. Cellular machinery to fuse antimicrobial autophagosome with lysosome. *Commun Integr Biol* 3:385-387.
54. Pryor, P.R., Mullock, B.M., Bright, N.A., Gray, S.R., and Luzio, J.P. 2000. The role of intraorganellar Ca(2+) in late endosome-lysosome heterotypic fusion and in the reformation of lysosomes from hybrid organelles. *J Cell Biol* 149:1053-1062.
55. Vergarajauregui, S., Martina, J.A., Puertollano, R. 2009. Identification of the penta-EF-hand protein ALG-2 as a Ca2+-dependent interactor of mucolipin-1. *J Biol Chem* 284:36357-36366.
56. Jeremic, A., Kelly, M., Cho, J.A., Cho, S.J., Horber, J.K., and Jena, B.P. 2004. Calcium drives fusion of SNARE-apposed bilayers. *Cell Biol Int* 28:19-31.
57. Bhoopathi, P., Chetty, C., Gujrati, M., Dinh, D.H., Rao, J.S., and Lakka, S. 2010. Cathepsin B facilitates authophagy-mediated apoptosis in SPARC overexpressed primitive neuroectodermal tumor cells. *Cell Death Differ.*:[Epub ahead of print].
58. Bidere, N., Lorenzo, H.K., Carmona, S., Laforge, M., Harper, F., Dumont, C., and Senik, A. 2003. Cathepsin D triggers Bax activation, resulting in selective apoptosis-inducing factor (AIF) relocation in T lymphocytes entering the early commitment phase to apoptosis. *J Biol Chem* 278:31401-31411.
59. Guicciardi, M.E., Deussing, J., Miyoshi, H., Bronk, S.F., Svingen, P.A., Peters, C., Kaufmann, S.H., and Gores, G.J. 2000. Cathepsin B contributes to TNF-alpha-mediated hepatocyte apoptosis by promoting mitochondrial release of cytochrome c. *J Clin Invest* 106:1127-1137.

60. Gonzalez-Noreiga, A., Grubb, J.H., Talkad, V., Sly, W.S. 1980. Chloroquine inhibits lysosomal enzyme pinocytosis and enhances lysosomal enzyme secretion by impairing receptor recycling. *J Cell Biol* 85:839-852.
61. Tapper, H., and Sundler, R. 1995. Bafilomycin A1 inhibits lysosomal, phagosomal, and plasma membrane H(+)-ATPase and induces lysosomal enzyme secretion in macrophages. *J Cell Physiol* 163:137-144.
62. Yamamoto, A., Tagawa, Y., Yoshimori, T., Moriyama, Y., Masaki, R., and Tashiro, Y. 1998. Bafilomycin A1 prevents maturation of autophagic vacuoles by inhibiting fusion between autophagosomes and lysosomes in rat hepatoma cell line, H-4-II-E cells. *Cell Struct Funct* 23:33-42.
63. Schneider, D.L. 1981. ATP-dependent acidification of intact and disrupted lysosomes. Evidence for an ATP-driven proton pump. *J Biol Chem* 256:3858-3864.
64. Reeves, J.P., and Reames, T. 1981. Atp Stimulates Amino-Acid Accumulation by Lysosomes Incubated with Amino-Acid Methyl-Esters - Evidence for a Lysosomal Proton Pump. *Journal of Biological Chemistry* 256:6047-6053.
65. Morgan, E.H., and Oates, P.S. 2002. Mechanisms and regulation of intestinal iron absorption. *Blood Cells Mol Dis* 29:384-399.
66. Andrews, N.C., and Schmidt, P.J. 2007. Iron homeostasis. *Annu Rev Physiol* 69:69-85.
67. Scott, C.C., and Gruenberg, J. 2011. Ion flux and the function of endosomes and lysosomes: pH is just the start: the flux of ions across endosomal membranes influences endosome function not only through regulation of the luminal pH. *Bioessays* 33:103-110.
68. Galione, A., Evans, A.M., Ma, J., Parrington, J., Arredouani, A., Cheng, X., and Zhu, M.X. 2009. The acid test: the discovery of two-pore channels (TPCs) as NAADP-gated endolysosomal Ca(2+) release channels. *Pflugers Arch* 458:869-876.
69. Graves, A.R., Curran, P.K., Smith, C.L., and Mindell, J.A. 2008. The Cl-/H+ antiporter ClC-7 is the primary chloride permeation pathway in lysosomes. *Nature* 453:788-792.
70. Kasper, D., Planells-Cases, R., Fuhrmann, J.C., Scheel, O., Zeitz, O., Ruether, K., Schmitt, A., Poet, M., Steinfeld, R., Schweizer, M., et al. 2005. Loss of the chloride channel ClC-7 leads to lysosomal storage disease and neurodegeneration. *Embo J* 24:1079-1091.
71. Karageorgos, L.E., Isaac, E.L., Brooks, D.A., Ravenscroft, E.M., Davey, R., Hopwood, J.J., Meikle, P.J. 1997. Lysosomal biogenesis in lysosomal storage disorders. *Exp Cell Res* 234:85-97.
72. Pereira, V.G., Gazarini, M.L., Rodrigues, L.C., da Silva, F.H., Han, S.W., Martins, A.M., Tersariol, I.L., D'Almeida, V. 2010. Evidence of lysosomal membrane permeabilization in mucopolysaccharidosis type I: rupture of calcium and proton homeostasis. *J Cell Physiol* 223:335-342.
73. Palmieri, M., Impey, S., Kang, H., di Ronza, A., Pelz, C., Sardiello, M., and Ballabio, A. 2011. Characterization of the CLEAR network reveals an integrated control of cellular clearance pathways. *Hum Mol Genet* 20:3852-3866.
74. Rosenfeld, M.G., Kreibich, G., Popov, D., Kato, K., Sabatini, D.D. 1982. Biosynthesis of lysosomal hydrolases: their synthesis in bound polysomes and the role of co- and post-translational processing in determining their subcellular distribution. *J Cell Biol* 93:135-143.

75. Erickson, A.H., Walter, P., Blobel, G. 1983. Translocation of a lysosomal enzyme across the microsomal membrane requires signal recognition particle. *Biochem Biophys Res Commun* 115:275-280.
76. Imperiali, B., Rickert, K.W. 1995. Conformational implications of asparagine-linked glycosylation. *Proc Natl Acad Science* 92:97-101.
77. Pohl, S., Marschner, K., Storch, S., and Braulke, T. 2009. Glycosylation- and phosphorylation-dependent intracellular transport of lysosomal hydrolases. *Biol Chem* 390:521-527.
78. Dierks, T., Schmidt, B., Figura, K.V. 1997. Conversion of cysteine to formylglycine: A protein modification in the endoplasmic reticulum. *Proc Natl Acad Science* 94:11963-11968.
79. Reitman, M.L., and Kornfeld, S. 1981. Lysosomal enzyme targeting. N-Acetylglucosaminylphosphotransferase selectively phosphorylates native lysosomal enzymes. *J Biol Chem* 256:11977-11980.
80. Waheed, A., Hasilik, A., and von Figura, K. 1982. UDP-N-acetylglucosamine:lysosomal enzyme precursor N-acetylglucosamine-1-phosphotransferase. Partial purification and characterization of the rat liver Golgi enzyme. *J Biol Chem* 257:12322-12331.
81. Goldberg, D.E., and Kornfeld, S. 1981. The phosphorylation of beta-glucuronidase oligosaccharides in mouse P388D1 cells. *J Biol Chem* 256:13060-13067.
82. Lazzarino, D.A., and Gabel, C.A. 1989. Mannose processing is an important determinant in the assembly of phosphorylated high mannose-type oligosaccharides. *J Biol Chem* 264:5015-5023.
83. Varki, A., and Kornfeld, S. 1981. Purification and characterization of rat liver alpha-N-acetylglucosaminyl phosphodiesterase. *J Biol Chem* 256:9937-9943.
84. Braulke, T., and Bonifacino, J.S. 2009. Sorting of lysosomal proteins. *Biochim Biophys Acta.* 1793:604-614.
85. Puertollano, R., van der Wel, N.N., Greene, L.E., Eisenberg, E., Peters, P.J., and Bonifacino, J.S. 2003. Morphology and dynamics of clathrin/GGA1-coated carriers budding from the trans-Golgi network. *Mol Biol Cell* 14:1545-1557.
86. Natowicz, M.R., Chi, M.M., Lowry, O.H., Sly, W.S. 1979. Enzymatic identification of mannose 6-phosphate on the recognition marker for receptor-mediated pinocytosis of beta-glucuronidase by human fibroblasts *Proc Natl Acad Science* 76:4322-4326.
87. van Meel, E., and Klumperman, J. 2008. Imaging and imagination: understanding the endo-lysosomal system. *Histochem Cell Biol* 129:253-266.
88. Stennicke, H.R., and Salvesen, G.S. 2000. Caspases - controlling intracellular signals by protease zymogen activation. *Biochim Biophys Acta* 1477:299-306.
89. Oda, K., Nishimura, Y., Ikehara, Y., and Kato, K. 1991. Bafilomycin A1 inhibits the targeting of lysosomal acid hydrolases in cultured hepatocytes *Biochem Biophys Res Commun* 178:369-377.
90. Lefrancois, S., Zeng, J., Hassan, A.J., Canuel, M., and Morales, C.R. 2003. The lysosomal trafficking of sphingolipid activator proteins (SAPs) is mediated by sortilin. *EMBO J* 22:6430-6437.
91. Ni, X., and Morales, C.R. 2006. The lysosomal trafficking of acid sphingomyelinase is mediated by sortilin and mannose 6-phosphate receptor. *Traffic* 7:889-902.
92. Reczek, D., Schwake, M., Schroder, J., Hughes, H., Blanz, J., Jin, X., Brondyk, W., Van Patten, S., Edmunds, T., and Saftig, P. 2007. LIMP-2 is a receptor for lysosomal

mannose-6-phosphate-independent targeting of beta-glucocerebrosidase. *Cell* 131:770-783.
93. Katzmann, D.J., Babst, M., and Emr, S.D. 2001. Ubiquitin-dependent sorting into the multivesicular body pathway requires the function of a conserved endosomal protein sorting complex, ESCRT-I. *Cell* 106:145-155.
94. Honing, S., Griffith, J., Geuze, H.J., and Hunziker, W. 1996. The tyrosine-based lysosomal targeting signal in lamp-1 mediates sorting into Golgi-derived clathrin-coated vesicles. *EMBO J* 15:5230-5239.
95. Hunziker, W., and Geuze, H.J. 1996. Intracellular trafficking of lysosomal membrane proteins. *Bioessays* 18:379-389.
96. Meyer, C., Zizioli, D., Lausmann, S., Eskelinen, E.L., Hamann, J., Saftig, P., von Figura, K., and Schu, P. 2000. mu1A-adaptin-deficient mice: lethality, loss of AP-1 binding and rerouting of mannose 6-phosphate receptors. *EMBO J* 19:2193-2203.
97. Janvier, K., and Bonifacino, J.S. 2005. Role of the endocytic machinery in the sorting of lysosome-associated membrane proteins. *Mol Biol Cell* 16:4231-4242.
98. Pak, Y., Glowacka, W.K., Bruce, M.C., Pham, N., and Rotin, D. 2006. Transport of LAPTM5 to lysosomes requires association with the ubiquitin ligase Nedd4, but not LAPTM5 ubiquitination. *J Cell Biol* 175:631-645.
99. Dierks, T., Schmidt, B., Borissenko, L.V., Peng, J., Preusser, A., Mariappan, M., and von Figura, K. 2003. Multiple sulfatase deficiency is caused by mutations in the gene encoding the human C(alpha)-formylglycine generating enzyme. *Cell* 113:435-444.
100. Reuser, A.J., Koster, J.F., Hoogeveen, A., and Galjaard, H. 1978. Biochemical, immunological, and cell genetic studies in glycogenosis type II. *Am J Hum Genet* 30:132-143.
101. Takahashi, T., Suchi, M., Desnick, R.J., Takada, G., and Schuchman, E.H. 1992. Identification and expression of five mutations in the human acid sphingomyelinase gene causing types A and B Niemann-Pick disease. Molecular evidence for genetic heterogeneity in the neuronopathic and non-neuronopathic forms. *J Biol Chem* 267:12552-12558.
102. Hers, H.G. 1963. alpha-Glucosidase deficiency in generalized glycogenstorage disease (Pompe's disease). *Biochem J* 86:11-16.
103. Takahashi, K., Naito, M., and Suzuki, Y. 1987. Genetic mucopolysaccharidoses, mannosidosis, sialidosis, galactosialidosis, and I-cell disease. Ultrastructural analysis of cultured fibroblasts. *Acta Pathol Jpn* 37:385-400.
104. Lubensky, I.A., Schiffmann, R., Goldin, E., and Tsokos, M. 1999. Lysosomal inclusions in gastric parietal cells in mucolipidosis type IV: a novel cause of achlorhydria and hypergastrinemia. *Am J Surg Pathol* 23:1527-1531.
105. Beltroy, E.P., Richardson, J.A., Horton, J.D., Turley, S.D., and Dietschy, J.M. 2005. Cholesterol accumulation and liver cell death in mice with Niemann-Pick type C disease. *Hepatology* 42:886-893.
106. Wei, H., Kim, S.J., Zhang, Z., Tsai, P.C., Wisniewski, K.E., and Mukherjee, A.B. 2008. ER and oxidative stresses are common mediators of apoptosis in both neurodegenerative and non-neurodegenerative lysosomal storage disorders and are alleviated by chemical chaperones. *Hum Mol Genet* 17:469-477.
107. Fu, R., Yanjanin, N.M., Bianconi, S., Pavan, W.J., and Porter, F.D. 2010. Oxidative stress in Niemann-Pick disease, type C. *Mol Genet Metab* 101:214-218.

108. Ginzburg, L., and Futerman, A.H. 2005. Defective calcium homeostasis in the cerebellum in a mouse model of Niemann-Pick A disease. *J Neurochem* 95:1619-1628.
109. Woloszynek, J.C., Kovacs, A., Ohlemiller, K.K., Roberts, M., and Sands, M.S. 2009. Metabolic adaptations to interrupted glycosaminoglycan recycling. *J Biol Chem* 284:29684-29691.
110. Waheed, A., Hasilik, A., Cantz, M., and von Figura, K. 1982. Phosphorylation of lysosomal enzymes in fibroblasts. Marked deficiency of N-acetylglucosamine-1-phosphotransferase in fibroblasts of patients with mucolipidosis III. *Hoppe Seylers Z Physiol Chem* 363:169-178.
111. Raghavan, S., Leshinsky, E., and Kolodny, E.H. 1999. G(M2)-ganglioside metabolism in situ in mucolipidosis IV fibroblasts. *Neurochem Res* 24:475-479.
112. Pacheco, C.D., Kunkel, R., and Lieberman, A.P. 2007. Autophagy in Niemann-Pick C disease is dependent upon Beclin-1 and responsive to lipid trafficking defects. *Hum Mol Genet* 16:1495-1503.
113. Mancini, G.M., Hoogeveen, A.T., Galjaard, H., Mansson, J.E., and Svennerholm, L. 1986. Ganglioside GM1 metabolism in living human fibroblasts with beta-galactosidase deficiency. *Hum Genet* 73:35-38.
114. Lieser, M., Harms, E., Kern, H., Bach, G., and Cantz, M. 1989. Ganglioside GM3 sialidase activity in fibroblasts of normal individuals and of patients with sialidosis and mucolipidosis IV. Subcellular distribution and and some properties. *Biochem J* 260:69-74.
115. Bargal, R., Zeigler, M., Abu-Libdeh, B., Zuri, V., Mandel, H., Ben Neriah, Z., Stewart, F., Elcioglu, N., Hindi, T., Le Merrer, M., et al. 2006. When Mucolipidosis III meets Mucolipidosis II: GNPTA gene mutations in 24 patients. *Mol Genet Metab* 88:359-363.
116. Hickman, S., and Neufeld, E.F. 1972. A hypothesis for I-cell disease: defective hydrolases that do not enter lysosomes. *Biochem Biophys Res Commun* 49:992-999.
117. Conzelmann, E., Sandhoff, K., Nehrkorn, H., Geiger, B., and Arnon, R. 1978. Purification, biochemical and immunological characterisation of hexosaminidase A from variant AB of infantile GM2 gangliosidosis. *Eur J Biochem* 84:27-33.
118. Conzelmann, E., and Sandhoff, K. 1978. AB variant of infantile GM2 gangliosidosis: deficiency of a factor necessary for stimulation of hexosaminidase A-catalyzed degradation of ganglioside GM2 and glycolipid GA2. *Proc Natl Acad Sci U S A* 75:3979-3983.
119. Sharp, J.D., Wheeler, R.B., Lake, B.D., Savukoski, M., Jarvela, I.E., Peltonen, L., Gardiner, R.M., and Williams, R.E. 1997. Loci for classical and a variant late infantile neuronal ceroid lipofuscinosis map to chromosomes 11p15 and 15q21-23. *Hum Mol Genet* 6:591-595.
120. Ranta, S., Zhang, Y., Ross, B., Lonka, L., Takkunen, E., Messer, A., Sharp, J., Wheeler, R., Kusumi, K., Mole, S., et al. 1999. The neuronal ceroid lipofuscinoses in human EPMR and mnd mutant mice are associated with mutations in CLN8. *Nat Genet* 23:233-236.
121. Kousi, M., Siintola, E., Dvorakova, L., Vlaskova, H., Turnbull, J., Topcu, M., Yuksel, D., Gokben, S., Minassian, B.A., Elleder, M., et al. 2009. Mutations in CLN7/MFSD8 are a common cause of variant late-infantile neuronal ceroid lipofuscinosis. *Brain* 132:810-819.

122. Kitzmuller, C., Haines, R., Sandra, C., Daniel, C.F., and Mole, S.E. 2007. A function retained by the common mutant CLN3 protein is responsible for the late onset of juvenile neuronal ceroid lipofuscinosis. *Human Molecular Genetics* 17:303-312.
123. Meikle, P.J., Ranieri, E., Ravenscroft, E.M., Hua, C.T., Brooks, D.A., and Hopwood, J.J. 1999. Newborn screening for lysosomal storage disorders. *Southeast Asian J Trop Med Public Health* 30 Suppl 2:104-110.
124. Meikle, P.J., Hopwood, J.J., Clague, A.E., and Carey, W.F. 1999. Prevalence of lysosomal storage disorders. *JAMA* 281:249-254.
125. Applegarth, D.A., Toone, J.R., and Lowry, R.B. 2000. Incidence of inborn errors of metabolism in British Columbia, 1969-1996. *Pediatrics* 105:e10.
126. Hawkins-Salsbury, J.A., Reddy, A.S., and Sands, M.S. 2011. Combination therapies for lysosomal storage disease: is the whole greater than the sum of its parts? *Hum Mol Genet* 20:R54-60.
127. Hilz, M.J., Marthol, H., Schwab, S., Kolodny, E.H., Brys, M., and Stemper, B. 2010. Enzyme replacement therapy improves cardiovascular responses to orthostatic challenge in Fabry patients. *J Hypertens* 28:1438-1448.
128. Hilz, M.J., Brys, M., Marthol, H., Stemper, B., and Dutsch, M. 2004. Enzyme replacement therapy improves function of C-, Adelta-, and Abeta-nerve fibers in Fabry neuropathy. *Neurology* 62:1066-1072.
129. Spencer, B.J., and Verma, I.M. 2007. Targeted delivery of proteins across the blood-brain barrier. *Proc Natl Acad Sci U S A* 104:7594-7599.
130. Boado, R.J., Zhang, Y., Wang, Y., and Pardridge, W.M. 2008. GDNF fusion protein for targeted-drug delivery across the human blood-brain barrier. *Biotechnol Bioeng* 100:387-396.
131. Schiffmann, R. 2010. Therapeutic approaches for neuronopathic lysosomal storage disorders. *J Inherit Metab Dis* 33:373-379.
132. Prasad, V.K., and Kurtzberg, J. 2008. Emerging trends in transplantation of inherited metabolic diseases. *Bone Marrow Transplant* 41:99-108.
133. Escolar, M.L., Poe, M.D., Provenzale, J.M., Richards, K.C., Allison, J., Wood, S., Wenger, D.A., Pietryga, D., Wall, D., Champagne, M., et al. 2005. Transplantation of umbilical-cord blood in babies with infantile Krabbe's disease. *N Engl J Med* 352:2069-2081.
134. Jeyakumar, M., Thomas, R., Elliot-Smith, E., Smith, D.A., van der Spoel, A.C., d'Azzo, A., Perry, V.H., Butters, T.D., Dwek, R.A., and Platt, F.M. 2003. Central nervous system inflammation is a hallmark of pathogenesis in mouse models of GM1 and GM2 gangliosidosis. *Brain* 126:974-987.
135. Orchard, P.J., Blazar, B.R., Wagner, J., Charnas, L., Krivit, W., and Tolar, J. 2007. Hematopoietic cell therapy for metabolic disease. *J Pediatr* 151:340-346.
136. Oberle, C., Huai, J., Reinheckel, T., Tacke, M., Rassner, M., Ekert, P.G., Buellesbach, J., and Borner, C. 2010. Lysosomal membrane permeabilization and cathepsin release is a Bax/Bak-dependent, amplifying event of apoptosis in fibroblasts and monocytes. *Cell death and differentiation* 17:1167-1178.
137. Michallet, M., Saltel, F., Preville, X., Flacher, M., Revillard, JP., Genestier, L. 2003. Cathepsin-B-dependent apoptosis triggered by antithymocyte globulins: a novel mechanism of T-cell depletion. *Blood* 102:3719-3726.

138. Kagedal, K., Johansson, U., and Ollinger, K. 2001. The lysosomal protease cathepsin D mediates apoptosis induced by oxidative stress. *FASEB J* 15:1592-1594.
139. Joy, B., Sivadasan, R., Abraham, T.E., John, M., Sobhan, P.K., Seervi, M., and Santhoshkumar, T.R. 2009. Lysosomal destabilization and cathepsin B contributes for cytochrome c release and caspase activation in embelin-induced apoptosis. *Mol Carcinog.*:[Epub ahead of print].
140. Hsu, K.F., Wu, C.L., Huang, S.C., Wu, C.M., Hsiao, J.R., Yo, Y.T., Chen, Y.H., Shiau, A.L., and Chou, C.Y. 2009. Cathepsin L mediates resveratrol-induced autophagy and apoptotic cell death in cervical cancer cells. *Autophagy* 5:451-460.
141. Press, E.M., Porter, R.R., and Cebra, J. 1960. The isolation and properties of a proteolytic enzyme, cathepsin D, from bovine spleen. *Biochem J* 74:501-514.
142. Greenbaum, L.M., and Fruton, J.S. 1957. Purification and properties of beef spleen cathepsin B. *J Biol Chem* 226:173-180.
143. Chan, S.J., San Segundo, B., McCormick, M.B., and Steiner, D.F. 1986. Nucleotide and predicted amino acid sequences of cloned human and mouse preprocathepsin B cDNAs. *Proc Natl Acad Sci U S A* 83:7721-7725.
144. Mach, L., Schwihla, H., Stuwe, K., Rowan, A.D., Mort, J.S., and Glossl, J. 1993. Activation of procathepsin B in human hepatoma cells: the conversion into the mature enzyme relies on the action of cathepsin B itself. *Biochem J.* 293:437-442.
145. Musil, D., Zucic, D., Turk, D., Engh, R.A., Mayr, I., Huber, R., Popovic, T., Turk, V., Towatari, T., Katunuma, N., et al. 1991. The refined 2.15 A X-ray crystal structure of human liver cathepsin B: the structural basis for its specificity. *EMBO J* 10:2321-2330.
146. Illy, C., Quraishi, O., Wang, J., Purisima, E., Vernet, T., and Mort, J.S. 1997. Role of the occluding loop in cathepsin B activity. *J Biol Chem* 272:1197-1202.
147. Mellor, G.W., Thomas, E.W., Topham, C.M., and Brocklehurst, K. 1993. Ionization characteristics of the Cys-25/His-159 interactive system and of the modulatory group of papain: resolution of ambiguity by electronic perturbation of the quasi-2-mercaptopyridine leaving group in a new pyrimidyl disulphide reactivity probe. *Biochem J* 290 ( Pt 1):289-296.
148. Keillor, J.W., Neverov, A.A., and Brown, R.S. 1994. Catalysis of Amide Hydrolysis and Formation under Neutral Conditions by a Zwitterionic Imidazolium Thiolate. *J Am Chem Soc* 116:4669-4673.
149. Berti, P.J., and Storer, A.C. 1995. Alignment Phylogeny of the Papain Superfamily of Cysteine Proteases. *Journal of Molecular Biology* 246:273-283.
150. Hasnain, S., Hirama, T., Huber, C.P., Mason, P., and Mort, J.S. 1993. Characterization of Cathepsin-B Specificity by Site-Directed Mutagenesis - Importance of Glu(245) in the S2-P2 Specificity for Arginine and Its Role in Transition-State Stabilization. *Journal of Biological Chemistry* 268:235-240.
151. Gosalia, D.N., Salisbury, C.M., Ellman, J.A., and Diamond, S.L. 2005. High throughput substrate specificity profiling of serine and cysteine proteases using solution-phase fluorogenic peptide microarrays. *Mol Cell Proteomics* 4:626-636.
152. Krupa, J.C., Hasnain, S., Nagler, D.K., Menard, R., and Mort, J.S. 2002. S2' substrate specificity and the role of His110 and His111 in the exopeptidase activity of human cathepsin B. *Biochem J* 361:613-619.

153. Zhao, M., Antunes, F., Eaton, J.W., and Brunk, U.T. 2003. Lysosomal enzymes promote mitochondrial oxidant production, cytochrome c release and apoptosis. *Eur J Biochem* 270:3778-3786.
154. Werneburg, N.W., Guicciardi, M.E., Bronk, S.F., Gores, G.J. 2002. Tumor necrosis factor-α-associated lysosomal permeabilization is cathepsin B dependent. *Gastrointestinal and Liver Physiology* 283:947-956.
155. Luo, C.L., Chen, X.P., Yang, R., Sun, Y.X., Li, Q.Q., Bao, H.J., Cao, Q.Q., Ni, H., Qin, Z.H., and Tao, L.Y. 2010. Cathepsin B Contributes to Traumatic Brain Injury-Induced Cell Death Through a Mitochondria-Mediated Apoptotic Pathway. *Journal of Neuroscience Research* 88:2847-2858.
156. Broker, L.E., Huisman, C., Span, S.W., Rodriguez, J.A., Kruyt, F.A., and Giaccone, G. 2004. Cathepsin B mediates caspase-independent cell death induced by microtubule stabilizing agents in non-small cell lung cancer cells. *Cancer Res* 64:27-30.
157. Ostenfeld, M.S., Fehrenbacher, N., Hoyer-Hansen, M., Thomsen, C., Farkas, T., and Jaattela, M. 2005. Effective tumor cell death by sigma-2 receptor ligand siramesine involves lysosomal leakage and oxidative stress. *Cancer Res* 65:8975-8983.
158. Blomgran, R., Zheng, L., and Stendahl, O. 2007. Cathepsin-cleaved Bid promotes apoptosis in human neutrophils via oxidative stress-induced lysosomal membrane permeabilization. *J Leukoc Biol* 81:1213-1223.
159. Droga-Mazovec, G., Bojic, L., Petelin, A., Ivanova, S., Romih, R., Repnik, U., Salvesen, G.S., Stoka, V., Turk, V., and Turk, B. 2008. Cysteine cathepsins trigger caspase-dependent cell death through cleavage of bid and antiapoptotic Bcl-2 homologues. *J Biol Chem* 283:19140-19150.
160. LaPlante, J.M., Ye, C.P., Quinn, S.J., Goldin, E., Brown, E.M., Slaugenhaupt, S.A., and Vassilev, P.M. 2004. Functional links between mucolipin-1 and Ca2+-dependent membrane trafficking in mucolipidosis IV. *Biochem Biophys Res Commun* 322:1384-1391.
161. Dong, X.P., Cheng, X., Mills, E., Delling, M., Wang, F., Kurz, T., and Xu, H. 2008. The type IV mucolipidosis-associated protein TRPML1 is an endolysosomal iron release channel. *Nature* 455:992-996.
162. Miedel, M.T., Rbaibi, Y., Guerriero, C.J., Colletti, G., Weixel, K.M., Weisz, O.A., and Kiselyov, K. 2008. Membrane traffic and turnover in TRP-ML1-deficient cells: a revised model for mucolipidosis type IV pathogenesis. *J Exp Med* 205:1477-1490.
163. Bargal, R., Avidan, N., Ben-Asher, E., Olender, Z., Zeigler, M., Frumkin, A., Raas-Rothschild, A., Glusman, G., Lancet, D., and Bach, G. 2000. Identification of the gene causing mucolipidosis type IV. *Nat Genet* 26:118-123.
164. Falardeau, J.L., Kennedy, J.C., Acierno, J.S., Jr., Sun, M., Stahl, S., Goldin, E., and Slaugenhaupt, S.A. 2002. Cloning and characterization of the mouse Mcoln1 gene reveals an alternatively spliced transcript not seen in humans. *BMC Genomics* 3:3.
165. Vergarajauregui, S., Connelly, P.S., Daniels, M.P., Puertollano, R. 2008. Autophagic dysfunction in mucolipidosis type IV patients. *Human Molecular Genetics* 17:2723-2737.
166. Raychowdhury, M.K., Gonzalez-Perrett, S., Montalbetti, N., Timpanaro, G.A., Chasan, B., Goldmann, W.H., Stahl, S., Cooney, A., Goldin, E., and Cantiello, H.F. 2004. Molecular pathophysiology of mucolipidosis type IV: pH dysregulation of the mucolipin-1 cation channel. *Hum Mol Genet* 13:617-627.

167. Bargal, R., and Bach, G. 1997. Mucolipidosis type IV: abnormal transport of lipids to lysosomes. *J Inherit Metab Dis* 20:625-632.
168. Pryor, P.R., Reimann, F., Gribble, F.M., and Luzio, J.P. 2006. Mucolipin-1 Is a Lysosomal Membrane Protein Required for Intracellular Lactosylceramide Traffic. *Traffic* 7:1388-1398.
169. Fares, H., and Greenwald, I. 2001. Regulation of endocytosis by CUP-5, the Caenorhabditis elegans mucolipin-1 homolog. *Nat Genet* 28:64-68.
170. Treusch, S., Knuth, S., Slaugenhaupt, S.A., Goldin, E., Grant, B.D., and Fares, H. 2004. Caenorhabditis elegans functional orthologue of human protein h-mucolipin-1 is required for lysosome biogenesis. *Proc Natl Acad Sci U S A* 101:4483-4488.
171. Pagano, R.E. 2003. Endocytic trafficking of glycosphingolipids in sphingolipid storage diseases. *Philos Trans R Soc Lond B Biol Sci* 358:885-891.
172. Tellez-Nagel, I., Rapin, I., Iwamoto, T., Johnson, A.B., Norton, W.T., and Nitowsky, H. 1976. Mucolipidosis IV. Clinical, ultrastructural, histochemical, and chemical studies of a case, including a brain biopsy. *Arch Neurol* 33:828-835.
173. Kenyon, K.R., Maumenee, I.H., Green, W.R., Libert, J., and Hiatt, R.L. 1979. Mucolipidosis IV. Histopathology of conjunctiva, cornea, and skin. *Arch Ophthalmol* 97:1106-1111.
174. Goebel, H.H., Kohlschutter, A., and Lenard, H.G. 1982. Morphologic and chemical biopsy findings in mucolipidosis IV. *Clin Neuropathol* 1:73-82.
175. Zlotogora, J., Ben Ezra, D., Livni, N., Ashkenazi, A., and Cohen, T. 1983. A muscle disorder as presenting symptom in a child with mucolipidosis IV. *Neuropediatrics* 14:104-105.
176. Abraham, F.A., Brand, N., Blumenthal, M., and Merin, S. 1985. Retinal function in mucolipidosis IV. *Ophthalmologica* 191:210-214.
177. Riedel, K.G., Zwaan, J., Kenyon, K.R., Kolodny, E.H., Hanninen, L., and Albert, D.M. 1985. Ocular abnormalities in mucolipidosis IV. *Am J Ophthalmol* 99:125-136.
178. Weitz, R., and Kohn, G. 1988. Clinical spectrum of mucolipidosis type IV. *Pediatrics* 81:602-603.
179. Chitayat, D., Meunier, C.M., Hodgkinson, K.A., Silver, K., Flanders, M., Anderson, I.J., Little, J.M., Whiteman, D.A., and Carpenter, S. 1991. Mucolipidosis type IV: clinical manifestations and natural history. *Am J Med Genet* 41:313-318.
180. Frei, K.P., Patronas, N.J., Crutchfield, K.E., Altarescu, G., and Schiffmann, R. 1998. Mucolipidosis type IV: characteristic MRI findings. *Neurology* 51:565-569.
181. Schiffmann, R., Dwyer, N.K., Lubensky, I.A., Tsokos, M., Sutliff, V.E., Latimer, J.S., Frei, K.P., Brady, R.O., Barton, N.W., Blanchette-Mackie, E.J., et al. 1998. Constitutive achlorhydria in mucolipidosis type IV. *Proc Natl Acad Sci U S A* 95:1207-1212.
182. Siegel, H., Frei, K., Greenfield, J., Schiffmann, R., and Sato, S. 1998. Electroencephalographic findings in patients with mucolipidosis type IV. *Electroencephalogr Clin Neurophysiol* 106:400-403.
183. Schaheen, L., Patton, G., Fares, H. 2006. Suppression of the cup-5 mucolipidosis type IV-related lysosomal dysfunction by the inactivation of an ABC transporter in C. elegans. *Development* 133:3939-3948.
184. Laplante, J.M., Sun, M., Falardeau, J., Dai, D., Brown, E.M., Slaugenhaupt, S.A., and Vassilev, P.M. 2006. Lysosomal exocytosis is impaired in mucolipidosis type IV. *Mol Genet Metab* 89:339-348.

185. Venugopal, B., Mesires, N.T., Kennedy, J.C., Curcio-Morelli, C., Laplante, J.M., Dice, J.F., Slaughenhaupt, S.A. 2009. Chaperone-mediated autophagy is defective in mucolipidosis type IV. *J Cell Physiol* 219:344-353.
186. Soyombo, A.A., Tjon-Kon-Sang, S., Rbaibi, Y., Bashllari, E., Bisceglia, J., Muallem, S., and Kiselyov, K. 2006. TRP-ML1 regulates lysosomal pH and acidic lysosomal lipid hydrolytic activity. *J Biol Chem* 281:7294-7301.
187. Grimm, C., Cuajungco, M.P., van Aken, A.F., Schnee, M., Jors, S., Kros, C.J., Ricci, A.J., and Heller, S. 2007. A helix-breaking mutation in TRPML3 leads to constitutive activity underlying deafness in the varitint-waddler mouse. *Proc Natl Acad Sci U S A.*
188. Dong, X., Cheng, X., E., M., M., D., F., W., Kurz, T., and Xu, H. 2008. The type IV mucolipidosis-associated protein TRPML1 is an endolysosomal iron release channel. *Nature* 455:992-996.
189. Goldin, E., Caruso, R.C., Benko, W., Kaneski, C.R., Stahl, S., Schiffmann, R. 2008. Isolated ocular disease is associated with decreased mucolipin-1 channel conductance. *Investigative Ophthalmology* 49:3134-3142.
190. Thompson, E.G., Schaheen, L., Dang, H., and Fares, H. 2007. Lysosomal trafficking functions of mucolipin-1 in murine macrophages. *BMC Cell Biology* 8:54.
191. Kogot-Levin, A., Ziegler, M., Ornoy, A., Bach, G. 2009. Mucolipidosis type IV: the effect of increased lysosomal pH on the abnormal lysosomal storage. *Pediatr Res* 65:686-690.
192. Bentley, M., Nycz, D.C., Joglekar, A., Fertschai, I., Malli, R., Graier, W.F., and Hay, J.C. 2010. Vesicular calcium regulation coat retention, fusogenicity, and size of pre-Golgi intermediates. *Mol Biol Cell* 21:1033-1046.
193. Gaetke, L.M., and Chow, C.K. 2003. Copper toxicity, oxidative stress, and antioxidant nutrients. *Toxicology* 189:147-163.
194. Eaton, J.W., and Qian, M. 2002. Molecular bases of cellular iron toxicity. *Free Radic Biol Med* 32:833-840.
195. Pfeiffer, R.F. 2007. Wilson's Disease. *Seminars in Neurology* 27:123-132.
196. Llanos, R.M., and Mercer, J.F. 2002. The molecular basis of copper homeostasis copper-related disorders. *DNA Cell Biol* 21:259-270.
197. Harris, E.D. 2000. Cellular copper transport and metabolism. *Annu Rev Nutr* 20:291-310.
198. Mims, M., and Prchal, J. 2005. Divalent metal transporter 1. *Hematology* 10:339-345.
199. Terman, A., and Brunk, U.T. 2004. Lipofuscin. *Int J Biochem Cell Biol* 36:1400-1404.
200. Brunk, U.T., Jones, C.B., and Sohal, R.S. 1992. A novel hypothesis of lipofuscinogenesis and cellular aging based on interactions between oxidative stress and autophagocytosis. *Mutat Res* 275:395-403.
201. Cisternas, F.A., Tapia, G., Arredondo, M., Cartier-Ugarte, D., Romanque, P., Sierralta, W.D., Vial, M.T., Videla, L.A., and Araya, M. 2005. Early histological and functional effects of chronic copper exposure in rat liver. *Biometals* 18:541-551.
202. Schneider, P., Korolenko, T.A., and Busch, U. 1997. A review of drug-induced lysosomal disorders of the liver in man and laboratory animals. *Microsc Res Tech* 36:253-275.
203. Pourahmad, J., Ross, S., and O'Brien, P.J. 2001. Lysosomal involvement in hepatocyte cytotoxicity induced by Cu(2+) but not Cd(2+). *Free Radic Biol Med* 30:89-97.
204. Terman, A., Kurz, T., Gustafsson, B., and Brunk, U.T. 2006. Lysosomal labilization. *IUBMB Life* 58:531-539.

205. Brunk, U.T., and Terman, A. 2002. The mitochondrial-lysosomal axis theory of aging: accumulation of damaged mitochondria as a result of imperfect autophagocytosis. *Eur J Biochem* 269:1996-2002.
206. Stroikin, Y., Dalen, H., Loof, S., and Terman, A. 2004. Inhibition of autophagy with 3-methyladenine results in impaired turnover of lysosomes and accumulation of lipofuscin-like material. *Eur J Cell Biol* 83:583-590.
207. Walls, K.C., Klocke, B.J., Saftig, P., Shibata, M., Uchiyama, Y., Roth, K.Y., and Shacka, J.J. 2007. Altered Regulation of Phosphatidylinositol 3-kinase Signaling in Cathepsin D-Deficient Brain. *Autophagy* 3.
208. Pan, T., Kondo, S., Le, W., and Jankovic, J. 2008. The role of autophagy-lysosome pathway in neurodegeneration associated with Parkinson's disease. *Brain* 131:1969-1978.
209. Kiselyov, K., Jennigs, J.J., Jr., Rbaibi, Y., and Chu, C.T. 2007. Autophagy, mitochondria and cell death in lysosomal storage diseases. *Autophagy* 3:259-262.
210. Takamura, A., Higaki, K., Kajimaki, K., Otsuka, S., Ninomiya, H., Matsuda, J., Ohno, K., Suzuki, Y., and Nanba, E. 2008. Enhanced autophagy and mitochondrial aberrations in murine G(M1)-gangliosidosis. *Biochem Biophys Res Commun* 367:616-622.
211. Terman, A., Dalen, H., Eaton, J.W., Neuzil, J., and Brunk, U.T. 2004. Aging of cardiac myocytes in culture: oxidative stress, lipofuscin accumulation, and mitochondrial turnover. *Ann N Y Acad Sci* 1019:70-77.
212. King, T.P., and Bremner, I. 1979. Autophagy and apoptosis in liver during the prehaemolytic phase of chronic copper poisoning in sheep. *J Comp Pathol* 89:515-530.
213. Kiselyov, K., Colletti, G.A., Terwilliger, A., Ketchum, K., Lyons, C.W., Quinn, J., and Muallem, S. 2011. TRPML: transporters of metals in lysosomes essential for cell survival? *Cell Calcium* 50:288-294.
214. Eichelsdoerfer, J.L., Evans, J.A., Slaugenhaupt, S.A., and Cuajungco, M.P. 2010. Zinc dyshomeostasis is linked with the loss of mucolipidosis IV-associated TRPML1 ion channel. *J Biol Chem* 285:34304-34308.
215. Bach, G. 2001. Mucolipidosis type IV. *Mol Genet Metab* 73:197-203.
216. Bargal, R., Avidan, N., Olender, T., Ben Asher, E., Zeigler, M., Raas-Rothschild, A., Frumkin, A., Ben-Yoseph, O., Friedlender, Y., Lancet, D., et al. 2001. Mucolipidosis type IV: novel MCOLN1 mutations in Jewish and non-Jewish patients and the frequency of the disease in the Ashkenazi Jewish population. *Hum Mutat* 17:397-402.
217. Altarescu, G., Sun, M., Moore, D.F., Smith, J.A., Wiggs, E.A., Solomon, B.I., Patronas, N.J., Frei, K.P., Gupta, S., Kaneski, C.R., et al. 2002. The neurogenetics of mucolipidosis type IV. *Neurology* 59:306-313.
218. Bargal, R., Goebel, H.H., Latta, E., and Bach, G. 2002. Mucolipidosis IV: novel mutation and diverse ultrastructural spectrum in the skin. *Neuropediatrics* 33:199-202.
219. Folkerth, R.D., Alroy, J., Lomakina, I., Skutelsky, E., Raghavan, S.S., and Kolodny, E.H. 1995. Mucolipidosis IV: morphology and histochemistry of an autopsy case. *J Neuropathol Exp Neurol* 54:154-164.
220. Bozzato, A., Barlati, S., Borsani, G. 2008. Gene expression profiling of mucolipidosis type IV fibroblasts reveals deregulation of genes with relevant functions in lysosome physiology. *Biochim Biophys Acta.* 1782:250-258.
221. Chandra, M., Zhou, H., Li, Q., Muallem, S., Hofmann, S.L., and Soyombo, A.A. 2011. A Role for the Ca(2+) Channel TRPML1 in Gastric Acid Secretion, Based on Analysis of Knockout Mice. *Gastroenterology* 140:857-867.

222. Settembre, C., Fraldi, A., Jahreiss, L., Spampanato, C., Venturi, C., Medina, D., de Pablo, R., Tacchetti, C., Rubinsztein, D.C., and Ballabio, A. 2008. A block of autophagy in lysosomal storage disorders. *Hum Mol Genet* 17:119-129.
223. Settembre, C., Fraldi, A., Rubinsztein, D.C., and Ballabio, A. 2008. Lysosomal storage diseases as disorders of autophagy. *Autophagy* 4:113-114.
224. Vergarajauregui, S., Connelly, P.S., Daniels, M.P., and Puertollano, R. 2008. Autophagic dysfunction in mucolipidosis type IV patients. *Hum Mol Genet* 17:2723-2737.
225. Ballabio, A., and Gieselmann, V. 2009. Lysosomal disorders: from storage to cellular damage. *Biochim Biophys Acta* 1793:684-696.
226. Venugopal, B., Browning, M.F., Curcio-Morelli, C., Varro, A., Michaud, N., Nanthakumar, N., Walkley, S.U., Pickel, J., and Slaugenhaupt, S.A. 2007. Neurologic, gastric, and opthalmologic pathologies in a murine model of mucolipidosis type IV. *Am J Hum Genet* 81:1070-1083.
227. Curcio-Morelli C, C.F., Micsenyi MC, Cao Y, Venugopal B, Browning MF, Dobrenis K, Cotman SL, Walkley SU, Slaugenhaupt SA. 2010. Macroautophagy is defective in mucolipin-1-deficient mouse neurons. *Neurobiol Dis* 40:370-377.
228. Cheriyath, V., Kuhns, M.A., Kalaycio, M.E., and Borden, E.C. 2011. Potentiation of apoptosis by histone deacetylase inhibitors and doxorubicin combination: cytoplasmic cathepsin B as a mediator of apoptosis in multiple myeloma. *British Journal of Cancer* in press.
229. Rommelaere, G., Michel, S., Mercy, L., Fattaccioli, A., Demazy, C., Ninane, N., Houbion, A., Renard, P., and Arnould, T. 2010. Hypersensitivity of mtDNA-depleted cells to staurosporine-induced apoptosis: the roles of Bcl-2 downregulation and cathepsin B. *Am J Physiol Cell Physiol*.
230. Seglen, P.O., Gordon, P.B., Grinde, B., Solheim, A., Kovacs, A.L., and Poli, A. 1981. Inhibitors and pathways of hepatocytic protein degradation. *Acta Biol Med Ger* 40:1587-1598.
231. Scornik, O.A. 1984. Effects of inhibitors of protein degradation on the rate of protein synthesis in Chinese hamster ovary cells. *J Cell Physiol* 121:257-262.
232. Boya, P., Gonzalez-Polo, R.A., Poncet, D., Andreau, K., Vieira, H.L., Roumier, T., Perfettini, J.L., and Kroemer, G. 2003. Mitochondrial membrane permeabilization is a critical step of lysosome-initiated apoptosis induced by hydroxychloroquine. *Oncogene* 22:3927-3936.
233. Ferri, K.F., and Kroemer, G. 2001. Organelle-specific initiation of cell death pathways. *Nat Cell Biol* 3:E255-263.
234. Yueng, B.H.Y., Huang, D.C., Sinicrope, F.A. 2006. PS-341 (Bortezomib) Induces Lysosomal Cathepsin B Release and a Caspase-2-dependent Mitochondrial Permeabilization and Apoptosis in Human Pancreatic Cancer Cells. *J Biol Chem* 281:11923-11932.
235. Uchiyama, Y. 2001. Autophagic cell death and its execution by lysosomal cathepsins. *Arch Histol Cytol* 64:233-246.
236. Krepela, E. 2001. Cysteine proteinases in tumor cell growth and apoptosis. *Neoplasma* 48:332-349.
237. Bursch, W. 2001. The autophagosomal-lysosomal compartment in programmed cell death. *Cell Death Differ* 8:569-581.

238. Yuan, X.M., Li, W., Brunk, U.T., Dalen, H., Chang, Y.H., and Sevanian, A. 2000. Lysosomal destabilization during macrophage damage induced by cholesterol oxidation products. *Free Radic Biol Med* 28:208-218.
239. Isahara, K., Ohsawa, Y., Kanamori, S., Shibata, M., Waguri, S., Sato, N., Gotow, T., Watanabe, T., Momoi, T., Urase, K., et al. 1999. Regulation of a novel pathway for cell death by lysosomal aspartic and cysteine proteinases. *Neuroscience* 91:233-249.
240. Liu, L., Zhang, Z., and Xing, D. 2011. Cell death via mitochondrial apoptotic pathway due to activation of Bax by lysosomal photodamage. *Free radical biology & medicine* 51:53-68.
241. Sun, L., Zhao, Y., Li, X., Yuan, H., Cheng, A., and Lou, H. 2010. A lysosomal-mitochondrial death pathway is induced by solamargine in human K562 leukemia cells. *Toxicology in vitro : an international journal published in association with BIBRA* 24:1504-1511.
242. Cregan, S.P., Fortin, A., MacLaurin, J.G., Callaghan, S.M., Cecconi, F., Yu, S.W., Dawson, T.M., Dawson, V.L., Park, D.S., Kroemer, G., et al. 2002. Apoptosis-inducing factor is involved in the regulation of caspase-independent neuronal cell death. *J Cell Biol* 158:507-517.
243. Orrenius, S. 2004. Mitochondrial regulation of apoptotic cell death. *Toxicol Lett* 149:19-23.
244. Polster, B.M., and Fiskum, G. 2004. Mitochondrial mechanisms of neural cell apoptosis. *J Neurochem* 90:1281-1289.
245. Shimizu, S., Kanaseki, T., Mizushima, N., Mizuta, T., Arakawa-Kobayashi, S., Thompson, C.B., and Tsujimoto, Y. 2004. Role of Bcl-2 family proteins in a non-apoptotic programmed cell death dependent on autophagy genes. *Nat Cell Biol* 6:1221-1228.
246. von Schantz, C., Saharinen, J., Kopra, O., Cooper, J.D., Gentile, M., Hovatta, I., Peltonen, L., Jalanko, A. 2008. Brain gene expression profiles of Cln1 and Cln5 deficient mice unravels common molecular pathways underlying neuronal degeneration in NCL diseases. *BMC Genomics* 9.
247. Bach, G., and Desnick, R.J. 1988. Lysosomal accumulation of phospholipids in mucolipidosis IV cultured fibroblasts. *Enzyme* 40:40-44.
248. Bargal, R., and Bach, G. 1989. Phosphatidylcholine storage in mucolipidosis IV. *Clin Chim Acta* 181:167-174.
249. Weimer, J.M., Kriscenski-Perry, E., Elshatory, Y., Pearce, D.A. 2002. The Neuronal Ceroid Lipofuscinoses. *NeuroMolecular Medicine* 1:111-124.
250. Das, A.K., Lu, J-Y., Hofmann, S.L. 2001. Biochemical analysis of mutations in palmitoyl-protein thioesterase causing infantile and late-onset forms of neuronal ceroid lipofuscinosis. *Human Molecular Genetics* 10.
251. Lehtovirta, M., Kyttala, A., Eskelinen, E.L., Hess, M., Heinonen, O., Jalanko, A. 2001. Palmitoyl protein thioesterase (PPT1) localizes into synaptosomes and synaptic vesicles in neurons: implications for infantile neuronal ceroid lipofuscinses (INCL). *Human Molecular Genetics* 10:69-75.
252. Verkruyse, L.A., Hoffman, S.L. 1996. Lysosomal targeting of palmitoyl-protein thioesterase. *J Biol Chem* 271:15831-15836.

253. Bozzato, A., Barlati, S., and Borsani, G. 2008. Gene expression profiling of mucolipidosis type IV fibroblasts reveals deregulation of genes with relevant functions in lysosome physiology. *Biochim Biophys Acta* 1782:250-258.
254. von Schantz, C., Saharinen, J., Kopra, O., Cooper, J.D., Gentile, M., Hovatta, I., Peltonen, L., and Jalanko, A. 2008. Brain gene expression profiles of Cln1 and Cln5 deficient mice unravels common molecular pathways underlying neuronal degeneration in NCL diseases. *BMC Genomics* 9.
255. Klein, E., Koch, S., Borm, B., Neumann, J., Herzog, V., Koch, N., and Bieber, T. 2005. CD83 localization in a recycling compartment of immature human monocyte-derived dendritic cells. *International Immunology* 17:477-487.
256. Hirano, T., Kishi, M., Sugimoto, H., Taguchi, R., Obinata, H., Ohshima, N., Tatei, K., and Izumi, T. 2009. Thioesterase activity and subcellular localization of acylprotein thioesterase 1/lysophospholipase 1. *Biochem Biophys Acta* 1791:797-805.
257. Hentze, H., Lin, X.Y., Choi, M.S., and Porter, A.G. 2003. Critical role for cathepsin B in mediating caspase-1-dependent interleukin-18 maturation and caspase-1-independent necrosis triggered by the microbial toxin nigericin. *Cell Death Differ* 10:956-968.
258. Sarkar, A., Duncan, M., Hart, J., Hertlein, E., Guttridge, D.C., and Wewers, M.D. 2006. ASC directs NF-kappaB activation by regulating receptor interacting protein-2 (RIP2) caspase-1 interactions. *J Immunol* 176:4979-4986.
259. Wright, R.O., and Baccarelli, A. 2007. Metals and neurotoxicology. *Journal of Nutrition* 137:2809-2813.
260. Mehta, R., Templeton, D.M., and O'Brien P, J. 2006. Mitochondrial involvement in genetically determined transition metal toxicity II. Copper toxicity. *Chem Biol Interact* 163:77-85.
261. Huang, X.P., O'Brien, P.J., and Templeton, D.M. 2006. Mitochondrial involvement in genetically determined transition metal toxicity I. Iron toxicity. *Chem Biol Interact* 163:68-76.
262. Cuervo, A.M., Bergamini, E., Brunk, U.T., Droge, W., Ffrench, M., and Terman, A. 2005. Autophagy and aging: the importance of maintaining "clean" cells. *Autophagy* 1:131-140.
263. Stroikin, Y., Dalen, H., Brunk, U.T., and Terman, A. 2005. Testing the "garbage" accumulation theory of ageing: mitotic activity protects cells from death induced by inhibition of autophagy. *Biogerontology* 6:39-47.
264. Terman, A., Dalen, H., Eaton, J.W., Neuzil, J., and Brunk, U.T. 2003. Mitochondrial recycling and aging of cardiac myocytes: the role of autophagocytosis. *Exp Gerontol* 38:863-876.
265. Shiono, Y., Hayashi, H., Wakusawa, S., and Yano, M. 2001. Ultrastructural identification of iron and copper accumulation in the liver of a male patient with Wilson disease. *Med Electron Microsc* 34:54-60.
266. Hayashi, H., Yano, M., Fujita, Y., and Wakusawa, S. 2006. Compound overload of copper and iron in patients with Wilson's disease. *Med Mol Morphol* 39:121-126.
267. Georgopoulos, P.G., Roy, A., Yonone-Lioy, M.J., Opiekun, R.E., and Lioy, P.J. 2001. Environmental copper: its dynamics and human exposure issues. *J Toxicol Environ Health B Crit Rev* 4:341-394.
268. Prozialeck, W.C., Edwards, J.R., and Woods, J.M. 2006. The vascular endothelium as a target of cadmium toxicity. *Life Sci* 79:1493-1506.

269. Navarro Silvera, S.A., and Rohan, T.E. 2007. Trace elements and cancer risk: a review of the epidemiologic evidence. *Cancer Causes Control* 18:7-27.
270. Colletti, G.A., and Kiselyov, K. 2011. Trpml1. *Adv Exp Med Biol* 704:209-219.
271. Cheng, X., Shen, D., Samie, M., and Xu, H. 2010. Mucolipins: Intracellular TRPML1-3 channels. *FEBS Lett* 584:2013-2021.
272. Zeevi, D.A., Frumkin, A., and Bach, G. 2007. TRPML and lysosomal function. *Biochim Biophys Acta*.
273. Bach, G. 2005. Mucolipin 1: endocytosis and cation channel--a review. *Pflugers Arch* 451:313-317.
274. Slaugenhaupt, S.A. 2002. The molecular basis of mucolipidosis type IV. *Curr Mol Med* 2:445-450.
275. Abe, K., and Puertollano, R. 2011. Role of TRP Channels in the Regulation of the Endosomal Pathway. *Physiology (Bethesda)* 26:14-22.
276. Di Palma, F., Belyantseva, I.A., Kim, H.J., Vogt, T.F., Kachar, B., and Noben-Trauth, K. 2002. Mutations in Mcoln3 associated with deafness and pigmentation defects in varitint-waddler (Va) mice. *Proc Natl Acad Sci U S A* 99:14994-14999.
277. Lelouvier, B., and Puertollano, R. Mucolipin-3 regulates luminal calcium, acidification, and membrane fusion in the endosomal pathway. *J Biol Chem* 286:9826-9832.
278. Martina, J.A., Lelouvier, B., and Puertollano, R. 2009. The calcium channel mucolipin-3 is a novel regulator of trafficking along the endosomal pathway. *Traffic* 10:1143-1156.
279. Kim, H.J., Soyombo, A.A., Tjon-Kon-Sang, S., So, I., and Muallem, S. 2009. The Ca(2+) channel TRPML3 regulates membrane trafficking and autophagy. *Traffic* 10:1157-1167.
280. Puertollano, R., and Kiselyov, K. 2009. TRPMLs: in sickness and in health. *Am J Physiol Renal Physiol* 296:F1245-1254.
281. Chen, X., Hua, H., Balamurugan, K., Kong, X., Zhang, L., George, G.N., Georgiev, O., Schaffner, W., and Giedroc, D.P. 2008. Copper sensing function of Drosophila metal-responsive transcription factor-1 is mediated by a tetranuclear Cu(I) cluster. *Nucleic acids research* 36:3128-3138.
282. Desagher, S., Osen-Sand, A., Nichols, A., Eskes, R., Montessuit, S., Lauper, S., Maundrell, K., Antonsson, B., and Martinou, J.C. 1999. Bid-induced conformational change of Bax is responsible for mitochondrial cytochrome c release during apoptosis. *J Cell Biol* 144:891-901.
283. Zaidi, A.U., McDonough, J.S., Klocke, B.J., Latham, C.B., Korsmeyer, S.J., Flavell, R.A., Schmidt, R.E., and Roth, K.A. 2001. Chloroquine-induced neuronal cell death is p53 and Bcl-2 family-dependent but caspase-independent. *J Neuropathol Exp Neurol* 60:937-945.
284. Houseweart, M.K., Vilaythong, A., Yin, X.M., Turk, B., Noebels, J.L., and Myers, R.M. 2003. Apoptosis caused by cathepsins does not require Bid signaling in an in vivo model of progressive myoclonus epilepsy (EPM1). *Cell Death Differ* 10:1329-1335.
285. Persson, H.L. 2005. Iron-dependent lysosomal destabilization initiates silica-induced apoptosis in murine macrophages. *Toxicol Lett* 159:124-133.
286. Nagata, K., Zheng, L., Madathany, T., Castiglioni, A., Bartles, J., and Garcia-Anoveros, J. 2008. The varitint-waddler (Va) deafness mutation in TRPML3 generates constititutive, inward rectifying currents and causes cell degeneration. *Proc Natl Acad Science U.S.A.* 105:353-358.

287. Kim, H.J., Li, Q., Tjon-Kon-Sang, S., So, I., Kiselyov, K., and Muallem, S. 2007. Gain-of-function mutation in TRPML3 causes the mouse varitint-waddler phenotype. *J Biol Chem*.
288. Venkatachalam, K., Hofmann, T., and Montell, C. 2006. Lysosomal localization of TRPML3 depends on TRPML2 and the mucolipidosis-associated protein TRPML1. *J Biol Chem* 281:17517-17527.
289. Kim, J.H., Soyombo, A.A., Tjon-Kon-Sang, S., So, I., and Muallem, S. 2009. The $Ca^{2+}$ Channel TRPML3 Regulates Membrane Trafficking and Autophagy. *Traffic* 10:1157-1167.
290. Martina, J.A., Lelouvier, B., and Puertollano, R. 2009. The Calcium Channel Mucolipin-3 is a Novel Regulator of Trafficking Along the Endosomal Pathway. *Traffic* 10:1143-1156.
291. Long, S.B., Campbell, E.B., and Mackinnon, R. 2005. Crystal structure of a mammalian voltage-dependent Shaker family K+ channel. *Science* 309:897-903.
292. Long, S.B., Campbell, E.B., and Mackinnon, R. 2005. Voltage sensor of Kv1.2: structural basis of electromechanical coupling. *Science* 309:903-908.